PhD degree in Molecular Medicine (curriculum in Molecular Oncology)

European School of Molecular Medicine (SEMM),

University of Milan and University of Naples "Federico II"

Settore disciplinare: Bio/10

Characterization of the role of USP25 in EGFR endocytosis

Nadine Caroline Woessner

IFOM, Milan

Matricola n. R08892

Supervisor: Dr. Simona Polo

IFOM, Milan

Anno accademico 2013-2014

TABLE OF CONTENTS

LIST OF ABBREVIATIONS

AMSH	Associated molecule with the SH3 domain of STAM
AP-2	Adaptor protein 2
APP	Amyloid Precursor Protein
Arf6	ADP ribosylation factor
BTB	Bric-a-brac, Tramtrack, Broad-complex
Cbl	Casitas B-lineage lymphoma
CCP	Clathrin coated pit
CCV	Clathrin coated vesicle
Cdc42	Cell division control protein 42 homolog
CFTR	Cystic fibrosis transmembrane conductance regulator
CHC	Clathrin heavy chain
CHMP4C	Charged multivesicular body protein 4C
CLIC	Clathrin-independent carrier
CLC	Clathrin light chain
CME	Clathrin-mediated endocytosis
COP	Coat protein complex
CTD	C-terminal domain
CUE	Coupling of ubiquitin conjugation to ERAD
CUL	Cullin
Cys	Cysteine
DPW	Aspartic acid-proline-tryptophan
DUB	Deubiquitinating enzyme
EEA1	Early endosome antigen 1
EGF	Epidermal growth factor
EGFR	Epidermal growth factor receptor
EMT	Epithelial to mesenchymal transition
ENaC	Epithelial Na+ channel
Eps15	Epidermal growth factor receptor substrate 15
Eps15L1	Epidermal growth factor receptor substrate 15-like 1
Epsin	Eps15-interacting protein
ER	Endoplasmic reticulum
ERAD	ER-associated degradation
ESCRT	Endosomal sorting complex required for sorting
Faf	Fat facets
FYVE	Fab1, YotB, Vac1p, EEA1
Gap1	General amino-acid permease
G3BP1/2	Ras-GTPase-activating protein SH3 domain-binding protein
GDP	Guanosine diphosphate
GEEC	GPI-AP-enriched early endosomal compartment
GFP	Green fluorescent protein
GGA	Golgi-localized, gamma ear-containing, Arf-binding
GluR	Glutamate receptor
Gly	Glycine

GPCR	G protein-coupled receptor
GPI-AP	Glycosylphosphatidylinositol-anchored protein
Grb2	Growth factor receptor-bound protein
GTP	Guanosine triphosphate
HB-EGF	Heparin-binding EGF-like growth factor
HECT	Homologous to the E6-AP Carboxyl Terminus
HOIL-1	Haem-oxidized IRP2 ubiquitin ligase 1
HOIP	HOIL-1-interacting protein
Hrs	Hepatocyte growth factor-regulated Tyr-kinase substrate
IAV	Influenza A virus
IB	Immunoblot
ILV	Intraluminal vesicles
JAMM	JAB1/MPN/MOV34 metalloenzyme
Kd	Dissociation constant
KD	knock-down
kDa	Kilodalton
LAMP-1	Lysosome-associated membrane protein 1
LDL	Low-density lipoprotein
Lqf	Liquid factes
LRP6	Low-density receptor-related protein 6
LUBAC	Linear ubiquitin chain assembly complex
Lys	Lysine
MAPK	Mitogen-activated protein kinase
MARCH	Membrane-associated RING-CH
MCPIP1	Monocyte chemotactic protein-induced protein 1
Met	Methionine
MHCI	Major histocompatibility complex I
miR	microRNA
MIT	Microtubule interacting and trafficking
MIU	Motif interacting with ubiquitin
MJD	Machado Joseph Disease
MVB	Multivesicular body
MyBPC1	Myosin binding protein C1
NCE	Non-clathrin endocytosis
NEDD4	Neural precursor cell expressed developmentally down-regulated protein 4
NF-κB	Nuclear factor kappa B
NGF	Nerve growth factor
NSCLC	Non-small cell lung cancer
NTD	N-terminal domain
OTU	Ovarian tumour protease
PI3K	Phosphoinositide 3-kinase
PIP_2	Phosphatidylinositol-4,5-bisphosphate
pKa	Acid dissociation constant
PKC	Protein kinase C
PLA	Proximity ligation assays

PLCγ	Phospholipase Cγ
PM	Plasma membrane
RhoA	Ras homolog gene family, member A
RING	Really interesting gene
PtdIns3P	Phosphatidylinositol-3-phosphate
RBR	RING-between-RING
RTK	Receptor tyrosine kinase
SARA	SMAD anchor for receptor activation
SH3	Src homology 3
SIM	SUMO interaction domain
siRNA	Small interfering RNA
SMURF	Smad ubiquitin regulatory factor
SNX3	Sorting nexin 3
STAM	Signal transducing adaptor molecule
STAT	Signal transducers and activators of transcription
SV40	Simian virus 40
TCRα	T-cell receptor alpha
Tf	Transferrin
TFEB	Transcription factor EB
TfR	Transferrin receptor
TGFα	Transforming growth factor alpha
TGF-βR	Transforming growth factor beta receptor
TLR	Toll-like receptor
TOM1	Target of myb1
TP53	Tumour suppressor gene p53
TSG101	Tumour susceptibility gene 101
Tyr	Tyrosine
UBA	Ubiquitin associated
UBAP-1	Ubiquitin associated protein 1
UBD	Ubiquitin-binding domain
Ubl	Ubiquitin-like
UBX	Ubiquitin regulatory X
UCH	Ubiquitin C-terminal hydrolase
UIM	Ubiquitin-interacting motif
USP	Ubiquitin-specific protease
VHS	Vps27, Hrs, STAM
Vps	Vacuolar protein sorting

FIGURE AND TABLE INDEX

ABSTRACT

The epidermal growth factor receptor (EGFR) is involved in a broad range of cellular responses. Deregulated EGFR signalling is a significant feature in different stages of oncogenesis and it contributes to several cancer types. One important mechanism whereby cancer cells can obtain increased and uncontrolled EGFR signalling is to escape down-modulation of the receptor. Ubiquitination of EGFR and of members of the endocytic machinery has a key role in this process, regulating receptor internalization, trafficking and degradation. Deubiquitinating enzymes (DUBs) can reverse the ubiquitination process, antagonizing or even promoting receptor degradation.

To identify DUBs altering EGFR degradation we undertook a genome-wide small interfering RNA screen targeting all known active DUBs. In addition to previously described AMSH, USP8, USP2 and OTUD7B enzymes, we identified twelve novel DUBs affecting EGFR degradation by using immunoblot-based approaches complemented by an ELISA-based assay. Among them USP25, a member of the ubiquitin-specific protease (USP) family, displayed one of the strongest effects. We found that the degradation rate of EGFR is enhanced upon USP25 knock-down. Quantitative internalization assays revealed that depletion of USP25 leads to a faster internalization rate of EGFR. Consistently, overexpression of wild-type USP25, but not its catalytic inactive mutant, partially blocked EGFR internalization. Pathway analyses suggest that upon knock-down of USP25 a dynamin-independent endocytic route is activated, accounting for the increased EGFR internalization.

Furthermore, we scored an increase in the EGFR ubiquitination upon USP25 knock-down, in particular at early time points post EGF stimulation, suggesting that EGFR is a direct target of USP25. Details regarding the kind of ubiquitin chains attached to the EGFR in the absence of USP25 are still lacking and are currently under investigation. We

also validated the E3 ligase component Cullin 3 (CUL3) as USP25 interactor and we found that USP25 preferentially binds the neddylated active form of CUL3. Initial analyses with CUL3 suggest that ablation of USP25 and CUL3 have opposite effects on EGFR internalization and that the observed phenotypes compensate each other in double knock-down. Our data suggest that USP25 and CUL3 may form a stable complex with opposing activity on EGFR internalization, and led us to hypothesize that they are involved in a novel "quality control" mechanism working at the plasma membrane.

Taken together our study identifies USP25 as a novel negative regulator of EGFR ubiquitination and endocytosis, involved in early internalization events. USP25 may represent a suitable "druggable" target for pathological conditions where EGFR is deregulated and opens up a promising direction for future investigations.

INTRODUCTION

1 Endocytosis

Endocytosis is the process by which eukaryotic cells internalize extracellular materials together with components of the plasma membrane (PM), proteins and lipids. Over the years it became evident that endocytosis is not only a simple procedure for nutrient uptake and to transport material through the PM, but is involved in numerous aspects of cell signalling (Sigismund et al., 2012). There is increasing evidence that endocytosis might be involved in almost all cellular regulation processes (Sigismund et al., 2012). It remains unchallenged that endocytosis is the major mechanism of signal attenuation endowing the cell with spatial and temporal resolved messages (Gonnord et al., 2012). Hence, endocytosis provides the basis for communication and supply routes within cells.

1.1 Endocytic entry routes

The vital impact of endocytosis on cellular homeostasis is reflected by the number and complexity of cell entry routes. In spite of a complex diversity, all of them share four fundamental steps: (i) a specific binding event at the cell surface; (ii) PM budding and pinching off; (iii) tethering of the resulting vesicle; (iv) finally trafficking of the vesicle to a specific subcellular compartment. Traditionally entry routes are classified depending on the size of the initial membrane invagination. Particles larger than 500 nm, like bacteria or debris of apoptotic cells, are taken up only by specialized cells via phagocytosis (Swanson, 2008). The internalization of fluids is present in almost all eukaryotic cells and occurs by macropinocytosis (Lim & Gleeson, 2011). Phagocytosis and macropinocytosis require large rearrangements of the PM guided by actin cytoskeleton remodelling. Micropinocytosis instead is characterized by invaginations <200 nm and comprises clathrin-mediated endocytosis (CME) and non-clathrin endocytosis (NCE) (Doherty &

McMahon, 2009) (**Figure 1**). Both pathways are important for receptor-mediated endocytosis and are described in more detail in the following chapters.

1.1.1 Clathrin-mediated endocytosis (CME)

CME is the best-characterized pathway among the different entry routes and is ubiquitous to all eukaryotic cells (McMahon & Boucrot, 2011). The formation of clathrin coated pits (CCPs) is initiated by the association of PM-resident cargoes and clathrin, mediated by bridging molecules like adaptor protein 2 (AP-2). A clathrin coat is the three-dimensional grouping of triskelia. Each triskelion is composed by three clathrin heavy chains (CHCs) and three clathrin light chains (CLCs). The three CHCs provide the structural backbone of the clathrin lattice, while the three CLCs regulate the formation and disassembly of the clathrin coat (Edeling et al., 2006). Clathrin polymerization drives the invagination of the pit. More than 50 different proteins are associated with CCPs, providing a structural platform regulating interactions between adaptors and other endocytic proteins. The action of the GTPase dynamin leads to the scission of the pit and clathrin coated vesicles (CCVs) are released into the cytoplasm (McMahon & Boucrot, 2011). The immense number of proteins involved in CME has raised a debate about the existence of different CCPs for distinct cargoes and or intracellular fates (Johannessen et al., 2006; Puthenveedu & von Zastrow, 2006). A typical cargo which is exclusively internalized through CME is the Transferrin receptor (TfR) described in chapter 1.3.

1.1.2 Non-clathrin endocytosis (NCE)

In contrast to CME the NCE is much less understood. NCE describes a heterogeneous group of pathways with two characteristics: (i) they are insensitive to clathrin ablation (ii) but sensitive to cholesterol depletion; consequently they depend on cholesterol-rich PM

microdomains. Further classification occurs on the requirement of dynamin for vesicle scission in dynamin-dependent and dynamin-independent NCE pathways. A second level considers the existence of coat-like proteins required for membrane curvature and stabilization, as caveolins or flotillins, subdividing the pathways in caveolae-mediated or flotillin-mediated endocytosis, respectively (Maldonado-Baez et al., 2013). Finally the involvement of small GTPases which control the entry of specific cargoes, enables the grouping in Cdc42 (cell division control protein 42 homolog)-, RhoA- (Ras homolog gene family, member A) or Arf6 (ADP ribosylation factor)-regulated endocytic pathways (D'Souza-Schorey & Chavrier, 2006; Ellis & Mellor, 2000).

1.1.2.1 Caveolae-mediated endocytosis

Caveolae are small PM invaginations with a diameter of 60-80 nm. The typical protein coat of caveolae is formed by members of two families: caveolins and cavins (Bastiani et al., 2009; Rothberg et al., 1992). Caveolae are enriched for cholesterol, phosphatidylinositol-4, 5-bisphosphate (PIP_2) and sphingolipids, representing a subset of membrane rafts. Although the exact endocytic function of caveolae remains object of debate, several studies have identified common features to all caveolar entry mechanisms: they are dynamin-dependent (Henley et al., 1998), they require the activity of Src kinase and protein kinase C (PKC) and the recruitment of actin (Sharma et al., 2004). The caveolar pathway is involved in endocytosis of several ligands such as Transforming growth factor beta receptor (TGF-βR) (Di Guglielmo et al., 2003) and viruses, like Simian virus 40 (SV40) (Anderson et al., 1996). Beside the implication in NCE it was also postulated that they play a role in cell adhesion, signal transduction and redox signalling, lipid and cholesterol regulation as well as mechanosensing (Sigismund et al., 2012).

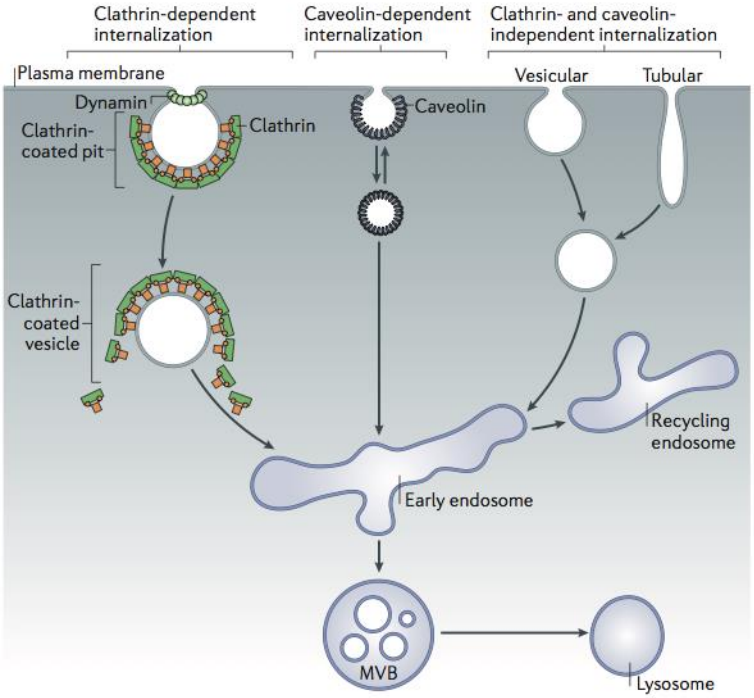

Figure 1: Micropinocytosis in mammalian cells

In mammalian cells exist multiple pathways of micropinocytosis. Clathrin-dependent internalization is dynamin-dependent and characterized by clathrin coated structures. Clathrin-independent pathways include caveolin-dependent endocytosis as well as various pathways with uncoated structures, some of which are vesicular and others are tubular. Internalized cargoes are first trafficked to the early endosomes and then either recycled back to the PM or sorted into multivesicular bodies (MVBs) and lysosomes for degradation [taken from (McMahon & Boucrot, 2011)].

1.1.2.2 CLIC/GEEC pathway

CLICs (clathrin-independent carriers) are uncoated tubular-vesicular structures which originate from the PM (Kirkham et al., 2005). They deliver cargoes to specific endosomes termed GEECs (GPI-AP-enriched early endosomal compartments) and bypass the Rab5 positive endosomal compartment. The CLIC/GEEC pathway is a dynamin-independent cdc42-dependent endocytic route and is the major pathway to internalize fluids, bulk membrane and glycosylphosphatidylinositol-anchored proteins (GPI-APs), for which CLICs/GEECs are selectively enriched (Sabharanjak et al., 2002).

1.2 Endocytic sorting

Once cargoes have entered the cell they are further trafficked to the early endosomes. These organelles serve as a first sorting station, where cargoes are subjected to distinct itineraries. In principle cargoes can have two fates: either recycling back to the PM or degradation in lysosomes, respectively. Small GTPases, mainly of the Rab-familiy, play an important role in sorting steps along the endosomal stations. They act like molecular switches, shifting between a GTP- (guanosine triphosphate) bound active state and a GDP- (guanosine diphosphate) bound inactive form. Cargoes destined for recycling are either shuttled through a fast Rab4-dependent pathway or a slow Rab8/Rab11-dependent recycling route back to the PM (Stenmark, 2009). The small GTPase Arf6 is involved in an additional recycling pathway, which is mainly used by receptors internalized through NCE, such as major histocompatibility complex I (MHCI) (D'Souza-Schorey & Chavrier, 2006).

The transition from early to late endosomes is embodied by a change of structure and composition of the compartments (**Figure 2**). Early endosomes are characterized by a predominantly tubulovesicular structure, the presence of Rab5 and high levels of phosphatidylinositol-3-phosphate (PtdIns3P). Rab5 mediates the transport from CCVs from the PM to the early endosomes and recruits the tethering protein early endosome antigen 1 (EEA1). The formation of small intraluminal vesicles (ILVs) produces morphologically distinct endosomes called multivesicular bodies (MVBs) and marks the transition state from the early to the late endocytic compartment (**Figure 2**). On a molecular basis the maturation from the early to the late endosomes is indicated by the replacement of Rab5 by Rab7 (`Rab-conversion´) and the presence of lysosome-associated membrane protein 1 (LAMP-1) (Stenmark, 2009).

MVBs and late endosomes are capable to fuse with lysosomes where degradation takes place. Ubiquitination is the major signal of cargoes designated for the degradative pathway. Targeting into the lysosomal pathway is facilitated by a conserved machinery

called endosomal sorting complex required for sorting (ESCRT). Four sequentially acting ESCRTs (ESCRT-0, -I, -II and –III) are recruited to early endosomes. These complexes facilitate three distinct but related functions: (i) recognition and clustering of ubiquitinated cargoes in the endosomal membrane; (ii) bending of the limiting membrane and sorting into endosomal invaginations; (iii) formation and scission of the ILVs that contain the sorted cargo (Hanson & Cashikar, 2012) (Further discussed in section 2.1.3.).

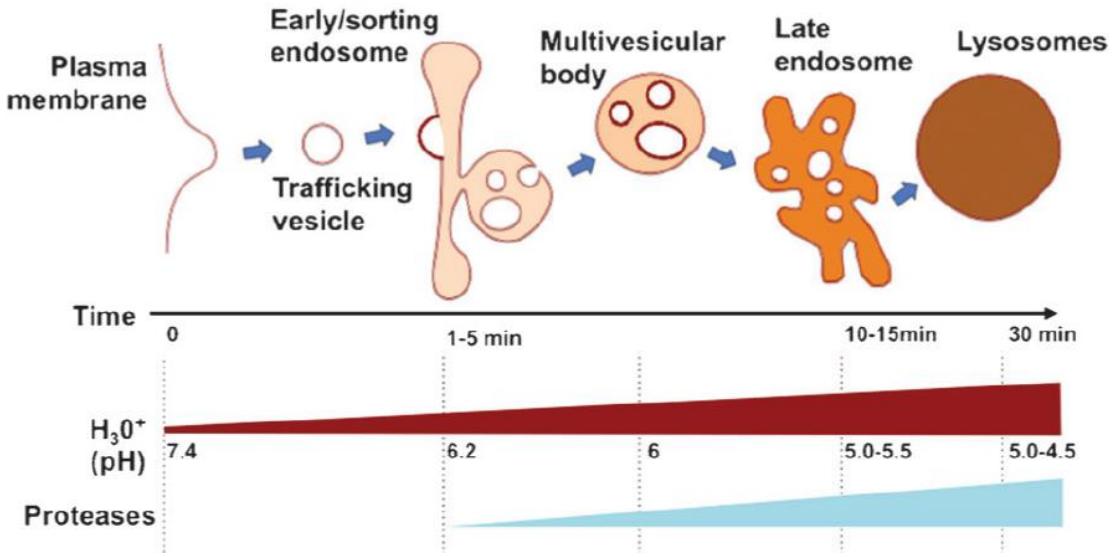

Figure 2: Itinerary of internalized cargoes

After internalization cargoes are subsequently routed in trafficking vesicles to the early/sorting endosomes, where they are further shuttled into MVBs and late endosomes. Finally the degradation of cargoes takes place in lysosomes. The time which it takes approximately to traffic the endocytosed material is plotted alongside the schematic representation of the different endocytic organelles. The internal pH decreases progressively, while the protease concentration increases on the way from early endosomes to lysosomes [taken from (Canton & Battaglia, 2012)].

1.3 Transferrin as a model substrate for CME

Transferrin (Tf) is an iron-binding protein that facilitates the iron uptake in cells. Tf loaded with iron binds to the TfR and is subsequently internalized through receptor-mediated endocytosis. This is one of the best understood biological processes and is undoubtedly clathrin-dependent (Mayle et al., 2012). The internalized complex is shuttled to the early

endocytic compartment where iron is released from Tf due to a decreased pH. Apo-transferrin and the TfR are routed either by a fast recycling pathway directly back to the PM or they are sorted to Rab11-positive recycling endosomes and taken back to the PM by a slow recycling pathway (Grant & Donaldson, 2009). At neutral pH they dissociate and both are ready for another round of iron uptake. Due to these characteristics, Tf is often used as a tool to illuminate the trafficking pathway of other cargoes or as a marker for the CME to investigate different endocytic entry routes or as a recycling marker, respectively.

1.4 Endocytosis and signalling

Endocytosis is the major mechanism to achieve signal attenuation by removing active signalling receptors from the cell surface. However recent studies have demonstrated that the influence of endocytosis on signal transduction is more wide-ranging. Moreover there are increasing evidences that there is a bi-directionality; endocytosis has a great impact on cell signalling, and conversely receptor signalling has an influence on the endocytic machinery (Hupalowska & Miaczynska, 2012).

1.4.1 Endocytosis regulates signalling

Binding of cognate ligands promotes the activation of the signalling cascade downstream of signalling receptors but also their internalization. The main purpose of this process is to diminish the number of receptors at the cell surface, thus downregulate the strength and duration of signalling (**Figure 3a**). Indeed, the long-term stimulation with ligand causes a reduced number of receptors at the cell surface. This negative feedback loop protects cells from excessive signalling (**Figure 3a**). In some cases removal of surface receptors does not correlate with a decrease in signalling but instead shifts the dose-response relationship, meaning that higher ligand concentrations are needed to trigger a signal response of the same magnitude. One example for this mechanism is the migration of cells in response to

soluble ligands. Distinct receptor tyrosine kinases (RTKs) and G protein-coupled receptors (GPCRs) are able to function as motogenic sensors and respond to chemotactic gradients (Dormann & Weijer, 2003). A shift in the dose-response to ligand concentration ensures that cells stop at their target sites, where the concentration of chemotactic factors is highest (Bailly et al., 2000).

Spatial and temporal regulation of signalling can be also achieved through a differential distribution of signalling molecules or specific phospholipids between the PM and the endosomal compartment. For example, GPCR signalling via PM-potassium channels is extinguished by the internalization of the receptor, since it requires the presence of receptors and potassium channels in the same membrane to form an active signalling complex (Mathie, 2007). Analogous is the phospholipase Cγ1 (PLCγ1) and phosphoinositide 3-kinase (PI3K) signalling by EGFR inhibited upon receptor internalization due to low PIP_2-levels in endosomes (Haugh & Meyer, 2002).

Another mechanism whereby endocytosis regulates cell signalling is the choice of the endocytic entry route through which receptors are internalized. The majority of signalling receptors can be internalized through CME as well as NCE. The selection of the internalization route determines the ratio of receptors recycled back to the PM or degraded in lysosomes, thereby controlling the final output in terms of signalling attenuation or prolonged signalling. For instance, TGFβ-receptors that are internalized through CME are recycled back to the PM and signalling is sustained. Inversely, receptors that enter the cell through NCE are ubiquitinated by the E3 ligase Smad ubiquitin regulatory factor (SMURF) resulting in receptor degradation and signal extinction (Di Guglielmo et al., 2003). An analogous regulation was found for the internalization and signalling of the epidermal growth factor receptor (EGFR) (Sigismund et al., 2008) (see also section 3). Other cargoes, like the Wnt3a-activated low-density receptor-related protein 6 (LRP6), use the two different internalization pathways in the opposite way. LRP6 signalling is coupled

with internalization through NCE, whereas the attenuation of signalling by receptor degradation is dependent on CME (Yamamoto et al., 2008).

1.4.2 Signalling regulates endocytosis

Converse events, regulation of the endocytic machinery through signalling, are rather complementary than contradictory. Rearrangements of the endocytic machinery induced by signalling affect the entire endocytic pathway, from vesicle internalization at the PM to the endosomal and lysosomal compartment (**Figure 3b**). It has been shown that stimulation of cells with epidermal growth factor (EGF) and nerve growth factor (NGF) can increase the density of CCPs at the PM. Ligand-induced activation of EGFR recruits CHC to the PM mediated by tyrosine (Tyr) phosphorylation of the CHC through c-Src (Wilde et al., 1999). More recent studies suggest that signalling events can even trigger the formation of `cargo-specialized´ coated pits as already previously mentioned (Johannessen et al., 2006; Puthenveedu & von Zastrow, 2006).

The endocytic machinery is regulated by receptor-mediated signalling also in later steps of the endocytic process. Live cell imaging studies show a decrease in the replacement of Rab5 by Rab7 in maturating endosomes by EGFR signalling (Rink et al., 2005). Thereby transport of receptors destined for degradation is slowed down, as demonstrated for low-density lipoprotein (LDL) (Poteryaev et al., 2010; Rink et al., 2005).

Moreover distinct stress-induced signalling pathways can control endocytosis by modulating specific transcriptional programs. Cell stress activates the transcription factor tumor suppressor gene p53 (TP53), which regulates several genes involved in endocytosis, like charged multivesicular body protein 4C (CHMP4C a subunit of the ESCRT-III complex) or caveolin-1. It has been shown that activation of TP53 leads to internalization and trafficking of caveolin-1 and EGFR to the late endocytic compartment. In this way the suppression of cell growth and division by the TP53 program is achieved through the

regulation of endocytosis (Yu et al., 2009). Another example is given by the regulation of lysosomal activity in response to cellular needs. It was found that numerous lysosomal genes are concomitantly transcribed. Lysosomal stress activates the transcription factor EB (TFEB), which induces the transcription of genes involved in the biogenesis and activation of lysosomes and results in increased protein clearance (Sardiello, Science, 2009).

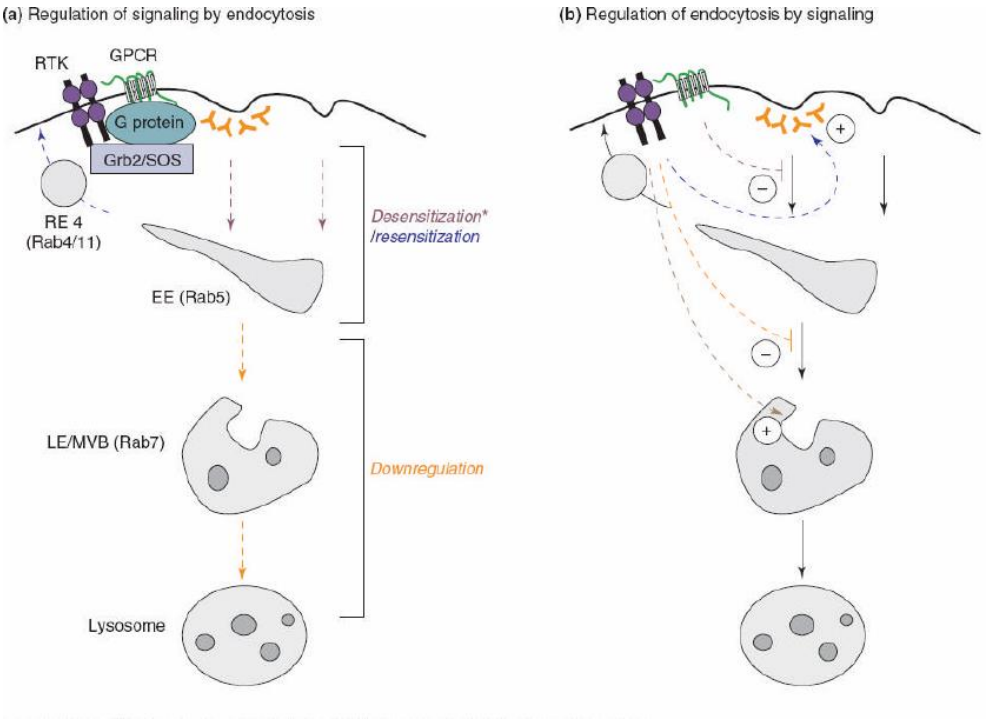

Figure 3: Reciprocal regulation between endocytosis and signalling

a) General regulatory effects of endocytosis on receptor-mediated signalling are depicted, using RTKs and GPCRs as examples. Receptor endocytosis causes attenuation of PM-associated signalling pathways or "desensitization" of cell signalling (violet arrows). The Recycling of receptors to the PM can reverse this process and leads to "resensitization" of cellular responsiveness (blue arrows). Degradation of internalized receptors in lysosomes results in receptor downregulation (orange arrows).
b) Examples of regulatory loops by which signalling regulates the endocytic pathway. EGFR signalling can promote under certain circumstances the formation of CCPs (dotted blue line), the formation of ILVs (dotted brown line) and inhibits the maturation of early to late endosomes (dotted orange line) [taken from (Zastrow & Sorkin, 2007)].

1.4.3 Signalling endosomes

A number of evidences show that signalling events are not only restricted to the PM. The concept of ´signalling endosomes´ derived from biochemical fractionation studies of RTK signalling components and the discovery that activated EGFR as well as several downstream effectors are present in endosomal membranes (Di Guglielmo et al., 1994). In general endosomes are characterized by a couple of features that give them the ability to act as signalling platform: (i) a small volume favours ligand-receptor binding and preserves receptor activity, (ii) slow sorting mechanisms and therefore long resident time, (iii) capacity to use microtubular transport for long distances, (iv) high levels of lipids and proteins which can act as scaffold for signalling platforms (Posor et al., 2014) and (v) a low pH, especially in late endosomes, promoting proteolysis of signalling molecules. Overall there are two known modes of endosomal signalling: either signalling originated from the PM is sustained, or specific signal complexes are assembled which are excluded at the PM or occur only with low efficiency (Sadowski et al., 2009; Scita & Di Fiore, 2010). The ability of a receptor to signal after internalization might be essential to ensure sufficient duration and intensity of signalling. Indeed several RTKs remain bound to the their ligands until late stage of the endosomal trafficking, including the EGFR-EGF complex (Sorkin & Von Zastrow, 2002). Several studies using small interfering RNAs (siRNAs) or dominant-negative mutants of proteins involved in internalization suggest that at least for some RTKs internalization is necessary to fully activate MAPK (mitogen-activated protein kinase) signalling (Lampugnani et al., 2006; Sigismund et al., 2008; Vieira et al., 1996). However this is still an open debate since some similar studies reach the opposite conclusion (DeGraff et al., 1999; Galperin & Sorkin, 2008; Johannessen et al., 2000). These differences reflect the complexity of the mammalian system that often does not permit generalization of concepts.

Endosome-specific signal systems are often based on the enrichment of PtdIns3P in endosomal membranes. One example is provided by the propagation of signalling from the TGFβ-receptor. SMAD2 and SMAD4 are recruited to endosomes by the adaptor proteins SARA (SMAD anchor for receptor activation) and endofilin. Both proteins contain a FYVE domain (Fab1, YotB, Vac1p, EEA1), which binds with high specificity to PtdIns3P. This ensures the efficient phosphorylation of SMAD2 by the internalized TGFβ-receptor and the formation of an active SMAD2-SMAD4 complex (Chen et al., 2007; Tsukazaki et al., 1998). However it has been reported that under certain circumstances TGFβ-receptor internalization is not necessary and SMAD signalling can be initiated already from the PM (Lu et al., 2002).

Taken together the hypothesis that signalling can also occur from endosomes is meanwhile well established in the field (Hupalowska & Miaczynska, 2012). Challenging future investigations will be to understand the physiological significance of signalling endosomes and if they are functionally distinct to signalling events on the PM or simply a spatial and temporal extension.

2 The ubiquitin system

The posttranslational modification of proteins with ubiquitin is in almost all cellular processes involved, including the regulation of endocytosis. Ubiquitin is a highly conserved protein of 76 amino acids, with only three conservative changes from yeast to human. There are four ubiquitin genes in humans whose translation products are fusion proteins. UBB and UBC encode polymeric head-to-tail concatemer of ubiquitin, whereas UBA52 and UB80 encode ribosomal-fused ubiquitin precursors (Lund et al., 1985). Ubiquitin can be covalently attached to proteins by the formation of an isopeptide bond between the carboxy group of its C-terminal glycine (Gly) and the ε-amino group of a

substrate lysine (Lys) residue (Hershko & Ciechanover, 1998). Ubiquitination occurs by the sequential action of three types of enzymes (**Figure 4**). First an ubiquitin-activating enzyme (E1) activates ubiquitin by the formation of a high-energy thiolester bond; this step is ATP-dependent. Then ubiquitin is passed to the active cysteine (Cys) of an ubiquitin-conjugating enzyme (E2) by transthiolation. The final step is accomplished by an ubiquitin ligase (E3) and results in the transfer of ubiquitin to a Lys side chain of the substrate (Komander & Rape, 2012).

Ubiquitin ligases are substrate specific and control the timing of transfer; hence they are the key regulatory determinants in the ubiquitination process (Ardley & Robinson, 2005). The relative high number of more than 600 E3 ubiquitin ligases compared to only around 40 E2s in humans, underscores the role of E3 ligases in substrate selection. There are two main families, the HECT- (Homologous to the E6-AP Carboxyl Terminus) and the RING- (Really Interesting New Gene) E3 ligases, which catalyse the transfer of ubiquitin in a different manner. Members of the HECT family harbour a catalytically active Cys on which ubiquitin is transferred from the E2 and forms a thiolester bond before it is finally conjugated to the substrate. Unlike the HECT-ligases, the RING finger E3s do not possess a catalytic active Cys and do not form any catalytic intermediate with ubiquitin. This class of E3 ligases serve as a scaffold to bring E2 and substrate in close proximity. Different studies suggest that RING finger domains can activate E2s allosterically (Metzger et al., 2014; Ozkan et al., 2005). Members of the RING-type family are functional as monomers, dimers or multi-subunit complexes, while HECT-E3s usually act as monomers. Recently a third group of E3 ubiquitin ligases was established. The RING-between-RING (RBR) family shares common features with both RING- and HECT-E3 ligase families. Similar to HECT-E3s, RBR ligases transfer ubiquitin directly from an intrinsic catalytic active Cys to substrates, but also recruit thiolester-bound E2 enzymes via a RING domain (Spratt et al., 2014). All twelve described RBR ligases are complex multidomain enzymes. The best

studied members are parkin, HOIP (HOIL-1-interacting protein) and HOIL-1 (haem-oxidized IRP2 ubiquitin ligase 1), both of which are components of the multiprotein complex LUBAC (linear ubiquitin chain assembly complex).

Proteins can be either monoubiquitinated or multiple monoubiquitinated by the attachment of several independent ubiquitin molecules. Since ubiquitin itself harbours seven Lys residues also chains of different linkages (Lys6, Lys11, Lys27, Lys29, Lys33, Lys48, Lys63 and linear chains on Methionine1 Met1) can be formed, allowing polyubiquitination of substrates (**Figure 4**). All these linkages have been detected in cells (Peng et al., 2003; Xu et al., 2009). Moreover, chains can be formed by either homotypic or heterotypic linkages. Different types of ubiquitin modifications serve as distinct signals and are associated with different cellular functions (Komander & Rape, 2012). It was demonstrated that substrates modified with four or more Lys48 linked ubiquitin moieties are targeted to the proteasome (Chau et al., 1989). Lys63 linked chains instead are mainly involved in DNA repair, transcriptional regulation, endocytosis and activation of protein kinases (Al-Hakim et al., 2010; Galan & Haguenauer-Tsapis, 1997; Huang & D'Andrea, 2006).

Ubiquitin modifications are recognized by proteins containing ubiquitin-binding domains (UBDs) which bind to ubiquitin in a non-covalent manner. UBDs are generally small stretches of 20 to 150 amino acids and are structurally diverse. More than 20 different UBDs have been identified in numerous proteins from which many exhibit a preference for certain ubiquitin-chains (Husnjak & Dikic, 2012). UBDs show a moderate to weak binding capacity with dissociation constants (Kds) for ubiquitin ranging from 5 to 500 μM. These high-specific, low-affinity interactions create a dynamic network, which can undergo rapid assembly and disassembly. When a higher affinity interaction is required, several possibilities can be envisioned: (i) enhancement by the presence of

several UBD motifs in the same protein, (ii) multimerization of UBD-containing proteins, (iii) secondary binding sites between the ubiquitin receptor and the ubiquitinated target.

Similar to phosphorylation also ubiquitination is a reversible process (**Figure 4**). Ubiquitin molecules can be removed from substrates by the action of deubiquitinating enzymes (DUBs) (see also chapter 2.2).

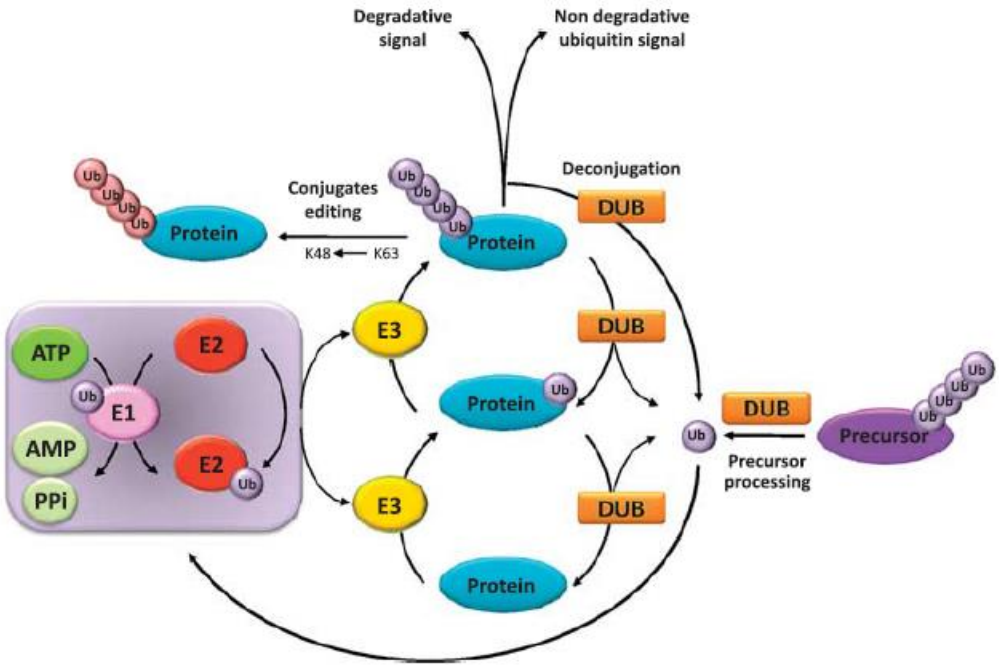

Figure 4: The ubiquitin system

Ubiquitin is conjugated by three sequentially acting enzymes: ubiquitin-activating enzyme E1, ubiquitin-conjugating enzymes E2s and ubiquitin ligases E3s. Substrates can be either monoubiquitinated or polyubiquitinated. Chains with different linkages serve as distinct signals and are involved in certain cellular processes. DUBs are able to remove ubiquitin from substrates and/or edit ubiquitin chains. Thereby DUB activity is necessary to generate free ubiquitin, rescue substrates destined for degradation and to change ubiquitin signals [taken from (Fraile et al., 2012)].

2.1 Ubiquitin in endocytosis

About twenty years ago, studies using the yeast *Saccharomyces cerevisiae* demonstrated that ubiquitin drives the internalization of several PM cargoes, including the mating pheromone a-factor transporter Ste6 (Kolling & Hollenberg, 1994) and the mating

pheromone α-factor Ste2 (Galan & Haguenauer-Tsapis, 1997; Hicke & Riezman, 1996). Experiments with ubiquitin mutants revealed that monoubiquitination is sufficient for Ste2 endocytosis (Terrell et al., 1998). For other PM cargoes instead, like the nutrient transporter Fur4 and general amino-acid permease (Gap1), polyubiquitination with Lys63 chains is essential for further trafficking (Lauwers et al., 2009) and to reach the maximal level of endocytosis (Galan & Haguenauer-Tsapis, 1997; Springael et al., 1999). Indeed, for many yeast membrane proteins, ubiquitination is both necessary and sufficient for endocytosis (Hicke & Riezman, 1996), although ubiquitin-independent endocytosis of cargoes has also been described (Chen & Davis, 2002).

2.1.1 Ubiquitination of cargoes

The role of ubiquitin in endocytosis in mammalian cells is far more complicated. It has been shown that ubiquitination is essential for the internalization of ion channels, like epithelial Na^+ channel (ENaC) (Staub et al., 1997). For many other endocytic cargoes, including RTKs and GPCRs, ubiquitination appears to be sufficient but not essential for their internalization (Haglund et al., 2003; Sigismund et al., 2005). Many of these receptors display ligand-induced modification with ubiquitin, but own also the possibility of ubiquitin-independent internalization. Analogous to the findings in yeast also in mammalian cells plasma membrane proteins are often modified with Lys63 chains, leading to an increased rate of endocytosis and a faster lysosomal transport (Barriere et al., 2007; Barriere et al., 2006). This might be due to a higher binding affinity of many UBDs of endocytic adaptor proteins for polyubiquitin rather than for monoubiquitin (Husnjak & Dikic, 2012).

One difficulty to establish the role of ubiquitin in the endocytosis of plasma membrane proteins is the fact that mammalian cells have several internalization pathways which often act in parallel (Acconcia et al., 2009) (see also chapter 1.1). Different

endocytic routes might have distinct sorting determinants and therefore depend or not on cargo ubiquitination. A critical example is represented by the EGFR and will be discussed in detail in chapter 3.

2.1.2 Ubiquitin and endocytic adaptors

Endocytic adaptor proteins are located at the PM and are thought to select cargoes and initiate the internalization process. Many of them contain UBDs, able to decipher the ubiquitin code from the cell surface. A common theme, the Ubiquitin-interacting motif (UIM) is present in several components of the downstream endocytic machinery, including epidermal growth factor receptor substrate 15 (Eps15), epidermal growth factor receptor substrate 15-like 1 (Eps15L1), Eps15-interacting protein 1 and 2 (Epsin1 and Epsin2) (Polo et al., 2002; van Delft et al., 1997). Eps15 and Epsins have multiple ubiquitin-interacting motifs (UIMs) through which they can bind to ubiquitinated membrane cargoes like the EGFR (Sigismund et al., 2005). Moreover the presence of several protein-protein interaction domains makes endocytic adaptor proteins to scaffolding proteins for the endocytic machinery. Next to ubiquitin via their UIMs, Eps15 and Epsins can bind the CHC and the clathrin adaptor molecule complex AP-2 through the clathrin box and the aspartic acid-proline-tryptophan (DPW) motifs, respectively. This allows the bridging of ubiquitinated cargoes to CCPs (**Figure 5**).

It has been shown that several endocytic adaptor proteins are also target for ubiquitin modifications. Followed by the stimulation of cells with growth factors Eps15, Epsin1 and Epsin2 (Polo et al.., 2002; van Delft et al.., 1997) and Hrs (Katz, Shtiegman et al.. 2002; Polo, Sigismund et al.. 2002) undergo a process that requires the integrity of UIM, and that is referred to as coupled monoubiquitination (Hicke et al., 2005). Several classes of UBDs, such as UIM, UBA (ubiquitin associated), MIU (motif interacting with ubiquitin) and CUE (coupling of ubiquitin conjugation to ERAD) can sustain this process

(Hicke et al., 2005). The phenomenon of coupled monoubiquitination was described for the first time for the UIM domain (Polo et al., 2002; van Delft et al., 1997) and the mechanistic basis for coupled monoubiquitination has been proposed (Fallon et al., 2006; Woelk et al., 2006). For the HECT E3 ligase neural precursor cell expressed developmentally down-regulated protein 4 (NEDD4), coupled monoubiquitination appears to involve self-ubiquitination followed by the interaction of the isopeptide-conjugated ubiquitin of the E3 with the UIM of the substrate (Polo et al., 2002; van Delft et al., 1997). The transfer of the thiolester-linked ubiquitin from the E3 to the substrate concludes the process. In the case of the RING-type ligase Parkin, coupled monoubiquitination requires the interaction of the Ubiquitin-like domain (Ubl) of Parkin with the UBD of the substrate, which is then followed by the transfer of ubiquitin directly from the E2 enzyme to the substrate (Fallon et al., 2006). A variant of the two proposed models that does not require E3 ligases has been suggested. In this model, a UBD-containing protein binds to an E2 enzyme through the interaction of the UBD with ubiquitin linked to E2 via a thiolester bond; then ubiquitin is directly transferred to the Lys residue within the substrate (Hoeller, Crosetto et al.. 2006). This process has been considered constitutive and is not linked to EGF stimulation.

The functional role of adaptor monoubiquitination is still under debate. One hypothesis, based on artificial chimeras, is that monoubiquitination of endocytic adaptors may cause a functional inhibition by facilitating a closed conformation through the intra-molecular binding of the attached ubiquitin to one of the UIMs (Hoeller et al., 2006). Other studies suggest that it serves as signal amplification thus enhancing the progression of ubiquitinated cargoes along the endocytic route (Polo, 2012). Our recent data indicate that Eps15 monoubiquitination is indeed a positive requirement for the EGFR internalization process rather than a negative signal that disassemble the receptor-adaptor complex. Monoubiquitinated Eps15 peaks concomitantly with unmodified Eps15 in gel filtration

analysis (Savio et al., manuscript in preparation) and is able to interact with activated EGFR (Sigismund et al., 2005) or its interactor AP-2 at the same level of unmodified Eps15 (Savio et al., manuscript in preparation). To further investigate the function of Eps15 monoubiquitination, we identified and mutagenized the Lys acceptor sites in Eps15. Interestingly, when tested in a rescue experiment the Eps15 6KR mutant was unable to reconstitute the impaired internalization of the Eps15/Eps15R/Epsin triple knock-down (KD) cells (Savio et al., manuscript in preparation).

2.1.3 Ubiquitin in endosomal sorting

Ubiquitin holds also in later steps of the endocytic pathway a critical regulatory role. Ubiquitinated internalized cargoes are subsequently sorted to the lysosomal endocytic compartment. The ESCRT machinery (see chapter 1.2) plays a major role in the generation of MVBs and in the sorting of ubiquitinated substrates into the ILVs. Numerous proteins of the ESCRT complex contain different UBDs. This equips the ESCRT machinery with the ability to capture and sort ubiquitinated cargoes into the MVB pathway (**Figure 5**). The ESCRT-0 complex is composed by two subunits: Hrs (hepatocyte growth factor-regulated Tyr-kinase substrate) and STAM (signal transducing adaptor molecule). Hrs contains two double-sided UIMs and one VHS (Vps27, Hrs, STAM) domain while STAM has one UIM and one VHS domain. Different studies in yeast and mammalian cells, in which one or several of those UBDs were mutated, could show that they are critical in the recognition and clustering of ubiquitinated cargoes in the membrane of early endosomes (Bilodeau et al., 2002; Raiborg et al., 2002; Ren & Hurley, 2010; Urbe et al., 2003). ESCRT-0 recruits the ESCRT-I complex, which consist of tumour susceptibility gene 101 (TSG101), ubiquitin associated protein 1 (UBAP-1), Vps28 and Vps37 and is capable to recruit the ESCRT-II complex, comprised by one molecule of Vps22 (EAP30) and Vps36 (EAP45) plus two molecules of Vps25 (EAP20) (**Figure 5**). Originally it was thought that the single

complexes act in a sequential manner. Recent studies instead suggest a model in which the ESCRT-0 complex recruits an ESCRT-I-ESCRT-II supercomplex. Multiple subunits of this supercomplex contain UBDs (including TSG101, Vps36 and UBAP-1) and coordinate cooperatively cargo sorting and packaging into subsequently formed buds (Shields & Piper, 2011). Finally the ESCRT-III complex, a dynamic polymer whose stoichiometry is not clearly defined, catalyses the scission of the formed buds and ILVs are released into the lumen of endosomes (Wollert et al., 2009) (**Figure 5**).

In addition there are a number of other ubiquitin-binding proteins present at the early endosomes. Eps15b, an isoform of Eps15 that is associated with Hrs, contains two UIMs. Eps15b is required for efficient lysosomal degradation of endocytosed EGFRs (Roxrud et al., 2008). Moreover GGA (Golgi-localized, gamma ear-containing, Arf-binding) proteins and TOM1 (target of myb1) have been discussed to be alternative members of the ESCRT-0 complex (**Figure 5**). Like the ESCRT-0 complex they contain UBDs as well as clathrin-binding domains allowing sorting of ubiquitinated cargoes in a similar mode (Katoh et al., 2004; Puertollano & Bonifacino, 2004).

One explanation for the array of UBDs in endocytic proteins involved in sorting might be to increase avidity for ubiquitin through multiple interactions. This is supported by the fact that the described UBDs have all low affinity to bind ubiquitin (Haglund & Dikic, 2012), necessary for on-off signalling-mediated events. Low affinity might facilitate the transfer of ubiquitinated cargoes from one ubiquitin-binding protein to another, ensuring the straightforward sorting. Furthermore it has been shown that many UBDs in endocytic proteins preferentially bind to Lys63 polyubiquitin chains (Dikic et al., 2009).

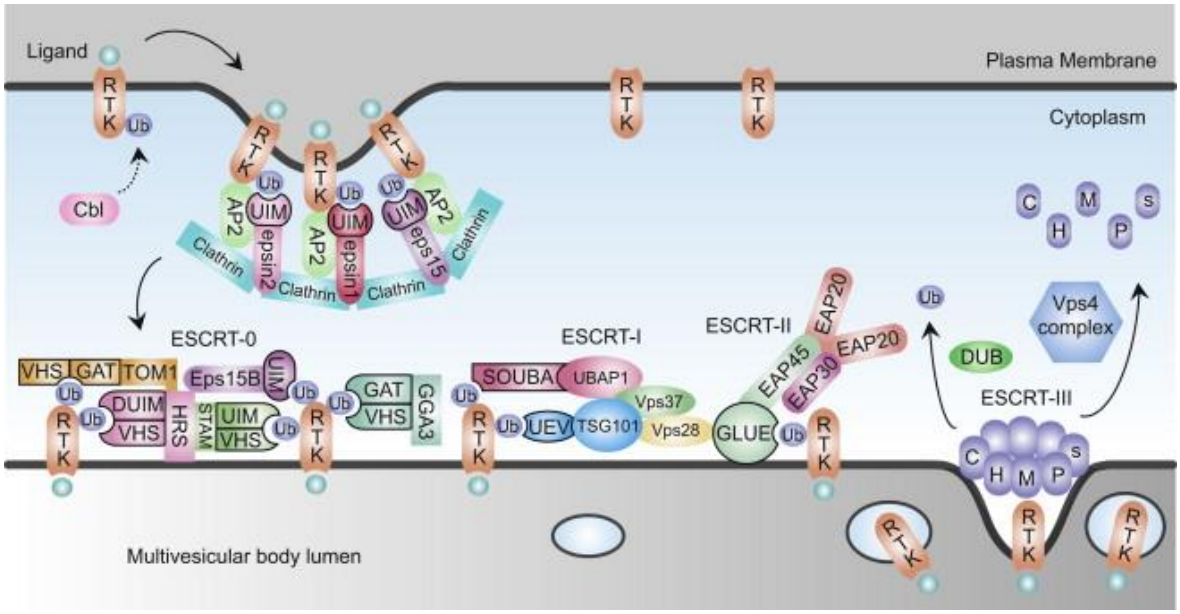

Figure 5: Regulation of RTK endocytosis via ubiquitin

Ubiquitinated receptors are recognized at the PM by UIM-containing proteins, like Eps15, Epsin1 and Epsin2. These adaptor proteins act as linkers and mediate the interaction of receptors with AP-2 and/or clathrin. At the early endocytic compartment ubiquitinated receptors are captured by the ESCRT machinery through multiple interactions with UBD-containing proteins. This ensures the correct sorting of ubiquitinated receptors destined for degradation into ILVs, thereby creating MVBs [taken from (Clague & Urbé, 2012)].

2.2 Deubiquitinating enzymes (DUBs) in endocytosis

Covalently attached ubiquitin can be removed by the action of DUBs. Overall DUB activity is directed to: (i) maintain the free ubiquitin pool, (ii) rescue proteins from ubiquitin-mediated degradation, (iii) control ubiquitin-mediated signalling events (**Figure 4**). The human genome encodes approximately 90 DUBs, predicted to be active. They can be subdivided into five families due to structural homology (**Figure 6**): (1) ubiquitin-specific proteases (USPs), (2) ubiquitin C-terminal hydrolases (UCHs), (3) ovarian tumour proteases (OTUs), (4) Josephins and (5) JAB1/MPN/MOV34 metalloenzymes (JAMMs). It needs to be mentioned that Liang et al. recently found a new domain in the monocyte chemotactic protein-induced protein 1 (MCPIP1) which displays deubiquitinating activity,

suggesting a new group of DUBs (Liang et al., 2010) (**Figure 6**). However, their expression seems to be restricted to bone marrow.

2.2.1 Mechanism of catalysis

DUBs belong to the superfamily of proteases, which are, based on the mechanism of catalysis, divided in aspartic, metallo, serine, threonine, and cysteine proteases. DUBs cover only two of them, metallo and cysteine proteases. The catalytic activity of cysteine protease DUBs depends on two or three critical amino acids, known as catalytic diad or triad, respectively. The pKa of the catalytic active Cys is lowered by a neighbouring histidine side chain. This allows a nucleophilic attack on the isopeptide bond between the C-terminus of ubiquitin and the Lys ε-amino group of the substrate. In some cases a glutamine, glutamate or asparagine residue aligns and polarizes the histidine chain, even though this is not essential for all cysteine proteases (Komander & Barford, 2008). Although cysteine DUBs have a remarkable variability in secondary structure, the catalytic active residues superpose with only minimal aberrations when bound to the C-terminus of ubiquitin (Komander & Barford, 2008). USPs, UCHs, OTUs and Josephins are cysteine proteases while JAMMs are metalloproteases. Generally metalloproteases use a zinc ion (Zn^{2+}) to polarize a water molecule which attacks the isopeptide bond and generates a non-covalent intermediate with the substrate. The metal ion is usually stabilized by an aspartate and two histidine residues. The intermediate is broken down through proton transfer from a water molecule and the DUB is released (Ambroggio et al., 2004).

2.2.2 DUB families

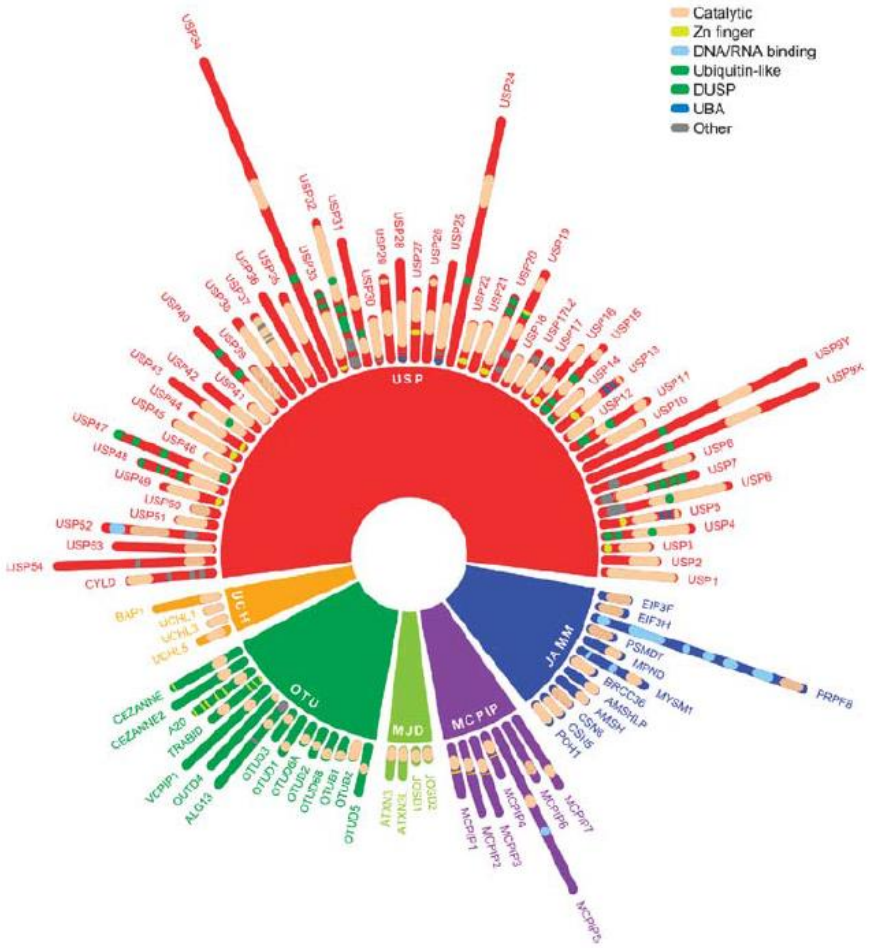

Figure 6: Classification of human DUBs

DUB families are represented by different colours: USPs, UCHs, OTUs, Josephins, JAMMs and MCPIPs. The length of the enzymes and the depicted domains correspond to the size of the protein in amino acids [taken from (Fraile et al., 2012)].

2.2.2.1 The USP family

The USP family is the largest and most diverse family in humans, with more than 50 DUBs. They all have in common a highly conserved and approximately 350 amino acid long USP domain, which harbours the catalytic active core (Clague et al., 2013; Komander et al., 2009). The USP domain consists of three subdomains which resemble the right hand: palm, thumb and fingers. Usually the apo-USP domains are in a non-productive catalytic conformation. Hence, the catalytic activity is regulated by substrate or scaffold-induced conformational changes. In this way the inappropriate cleavage of substrates is prevented (Komander et al., 2009). Many USP domains contain ubl domains which might have

regulatory function, as it was shown for USP4. The ubl in the USP domain of USP4 can bind the catalytic domain and competes with ubiquitinated substrates, thus USP4 activity is partially inhibited (Luna-Vargas et al., 2011). Furthermore, many USPs have large terminal extensions comprising additional domains, which might be important for their activity and for substrate specificity.

2.2.2.2 The UCH family

The UCH family was the first family that was identified (Pickart & Rose, 1985; Rose & Warms, 1983). So far, there are only four DUBs reported belonging to this group (UCHL1, UCHL3, UCHL5/UCH37 and BRCA1 associated protein-1) in humans. Based on *in vitro* enzymatic analyses it was suggested that they are mainly involved in the recycling of ubiquitin and in the co-translational processing of ubiquitin precursors (Larsen et al., 1998). In line with this hypothesis are high expression levels of UCH DUBs in humans and the lack of protein-protein interaction domains.

2.2.2.3 The OTU family

This family was identified due to their homology to the ovarian tumour gene involved in the development of ovaries in fruit flies (Goodrich et al., 2004; Steinhauer et al., 1989). The human genome encodes for sixteen OTU domain DUBs. They are characterized by a diverse ubiquitin chain linkage-specificity, even though the catalytic domain is structurally conserved between the different members (Mevissen et al., 2013).

2.2.2.4 The Josephin family

This family comprises five members and was named after the Machado Joseph Disease (MJD), a spinocerebellar ataxia. MJD is characterized by polyglutamine expansion in the ataxin 3 gene and the formation of cellular aggregates (Matos et al., 2011). The Josephin domain in the N-terminus possesses deubiquitinating activity, while the C-terminus contains two UIMs followed by the polyglutamine sequence and a third UIM (Burnett et

al., 2003). It is currently not known if the pathology of MJD is based on the depletion of this enzymatic activity.

2.2.2.5 The JAMM family

This family consists of twelve members that belong to the class of metalloproteases as above described. DUBs of this group are often found in huge protein complexes, like the ESCRT-machinery associated DUB AMSH (associated molecule with the SH3 domain of STAM) (McCullough et al., 2006) or the 26S proteasome-associated POH1 (also known as Rpn11) (Yao & Cohen, 2002).

2.2.3 DUB activity in early steps of endocytosis

DUBs represent an important group of regulatory enzymes controlling ubiquitin homeostasis. Hence DUB activity might be required in all ubiquitin-dependent steps in endocytosis discussed in chapter 2.1.

Systematic mutagenesis studies in yeast revealed that DUBs are functionally redundant (Amerik et al., 2000) and only a few with specific substrates have been identified so far. However, it has been shown that the DUB fat facets (faf) in *Drosophila melanogaster* regulates endocytosis by deubiquitinating the Epsin homologue liquid facets (lqf). The first indication came from genetic studies in which mutations in lqf were found to be dominant enhancers of the eye developmental defect observed in faf mutants (Cadavid et al., 2000). Subsequent biochemical studies examined that faf and lqf physically interact and ubiquitinated lqf is only detected when faf activity is impaired (Chen et al., 2002). Taken together these studies suggest that faf opposes the ubiquitin mediated proteasomal degradation of lqf in *D. melanogaster*. The relationship between the homologues of lqf (Epsin1) and faf (USP9X) is conserved also in mammalian cells. However, there might be some functional divergences since Epsin1 in humans is not a proteasomal substrate and is found to be monoubiquitinated instead of polyubiquitinated

(Polo et al., 2002; Oldham et al., 2002). Further studies could show that loss of Epsin1 monoubiquitination was prevented by depletion of USP9X in neuronal cells (Chen et al., 2003). Also recent data from our lab demonstrate that USP9X activity is critical for the monoubiquitination of endocytic adaptor proteins. Depletion of USP9X causes decreased ubiquitination levels of Eps15 and Epsins which in turn severely affects EGFR turnover, internalization and trafficking towards the lysosomes (Savio et al., manuscript in preparation).

There might be other DUBs regulating the internalization and endocytic trafficking of specific cargoes at the PM. For example GPCRs associate with β-arrestin adaptor proteins and both proteins are ubiquitinated before internalization. It has been shown that there is a correlation between the rate of recycled GPCR and the ubiquitination status of β-arrestin (Shenoy & Lefkowitz, 2003). USP33 can deubiquitinate GPCR as well as β-arrestin leading to fast recycling and stabilization of the GPCR-β-arrestin signalling complex (Shenoy et al., 2009).

2.2.4 DUB activity in later steps of endocytosis

The two so far best characterized DUBs involved in endocytosis and endosomal sorting are USP8 and AMSH. They are both localized at early endosomes, mediated by the interaction with STAM a member of the ESCRT-0 complex. Both enzymes share a binding site on STAM through a non-canonical Src homology 3 (SH3) binding motif (Kaneko et al., 2003; Kato et al., 2000; McCullough et al., 2006). Furthermore they possess a microtubule interacting and trafficking (MIT) domain that facilitates the interaction with members of the ESCRT-III complex (Hurley & Yang, 2008).

USP8 presumably exhibits multiple effects in the endocytic pathway, explaining the discrepancies found in literature. Two studies based on siRNA-mediated USP8 downregulation, showed that depletion of USP8 causes decreased degradation and

accumulation of ubiquitinated receptors on aberrantly enlarged early endosomes (Bowers et al., 2006; Row et al., 2006). Additionally it was found that the cellular levels of ESCRT-0 proteins are dramatically decreased under USP8 KD conditions, suggesting that USP8 activity is required to prevent Hrs and STAM from proteasomal degradation (Row et al., 2007). Both phenotypes could be rescued by the ectopic expression of GFP-tagged USP8, but not by catalytic inactive or MIT-domain mutant constructs (Row et al., 2007). A possible role of USP8 in sorting ubiquitinated receptors to lysosomal degradation is supported by the observation that USP8 not only deubiquitinates mono-ubiquitinated EGFR but can process also Lys48 and Lys63 chains (Row et al., 2006). In contrast with these studies is the observation of significantly reduced EGFR levels in conditional USP8 KD mice. Similar to transient depletion also in USP8 KD mice ESCRT-0 protein levels are decreased (Niendorf et al., 2007), suggesting a role for USP8 in the regulation of the endocytic machinery rather than targeting receptors directly. One explanation for these conflicting results might be a different level of depletion. Mizuno and colleagues proposed in their first study that KD of USP8 enhances EGFR degradation (Mizuno et al., 2005). In a subsequent second study instead they found that a more complete depletion blocks degradation and induces endosomal clustering (Mizuno et al., 2006), validating previous observations from other groups (Bowers et al., 2006; Row et al., 2006). A more recent publication instead reflated the hypothesis that USP8 KD enhances EGFR degradation via an Hrs-dependent pathway (Berlin et al., 2010). Altogether the function of USP8 in regulating receptors fate is still under debate.

The second in literature extensively discussed DUB involved in endosomal trafficking is AMSH, a member of the JAMM domain metalloprotease family. AMSH is deeply embedded in the endocytic machinery and interacts with several members of the ESCRT-complexes as well as with clathrin. The direct interaction with clathrin is crucial for the endosomal localization of AMSH (Nakamura et al., 2006). As many endocytic

proteins AMSH harbours a UIM domain to capture ubiquitinated substrates. AMSH was the first DUB for which a specificity for ubiquitin linkages was described. In vitro studies revealed that AMSH preferentially cleaves Lys63 chains (McCullough et al., 2006), the predominant form of receptor ubiquitination in the lysosomal pathway. Overexpression of a catalytic inactive mutant, supposed to work as `substrate trap`, leads to the accumulation of ubiquitin on endosomes, while KD of AMSH has no effect on total ubiquitin levels in cells (McCullough et al., 2004). Furthermore it has been shown that depletion of AMSH accelerates EGFR trafficking to lysosomes (Bowers et al., 2006; McCullough et al., 2004). Taken together this supports a basic model in which sorting of ubiquitinated receptors to lysosomes is dependent on the balance of E3 ligase and DUB activity. The principle of negative regulation of receptor degradation via DUB activity was also found for other membrane receptors. To give one example, siRNA mediated KD of USP10 in human airway epithelial cells accelerates the degradation of cystic fibrosis transmembrane conductance regulator (CFTR), while overexpression of wild-type USP10 promotes its endocytic recycling (Bomberger et al., 2010). Analogous to USP8 also USP10 is known to exert an indirect effect on receptor trafficking by regulating proteins of the sorting machinery. Overexpression of USP10 causes increased membrane levels of ENaC. This is due to USP10 activity which rescues a positive regulator of endosomal recycling, sorting nexin 3 (SNX3), from proteasomal degradation (Boulkroun et al., 2008).

The family of DUBs important in the endocytic process is still increasing. Recently, USP6 was found to specifically regulate the internalization and trafficking of cargoes entering cells through NCE (Funakoshi et al., 2014). USP6 also known as TRE17 was previously identified as an oncogene, even though the molecular mechanism and substrates involved in oncogenesis are not identified yet (Nakamura et al., 1992). It is known that USP6 localizes at endosomal membranes through its interaction with Arf6, a small GTPase involved in the recycling of NCE cargoes (Martinu et al., 2004). Funakoshi

et al. revealed that USP6 specifically counteracts membrane-associated RING-CH (MARCH) E3 ligases dependent ubiquitination of NCE cargoes, including CD44, CD98 and MHCI. They suggest that USP6 activity facilitates recycling of NCE cargoes back to the PM thereby increasing surface levels of CD44, CD98 and MHCI (Funakoshi et al., 2014).

2.2.5 DUB activity in the secretory pathway

Membrane proteins are synthesized and folded in the endoplasmic reticulum (ER), sorted into coat protein complex II (COPII) vesicles and shuttled to the Golgi complex. In contrast to the endocytic pathway ubiquitin is not directly involved in the sorting and trafficking of cargoes. However it is described that subunits of the secretory machinery are regulated via ubiquitin. Studies in *S. cerevisiae* could show that the yeast DUB Ubp3 forms an active deubiquitinating complex with Bre5, able to rescue the COPII subunit Sec23b and β´-COP (a COPI subunit) from proteasomal degradation (Cohen et al., 2003a; Cohen et al., 2003b). This ensures cellular homeostasis by the maintenance of an efficient secretory pathway. *In vitro* studies revealed that also the human homologues USP10 and G3BP (Ras-GTPase-activating protein SH3 domain-binding protein) are together in a complex (Soncini et al., 2001), suggesting that the functional relationship of a specific USP-type DUB and the protein transport between the ER and Golgi seems to be evolutionary conserved.

The most prominent role for ubiquitin in the secretory pathway is the quality control for protein folding in the ER. Misfolded luminal or integral membrane proteins are selected for ER-associated degradation (ERAD) (Ruggiano et al., 2014). Once detected, misfolded proteins are retrotranslocated from the ER to the cytoplasm and subjected to proteasomal degradation. In this process ERAD substrates are polyubiquitinated by E3 ligases such as Hrd1. Ubiquitinated proteins are recognized by the UBDs of ubiquitin

regulatory X (UBX) proteins, which recruit the AAA ATPase p97 (also known as VCP), whose activity is essential for the retrotranslocation. Therefore ubiquitination in this pathway is a recognition signal to recruit the driving force p97 rather than a determinant for sorting and trafficking (Lemus & Goder, 2014). In the last years several DUBs have been described to play a role in ERAD. USP19 is anchored in the ER membrane and involved in the unfolded protein response. It has been shown that USP19 can rescue two typical ERAD substrates, CFTRΔF508 as well as the T-cell receptor alpha (TCRα) from proteasomal degradation (Hassink et al., 2009). An array of DUBs have been described to interact with p97 or other components of the ERAD machinery, including, YOD1, VCPIP1, ataxin 3 and USP13 (Liu & Ye, 2012). The degree of redundancy of this p97-associated DUBs remains an open question.

3 The EGFR system

The EGFR, a receptor tyrosine kinase, is known to be a key regulator of normal cell growth and differentiation (Ullrich & Schlessinger, 1990); its aberrant activity is often associated with pathological processes (Roskoski, 2014a). The EGFR is the best characterized member of the ErbB-family, composed by EGFR/ErbB1, ErbB2, ErbB3 and ErbB4 (Carpenter, 2003; Citri et al., 2003). They all possess a similar structure that is composed by: a glycosylated extracellular N-terminal part containing a ligand-binding domain and a dimerization arm, a short hydrophobic transmembrane region, and an intracellular part harbouring the protein tyrosine kinase domain and a C-terminal regulatory region (Roskoski, 2014b). This structure enables signal transduction across the PM and the induction of distinct cellular responses (**Figure 7**).

3.1 Ligand-induced EGFR signal transduction

So far seven EGFR ligands have been identified to activate the receptor by binding to the extracellular domain, namely EGF, transforming growth factor alpha (TGFα), heparin-binding EGF-like growth factor (HB-EGF), amphiregulin, β-cellulin, epiregulin and epigen (Higashiyama et al., 1992; Massague, 1990; Shoyab et al., 1988; Strachan et al., 2001; Toyoda et al., 1995). One characteristic is a consensus sequence consisting of six spatially conserved Cys residues, known as the EGF motif. All ligands are type I transmembrane proteins which in order to be released are cleaved by cell surface proteases (Yarden, 2001). Binding of EGF to EGFR has been proposed to induce a conformational change exposing the dimerization arm and shifts the monomer-dimer equilibrium to the dimeric state (Ogiso et al., 2002). Subsequently the intrinsic tyrosine kinase domain is activated and key Tyr residues within the C-terminal region become phosphorylated and serve as specific docking sites. This promotes the recruitment of phosphotyrosine binding proteins thereby initiating several signalling pathways (**Figure** 7), including:

(1) the Ras/Raf/MAPK pathway; mediated by the adaptors growth factor receptor-bound protein (Grb2) and Shc (Cooper et al., 1984),

(2) the PI3K pathway acting through the kinase Akt and the transcription factor nuclear factor κB (NF-κB); mediated by the adaptors Grb2 and Grb2-associated binder 1 (Bjorge et al., 1990),

(3) the PLC-γ pathway and the downstream calcium- and PKC-mediated cascades (Meisenhelder et al., 1989)

(4) and the signal transducers and activators of transcription (STAT) pathway.

Since all these pathways are involved in cellular key programmes like survival, proliferation, differentiation and migration, EGFR signalling has to be tightly regulated. The major negative feedback regulation is the downmodulation of the receptor via endocytosis.

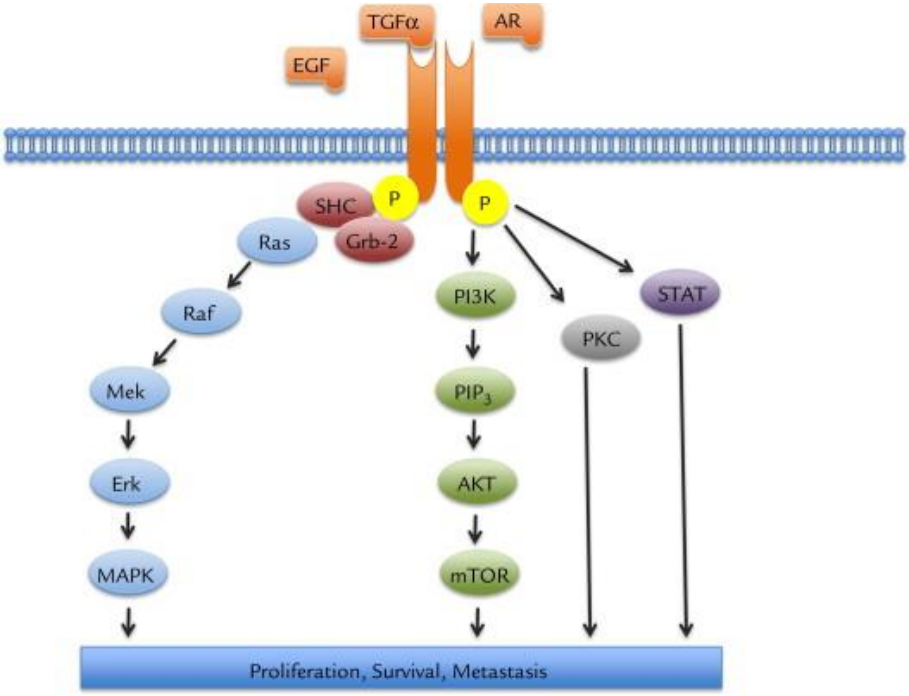

Figure 7: Schematic representation of the major EGFR signalling pathways

EGFR is activated upon binding of its cognate ligands, leading to dimerization, trans-phosphorylation and activation of signalling pathways. Key signalling molecules of the major EGFR signalling pathways are depicted [taken from (Goffin & Zbuk, 2013)].

3.2 EGFR endocytosis and trafficking

Activation of EGFR through binding of a cognate ligand activates signalling but also accelerates receptor endocytosis. EGFR can be internalized through both CME and NCE pathway (Sigismund et al., 2005) (**Figure 8**). The distribution of the receptor into these two entry routes has a major impact on the final fate of the EGFR and is mainly regulated by ligand concentration (Sigismund et al., 2008). CME is characterized by high internalization rates of EGFR and is already observed at low ligand concentrations (≤1-2 ng/ml). The rate of EGFR uptake decreases with increasing EGF concentrations, as NCE becomes active (Sigismund et al., 2013). There was a long-standing debate regarding the "physiological" concentrations of EGF, since there was a historical erroneous perception that only low doses of EGF are physiological. However, it is known that, while plasma EGF concentrations are around 1 ng/ml (Hayashi & Sakamoto, 1988), EGF levels in serum

as well as in distinct body fluids and organs are significantly higher (Oka & Orth, 1983; Westergaard et al., 1990). Therefore cells are exposed to a wide range of EGF ligand concentrations, ranging from a few to a few hundred ng/ml.

As already mentioned it has been shown that ligand concentrations can affect the choice of entry route (Sigismund et al., 2005). While at low doses of EGF (<3 ng/ml), receptors undergo exclusively CME, it was demonstrated by Sigismund et al. that at higher ligand concentrations (10-100 ng/ml) a substantial fraction of EGFR (~40%) is internalized via a clathrin-independent pathway (Sigismund et al., 2005). EGFRs internalized through CME are mostly recycled back to the plasma membrane and therefore signalling is sustained (**Figure 8**). By contrast, EGFRs entering cells through NCE are preferentially targeted to lysosomal degradation and signalling is attenuated (Sigismund et al., 2008). These results suggest that different internalization pathways evolved to deal with the huge variety of physiological EGF concentrations. This mechanism facilitates the maximization of the stimulation efficiency at low ligand concentrations by protecting receptors from degradation. On the other hand cells are protected from overstimulation by directing receptors to lysosomal degradation at high EGF concentrations (Sigismund et al., 2008). However, it has been shown that not all cell types act in this way, thus the presence and significance of the NCE pathway to internalize EGFR clearly depends on the cellular context (Kazazic et al., 2006; Sigismund et al., 2013).

3.3 Role of ubiquitin in EGFR endocytosis

Casitas B-lineage lymphoma c (c-Cbl) was found to be the major E3 ligase for many RTKs including the EGFR (Levkowitz et al., 1999; Levkowitz et al., 1998). Upon stimulation with growth factors c-Cbl is recruited to the PM and can bind either directly to the regulatory region of EGFR (Tyr1045-P) or indirectly through the interaction with the adaptor protein Grb2 (**Figure 8**). Mass spectrometry analysis examined that the kinase

domain of EGFR is mainly monoubiquitinated (~49% of the modified receptor) but also polyubiquitinated with Lys63 linked chains (~40%) (Huang et al., 2006). It is well established that ubiquitination is essential to target EGFR for lysosomal degradation (Haglund & Dikic, 2012; Huang et al., 2013) (see also chapter 2.1). The role of receptor ubiquitination in early endocytic steps instead is more complex and still not fully understood. This might be also due to the presence of multiple internalization pathways with different requirements. Indeed, it has been shown that EGFR ubiquitination is essential for NCE, while it is dispensable in clathrin-dependent endocytosis (Huang et al., 2007; Sigismund et al., 2005).

A recent study describes the molecular mechanism that regulates the transition from CME- to NCE-mediated EGFR endocytosis, by demonstrating that ubiquitination of EGFR at the PM is threshold controlled (Sigismund et al., 2013). Upon stimulation with growth factors EGFR becomes phosphorylated at distinct Tyr residues. This permits the cooperative binding of the E3 ligase c-Cbl, in complex with Grb2, at two specific EGFR phosphorylation sites (Tyr1068 and Tyr1086) or directly to pTyr1048. Increasing concentrations of EGF results in a higher probability of EGFR being simultaneously phosphorylated at Tyr1048 and one of the two other critical pTyr residues (Tyr1068 and Tyr1086), on the same EGFR moiety (**Figure 8**). Efficient recruitment of c-Cbl induces EGFR ubiquitination, thus being the major signal for lysosomal degradation and triggers the internalization via NCE (Sigismund et al., 2013).

The requirement of receptor ubiquitination for the initial steps of CME is rather controversial (Haglund & Dikic, 2012). The first indication that ubiquitination is dispensable for this pathway came from an EGFR mutant that lacks Tyr1045 and is therefore only weakly ubiquitinated. It has been shown that this mutant undergoes normal internalization via CME (Jiang & Sorkin, 2003). This is supported by further studies in which mutation of the three sites for Cbl binding (Sigismund et al., 2013) or the major

ubiquitination sites (16KR EGFR mutant) do not affect EGFR CME (Huang et al., 2007; Huang et al., 2006). Interestingly, the 16KR EGFR mutant still depends on the presence of c-Cbl for its internalization via CME. This might be due to a possible function of c-Cbl as adaptor protein or to the ubiquitination of other endocytic components of the clathrin machinery.

A recent study suggests that clathrin-dependent internalization of EGFR is regulated through multiple mechanisms (Goh et al., 2010). This is based on the observation of impaired internalization of EGFR mutated in 21 Lys residues known to be major sites of protein interactions or posttranslational modifications, respectively. Goh et al. propose that EGFR internalization is collectively regulated through ubiquitination of Lys residues in the kinase domain of EGFR, acetylation of Lys residues in the C-terminus and by the interaction with AP-2 or with the adaptor protein Grb2, respectively. All those mechanisms are thought to be redundant and their importance might vary depending on cell type and experimental conditions (Goh et al., 2010).

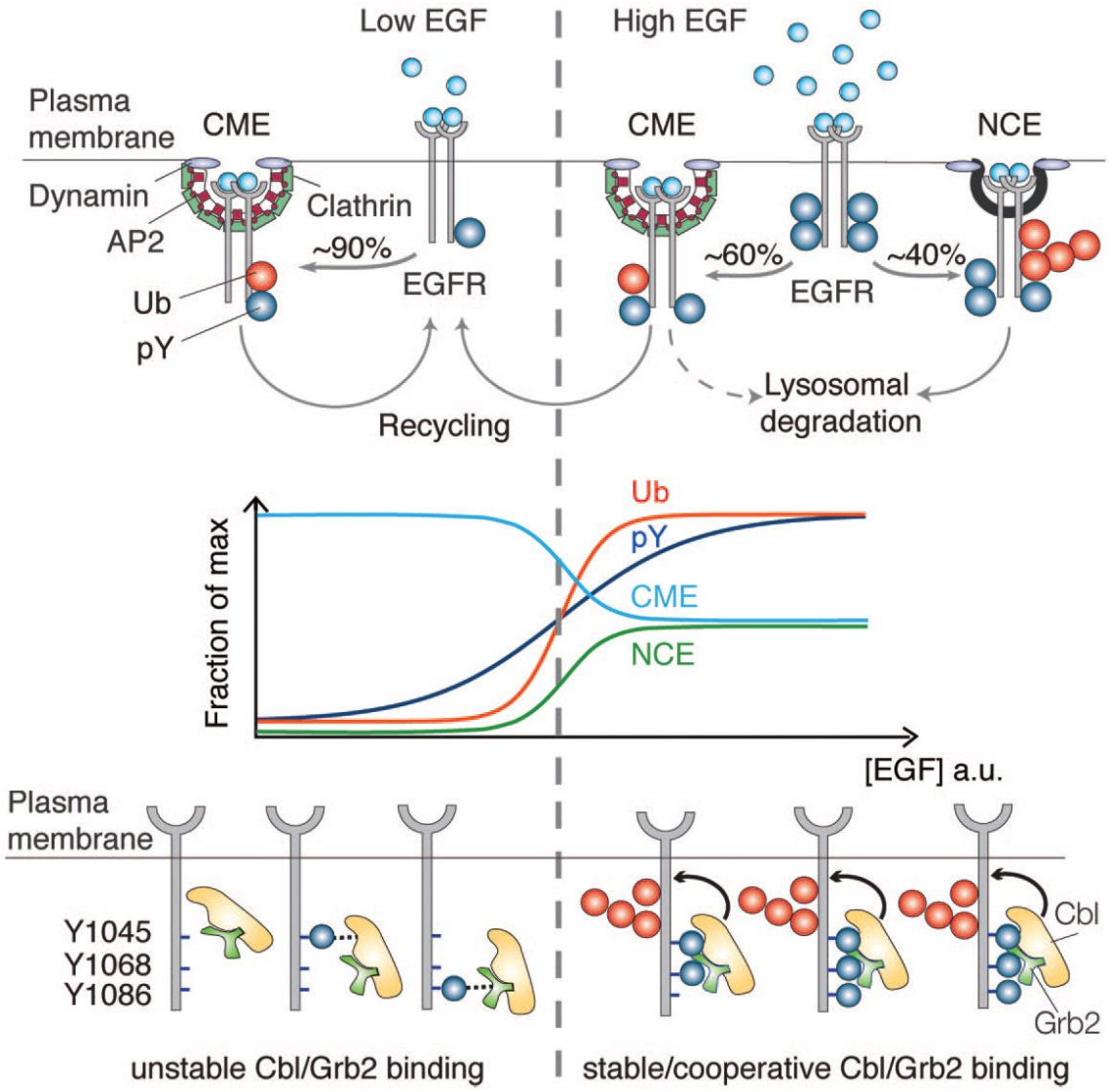

Figure 8: Ubiquitin regulates EGFR endocytosis

Depending on EGF concentration EGFR undergoes clathrin-dependent or clathrin-independent internalization. CME targets receptors predominantly to recycling and sustains the EGFR signalling capacity, while EGFR internalization via NCE is mostly associated with receptor degradation in the presence of high ligand concentrations. Middle: schematic representation of EGFR ubiquitination (Ub), phosphorylation (pY) and endocytic routes as a function of ligand concentration. Bottom: cooperativity mechanism responsible for the EGFR–Ub threshold. Three phosphotyrosines are critical for the cooperative recruitment of c-Cbl to active EGFR: pY1045 binds directly to c-Cbl, pY1068/pY1086 bind indirectly to c-Cbl:Grb2 complex [taken from (Polo et al., 2014)].

3.4 Role of DUBs in EGFR endocytosis

The two best studied DUBs involved in EGFR endocytosis are AMSH and USP8 (already described in chapter 2.2.4.). However the knowledge about the impact of DUBs in EGFR endocytosis was emerging in recent years. Cezanne-1 (also known as OTUD7B), a Lys11 chain specific DUB of the OTU family (Mevissen et al., 2013), was described to oppose EGFR degradation thus enhancing receptor signalling (Pareja et al., 2012). Cezanne-1 was found to be frequently amplified in breast cancer patients suggesting a role in tumour progression (Pareja et al., 2012). Analogous to these findings, it was reported that USP2a opposes EGFR degradation and co-localizes with EGFR at early endosomes (Liu et al., 2013). Overexpression of USP2a but not the catalytic inactive mutant caused a decrease in EGFR ubiquitination and prolonged downstream signalling. Depletion of USP2a displayed the reverse phenotype. Furthermore USP2a and EGFR were found to be concomitantly overexpressed in non-small cell lung cancers (NSCLC) (Liu et al., 2013). Recently, USP17 expanded the group of DUBs controlling EGFR endocytosis (Jaworski et al., 2014). It was reported that USP17 is essential for the internalization of EGFR and TfR via CME, and that the expression of USP17 is induced upon EGF stimulation. De la Vega et al. suggested that USP17 might play a general role in clathrin-dependent receptor endocytosis, presumably by regulating essential components of the endocytic machinery (Jaworski et al., 2014). USP18 instead was found in a siRNA screen to regulate EGFR expression on a translational level (Duex &Sorkin, 2009). Downregulation of USP18 leads to reduced translation of EGFR mRNA, while other RTKs are unaffected. Overexpression of USP18 shows the reverse phenotype. In a second study Duex et al. revealed that USP18 is a negative regulator of the microRNA miR7. Depletion of USP18 upregulates miR7, which in turn inhibits EGFR expression (Duex et al.., 2011).

4 USP25

USP25 belongs to the USP family of DUBs. It was first identified in 1999 in one of the lowest gene-density regions of the human genome (Valero et al., 1999). Since USP25 is located on the 21q chromosome it seems plausible to be involved in phenotypes of the Down's syndrome. Indeed, in average a 1.7-fold overexpression of USP25 was observed in trisomic versus disomic samples (Valero et al., 2001). However, due to the lack of detailed studies, the putative contribution of USP25 to the Down's syndrome phenotype remains so far unravelled.

Northern blot analyses proved that USP25 is ubiquitously expressed in human tissues at a basal level (Valero et al., 1999). There are three alternatively spliced isoforms of USP25 (Valero et al., 2001). The shortest USP-isoform (USP25a; 122kDa) misses exon 19 and was found to be expressed in all analysed tissues. The second isoform USP25b (126 kDa) contains exon 19b and displays low expression levels in all tissues detected except muscle and heart. USP25m (130 kDa) is the longest isoform comprising the whole exon 19 and is specifically expressed in heart and skeletal muscle (Valero et al., 2001). USP25 shares the same exon intron structure with USP28 and their nucleotide and amino acid identities are 56% and 51%, respectively, suggesting that they evolved from a common ancestor (Valero et al., 2001).

USP25 possesses three UBDs at the N-terminus, one UBA and two UIMs, which can bind ubiquitin in a non-covalent manner (**Figure 9**). Furthermore, a SUMO interaction domain (SIM) was found between the UBA domain and the first UIM (Meulmeester et al., 2008). As all DUBs of the USP-type USP25 has a USP domain, containing the catalytic triad, followed by a coiled coil domain, which also seems to be necessary for the catalytic activity (Denuc et al., 2009). Typically for USP-type DUBs, USP25 has no chain linkage-specificity and can cleave both Lys63 and Lys48 linked chains *in vitro* and *in vivo* (Zhong et al., 2013b).

Figure 9: Domain structure of USP25

USP25 has three UBDs at the N-terminus, one ubiquitin-associated (UBA) domain and two ubiquitin-interacting motifs (UIMs). A SUMO-interacting motif (SIM) is located between the first two UBDs. The catalytic core domain (USP) harbours the catalytic active Cys and is followed by a coiled coil region.

In recent years several functions and targets of USP25 emerged. For instance, the heart and muscle specific isoform USP25m was found to be upregulated during myogenesis (Bosch-Comas et al., 2006). USP25m interacts with three sarcomeric proteins involved in muscle differentiation and maintenance: actin alpha-1, filamin C and myosin binding protein C1 (MyBPC1). Overexpression of USP25m, but not other USP25 isoforms, rescues MyBPC1 from proteasomal degradation (Bosch-Comas et al., 2006).

It was reported that USP25 interacts with the E3 ligase Hrd1 as well as with the AAA ATPase VCP/p97, both known to be involved in the ERAD pathway (Blount et al., 2012). Overexpression of USP25 caused higher steady state levels of typical ERAD substrates, like CD3δ, a transmembrane subunit of the T cell receptor, and β-Amyloid Precursor Protein (APP). This depends on the catalytic activity and the UBDs of USP25, suggesting that USP25 is able to rescue ERAD substrates from proteasomal degradation by counteracting the E3 ligase Hrd1 (Blount et al., 2012).

USP25 is a target of several posttranslational modifications, regulating USP25 activity and expression levels. Phosphorylation of USP25 by the non-receptor tyrosine kinase SYK leads to decreased cellular levels of USP25 in a proteasome independent way (Cholay et al., 2010). This might be an additional level of regulation, since USP25 was

found by a high-throughput study for protein stability in HEK293T cells to be a target for proteasomal degradation (Yen et al., 2008).

An elegant publication of the Melchior lab describes USP25 as an interaction partner and target for SUMO2/3 (Meulmeester et al., 2008). They identified a SIM at the N-terminus that is essential for the specific binding of USP25 to SUMO2/3. Interestingly, USP25 is also a substrate for SUMO2/3 modifications at two Lys residues located within the first UIM (Lys99) or close to the second UIM (Lys141). Sumoylation of USP25 does not alter its catalytic activity, since ubiquitin-AMC can be still processed. However, modification with SUMO2/3 impaired ubiquitin binding and therefore the hydrolysis of ubiquitin chains was affected (Meulmeester et al., 2008). This might be provoked by a direct inhibition of the UBDs through the modification of the two Lys residues with SUMO2/3. Alternatively the SIM-SUMO interaction might cause a conformational change and consequently UBDs are inaccessible for ubiquitin chain binding. Lys99 was described to be a target for monoubiquitination as well. In contrast to sumoylation it was suggested that ubiquitination activates USP25, since a USP25 Lys99 mutant possess a decreased ability to rescue the specific substrate MyBPC1 from proteasomal degradation (Denuc et al., 2009).

Recently USP25 activity was connected to NF-κB signalling by different groups (Zhong et al., 2012; Zhong et al., 2013a; Zhong et al., 2013b). It has been shown that USP25 is a negative regulator of interleukin17-mediated signalling and inflammation by targeting TRAF5 and TRAF6 modified with Lys63 linked chains (Zhong et al., 2012). In a subsequent study Zhong and colleagues revealed a role for USP25 in Toll-like receptor (TLR) signalling and innate immunity, to specifically reverse the Lys48 chains on TRAF3 (Zhong et al., 2013a). Finally, it was reported that USP25 is a negative regulator of the virus-triggered type I interferon signalling pathway (Zhong et al., 2013b).

There is increasing evidence that USP25 might be also involved in oncogenesis. USP25 was found to be more than threefold overexpressed in breast cancer tissue in respect to normal adjacent tissue (Deng et al., 2007). Moreover, USP25 is implicated in the epithelial to mesenchymal transition (EMT) in NSCLC. Li and colleagues demonstrated that USP25 is a downstream target of miR-200c (Li et al., 2014). The expression of miR-200c negatively correlates with the clinical stage of lymph node metastasis in NSCLC patients, while overexpression of miR-200c inhibits migration, invasion and EMT *in vitro* and lung metastasis formation in mice. Furthermore, USP25 was found to be upregulated in NSCLC patients, correlating with clinical stage and lymphatic node metastasis. Taken together this suggests that expression of miR-200c has a tumour suppressive effect in NSCLC by downregulating USP25 mRNA levels (Li et al., 2014).

5 Cullin 3

5.1 Structure and regulation of Cullins

Cullins are multimeric protein complexes, which exert ubiquitin E3 ligase activity. They are composed by a Cullin scaffold protein that bridges a RING E3 ligase bound at the C-terminal domain (CTD), and a substrate adaptor bound at the N-terminal domain (NTD) (**Figure 10**). Two RING ligases (RBX1 and RBX2) are known to interact with the seven Cullin scaffold proteins (CUL1, CUL2, CUL3, CUL4a, CUL4b, CUL5, CUL6 and CUL7). The substrate specificity is determined by a substrate adaptor and each Cullin is associated with a different family of substrate receptors. In the case of CUL3 these are Bric-a-brac, Tramtrack, Broad-complex (BTB) domain containing proteins (Pintard et al., 2003; Xu et al., 2003). The combinatorial assembly allows a huge diversity of Cullin complexes, accounting for the multitude of cellular functions and known substrates (Genschik et al., 2013). Cullin activity is known to be regulated by neddylation (**Figure 10**). In its inactive

conformation the transfer of ubiquitin is sterically unlikely due to the distance between bound substrate and E2 enzyme. A dramatic conformational change upon neddylation of the Cullin C-terminus diminishes the gap between E2 and substrate, and allows the ubiquitin transfer (Duda et al., 2008).

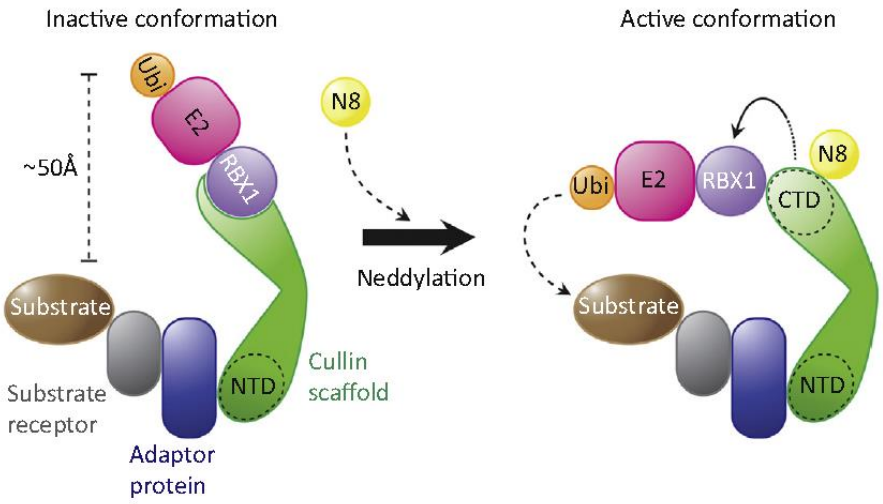

Figure 10: Structure and regulation of Cullins

The N-terminal domain (NTD) of a Cullin scaffold binds adaptor protein and substrate receptor, while the C-terminal domain (CTD) is associated with the E3 ligase (RBX1) and the E2 enzyme. In the unneddylated open conformation, substrate and the E2 loaded with ubiquitin are distant from each other. Upon neddylation of the CTD the Cullin complex undergoes a dramatic conformational change that brings substrate and E2 enzyme in close proximity, allowing ubiquitin transfer [taken from (Lu & Pfeffer, 2014)].

5.2 Cullin 3 in endocytosis

In recent years evidences that CUL3 has an impact on receptor endocytosis were increasing. In *Arabidopsis thaliana* a PM localized CUL3 dependent pathway controls the endocytosis of the photoreceptor phot1. Polyubiquitination directs phot1 to lysosomal degradation, while monoubiquitination or multi-monoubiquitination serves as a signal for recycling back to the PM, both mediated by $CUL3^{NPH3}$ (Roberts et al., 2011). Also in *Caenorhabditis elegans* a potential CUL3 pathway involved in receptor-mediated

endocytosis was reported. Based on a genetic screen in which *kel8* mutants (substrate receptor protein) accumulated glutamate receptors (GluRs) at postsynaptic membranes, it was suggested that $CUL3^{KEL8}$ ubiquitinates GluR-1, promoting its endocytosis and proteasomal degradation (Schaefer & Rongo, 2006). A recent publication proposes that CUL3-mediated ubiquitination regulates the trafficking along the endosomal pathway in mammalian cells (Huotari et al., 2012). The endosomal trafficking of two well-known cargoes, namely the influenza A virus (IAV) and the EGFR, is affected by the siRNA-mediated depletion of CUL3. While the IAV internalization is normal, the virus accumulates in the late endocytic compartment and is unable to penetrate into the cytoplasm, thus the infection cycle is disrupted. Also the lysosomal degradation of EGFR is significantly delayed and the receptors accumulate on late endosomes. While early endosomes appear morphologically normal, late endosomes are increased in size and mostly devoid of ILVs in CUL3-depleted cells. Taken together this suggests that CUL3-based E3 ligase complexes are required for the proper maturation of late endosomes (Huotari et al., 2012). However, the BTB domain-substrate receptors as well as the CUL3 endocytic targets remain unidentified and further studies are needed to refine the role of CUL3 in the endocytic pathway.

MATERIAL AND METHODS

1 Solutions

1.1 Phosphate-buffered saline

NaCl	137 mM
KCl	2.7 mM
Na_2HPO_4	10 mM
KH_2PO_4	2 mM

8 g of NaCl, 0.2 g of KCl, 1.44 g of Na_2HPO_4, and 0.24 g of KH_2PO_4 were dissolved in 800 ml of distilled water. The pH was adjusted to 7.4 with HCl and the volume was brought to 1 litre with distilled H_2O.

1.2 Tris-HCl (1 M)

121.1 g of Tris bae were dissolved in 800 ml distilled H_2O. The pH was adjusted to 7.4, 7.6 or 8.0 with HCl, and distilled H_2O was added to bring the volume up to 1 litre.

1.3 Tris-buffered saline (TBS)

NaCl	137 mM
KCl	2.7 mM
Tris-HCl pH 7.4	25 mM

8 g of NaCl, 0.2 g of KCl and 3 g of Tris base were dissolved in 800 ml of distilled H_2O. The pH was adjusted to 7.4 with HCl and distilled H_2O was added to bring the volume up to 1 litre.

1.4 10X SDS-PAGE running buffer

Glycine	192 mM
Tris-HCl, pH 8.3	250 mM
SDS	1%

1.5 10X transfer buffer

Glycine	192 mM
Tris-HCl, pH 8.3	250 mM

For 1X transfer buffer, the 10X stock was diluted 1:10 with ddH_2O and 20% v/v methanol.

1.6 50X TAE (Tris-Acetate-EDTA)

Tris base	2 M
Acetic acid	1 M
EDTA pH 8	10 mM

The pH was adjusted to 8.5 with HCl and distilled H_2O was added to bring the volume up to 1 litre.

2 Protein buffers

2.1 1X JS buffer

HEPES, pH 7.4	50 mM
NaCl	150 mM
Glycerol	10%
Triton X-100	1%

$MgCl_2$	1.5 mM
EGTA	5 mM

2.2 1X RIPA buffer

Tris HCl, pH 7.6	50 mM
NaCl	150 mM
NP-40	1%
SDS	0.1%
Deoxycholic acid	0.5%
EGTA	5 mM

500X Protease inhibitor cocktail from Calbiochem, sodium pyrophosphate pH 7.5 20 mM, sodium fluoride 250 mM, PMSF 2 mM, and sodium orthovanadate 10 mM were added to the buffer just before use.

2.3 1X Laemmli buffer

SDS	2%
Tris-HCl pH 6.8	62.5 mM
Glycerol	10%
Bromophenol blue	0.1%
β.Mercaptoethanol	5% (v/v)

SDS-PAGE sample buffer was prepared as a 4X or 2X stock solution and stored at -20°C, protected from light.

3 Reagents

Human recombinant EGF was from Vinci-Biochem. Human Transferrin and doxycycline hydrochloride was from SIGMA. Human ALEXA-EGF was from Molecular Probes. ^{125}I-EGF and ^{125}I-Tf was from Perkin Elmer.

3.1 Antibodies

The following antibodies were used (biochemistry): polyclonal anti-EGFR (home-made, directed against aa 1172-1186 of human EGFR), monoclonal anti-EGFR (m108 hybridoma, directed against the extracellular domain of human EGFR), monoclonal anti-Eps15 (home-made, directed against aa 2-330 of murine Eps15), polyclonal anti-USP25 (home-made, directed against human full length GST-USP25) and monoclonal anti-Epsin1/2 (home-made, directed against aa 249-401 of human Epsin1), polyclonal anti-USP25 (kindly provided by Frauke Melchior), anti-Hrs (kindly provided by Harald Stenmark) and anti-pY334-Hrs (kindly provided by Sylvie Urbé), anti-CUL3 (kindly provided by Matthias Peter). Anti-pY(1068)EGFR, anti-pY(1045)EGFR, anti-Akt (9272), anti-pS(473)Akt (3787), anti-phospho-p44/42-MAPK (Thr202/Tyr204, 4695), anti-phospho-p44/42 MAPK (Thr202/Tyr204) (Cell Signaling – 9106), were from Cell Signaling. Anti-vinculin (V9131) and anti-tubulin (T5168) were from SIGMA. Anti-USP10 (ab72486) was from abcam. Anti-CHC, anti-c-Cbl (clone 17), and anti-Grb2 were from BD Pharmingen. Anti-HA (clone 16B12) was from Convance. Anti-Cbl-b was from Santa Cruz, anti-Nedd4 was home-made. Anti-Ubiquitin: ZTA10, generated in-house, P4D1 from Santa Cruz or FK2 –Enzo Life Science BML-PW8810.

The following antibodies were used in immunofluorescence: anti-EGFR (13A9, kindly provided by GENENTECH), anti-USP25 (home-made), anti-EAA-1 (N-19, Santa Cruz), anti-Lamp-1 (CD107a, BD Pharmingen), secondary Ab conjugated to Cy3 or FITC from Amsherham or Alexa488, Alexa555 and Alexa647 from Molecular Probes.

3.2 RNAi oligos

3.2.1 Negative control siRNA

The following scrambled siRNA was used as a negative control in all assays:

UGCCUAAGGAGAGAAAGAGUUUCUC

3.2.2 Specific RNAi oligos

The following siRNAs were used as reported in the figures:

- USP25 S1 (Stealth Invitrogen): CAGGAGGAGACAACUUACUACCAAA
- USP25 S2 (Stealth Invitrogen): CACCAGAGAUUUGCAGGAAAGCAUA
- USP10 S1 (Stealth Invitrogen): CGGCCACCUGGAUAUUACAGCUAUU
- USP10 S2 (Stealth Invitrogen): CCAGGUGGUGAAACCAACUGCUGAA
- DynaminI (Riboxx): UUUCACAAUGGUCUCAAAGCCCCC
- DynaminII (Riboxx): UGAACUGCAGGAUCAUGUCCCCC
- Clathrin Heavy Chain (Riboxx): GAAGAACUCUUUGCCCGGAAAUUUA
- Reticulon-3 (Stealth Invitrogen): CCCUGAAACUCAUUAUUCGUCUCUU
- Cullin 3 (5): CAACACTTGGCAAGGAGACTT (Sumara et al., 2007)
- Cullin 3 (D2): CAAACTATTGCGGGTGACTTT (Sumara et al., 2007)

3.3 TaqMAN assays for qRT-PCR (Applied Biosystems)

- USP25: Hs00203650_m1
- EGFR: Hs01076078_m1
- Transferrin: Hs00951083_m1
- 18S: Hs99999901_s1
- GAPDH: Hs99999905_m1

4 Cloning techniques

4.1 Agarose gel electrophoresis

All cloning steps were performed according to standard protocols (Wood, et al., 1983). DNA samples were loaded on 0.8%-2% agarose gels along with DNA markers (1 kb DNA Ladder, NEB). Gels were made in TAE buffer containing Gel Red (Biotium), according to manufacturere´s instructions, and run at 100 V until desired separation was achieved. DNA bands were visualized under a UV lamp.

4.2 Minipreps

Individual colonies were used to inoculate 3 ml LB (containing the appropriate antibiotic) and grown overnight at 37°C. Bacteria were transferred to reaction tubes and centrifuged for 5 min at 16000 x g using a 5415 R centrifuge (Eppendorf). Minipreps were performed with the Wizard Plus SV Minipreps Kit (Promega) following manufacturer's instructions. DNA was eluted in 30 µl nuclease free H_2O.

4.3 Diagnostic DNA restriction

Between 0.5 and 5 µg DNA were digested for 2 h at 37°C with 10-20 units of restriction enzyme (New England Biolabs). For digestion, the volume was filled up to 20-50 µl with the appropriate buffer and distilled H_2O.

4.4 Large scale plasmid preparation

Cells containing transfected DNA were expanded into 250 ml cultures overnight. Plasmid DNA was isolated from these cells using the Qiagen Maxi-prep kit according to manufacturer's instructions.

4.5 Transformation of competent cells

An aliquot of competent cells (TOP10 from Invitrogen) was thawed on ice prior to the addition of plasmid DNA. Cells were incubated with DNA on ice for 30 min and then subjected to heat shock for 30 s at 42°C. Cells were returned on ice for 5 min. 300 µl of SOC was added and cells were incubated at 37°C for 60 min before plating them onto agar plates containing the appropriate antibiotic. Plates were incubated overnight at 37°C.

5 Constructs and plasmids

GFP-tagged human USP25 wild-type was kindly provided by Sylvie Urbé. The catalytic inactive mutant USP25C178A was cloned by site directed mutagenesis using the following oligonucleotide: CTA AAG AAT GTT GGC AAT ACT GCT TGG TTT AGT GCT GTT ATT C. Human USP10 wild-type and catalytic inactive mutant USP10C488A was kindly provided by Giulio Draetta. HA-tagged human CUL3 wild-type was kindly provided by Matthias Peter.

HA-tagged constructs for the stable cell lines were PCR subcloned into pSLIK vectors (Invitrogen), through restriction enzyme digestion (New England Biolabs) and ligation (New England Biolabs). The following oligonucleotides were used:

- HAUSP25SacIIfwd: GGC CCG CGG ATG TAC CCA TAT GAT GTT CCA GAT TAC GCT ACC GTG GAG CAG AAC GTG CTG CAG C
- USP25XhoIrev: GGC CTCGAG TTA TCT TCC ATC AGC AGG AGT TCG

The following oligonucleotides were cloned into the pENT (Invitrogen) for inducible stable KD cell lines:

- sh3746_USP25fwd: AGC GCG CAC TGT GTA CGA TAC ATA ATT AGT GAA GCC ACA GAT GTA ATT ATG TAT CGT ACA CAG TGC T
- sh3746_USP25rev: GGC AAG CAC TGT GTA CGA TAC ATA ATT ACA TCT GTG GCT TCA CTA ATT ATG TAT CGT ACA CAG TGC G

- sh2962_USP25fwd: AGC GCA CAG AGG ACA TGA TGA AGA ATT AGT GAA GCC ACA GAT GTA ATT CTT CAT CAT GTC CTC TGT A
- sh2962_USP25rev: GGC ATA CAG AGG ACA TGA TGA AGA ATT ACA TCT GTG GCT TCA CTA ATT CTT CAT CAT GTC CTC TGT G

All constructs were sequence verified.

6 Cell culture

6.1 Cell culture media

Human epithelial cervical cancer HeLa cells were grown in GlutaMAX™-Minimum Essential Medium (MEM, Gibco Invitrogen), supplemented with 10% Fetal Bovine Serum High Performance (South American from Invitrogen), sodium pyruvate 1 mM (Euroclone) and non-essential aminoacids (Euroclone).

HEK293T helper cells and human epithelial cervical cancer HeLa-Oslo cells were grown in Dulbecco's Modified Eagle's Medium (DMEM, Lonza), supplemented with 10% Fetal Bovine Serum High Performance (South American from Invitrogen) and 2 mM glutamine.

MDA-MB231 cells were grown in Gibco® RPMI 1640 medium (Gibco Invitrogen) supplemented with 10% Fetal Bovine Serum High Performance (North American from Invitrogen) and 2 mM glutamine.

6.2 Transfections

6.2.1 RNAi transfections

RNAi transfections were performed using Lipofectamine RNAi MAX reagent from Invitrogen, according to manufacturer's instructions. Oligos for mRNA silencing were designed with BLOCK-iT™ RNAi Designer from Invitrogen. Cells were subjected to a single transfection in suspension (in the case of dynamin and CUL3) or to double transfection (first KD in suspension and second KD in adhesion), with 10 nM RNAi oligo

(for clathrin and CUL3 KD 20 nM RNAi oligo was used) and analyzed 5 days after transfection (except for dynamin and CUL3, 2 days after transfection).

6.2.2 DNA transfections

DNA transfections were performed using Lipofectamine reagent from Invitrogen Life Technologies, according to manufacturer's instructions. Cells were plated at 80% confluency on 10 cm cell culture dishes. The day after cells were transfected with 5 µg DNA and 30 µl Lipofectamine. 24 h after transfection cells were lysed and subjected to immunoprecipitation or pull-down assay. In case of internalization assays with ALEXA-EGF cells were seeded on coverslips 24 h post-transfection and internalization assays were performed 48 h post-transfection.

6.3 Retroviral and lentiviral infection

Stable inducible USP25 KD or USP25 overexpression (USP25wt or USP25C178A) HeLa cells were produced by lentiviral infection. HA-USP25 wild-type, HA-USP25C178A or annealed oligonucleotides for USP25 KD were cloned into pENT and recombination into pSLIK_Neo was performed according to the standard protocol (Shin et al., 2006). All constructs were sequence verified. 10 ug of pSLIK constructs were transfected in HEK293T cells by $CaCl_2$ together with plasmids encoding for GAG, POL, ENV (VSVG), and REV retroviral proteins. After 24 h viral supernatant was collected and passed through PVDF 0.45 µm Millipore filters. The supernatant was used to infect HeLa target cells after adding 8 µg/ml polybrene. Medium was replaced with standard HeLa medium after two cycles of infection. 48 h after infection, selection of infected cells was performed by adding 400 µg/ml neomycin.

7 Protein procedures

7.1 Cell lysis

After washing with PBS 1X, cells were lysed directly in cell culture plates by adding JS or RIPA buffer. Lysates were collected by using a cell-scraper and clarified by centrifugation at 16000 x g for 20 min at 4ºC using a 5415 R centrifuge. Protein concentration was measured by Bradford assay (Biorad) following manufacturer's instructions.

7.2 SDS-Polyacrylamide gel electrophoresis (SDS-PAGE)

For the resolution of proteins gradient (4-20%) precast gels (Biorad) were used or were made from a 30%, 37,5:1 mix of acrylamide: bisacrylamide (Sigma). As polymerization catalysts, 10% ammonium persulphate (APS) and TEMED were used.

Separating gel mix

	Gel %		
	6	8	10
Acrylamide mix (ml)	2	2.7	3.3
1.5 M Tris HCl, pH 8.8 (ml)	2.5	2.5	2.5
ddH_2O (ml)	5.3	4.6	4
10% SDS (ml)	0.1	0.1	0.1
10% APS (ml)	0.1	0.1	0.1
TEMED (ml)	0.01	0.01	0.01
TOTAL (ml)	10	10	10

Stacking gel mix

Acrylamide mix (ml)	1.68
1 M Tris-HCl, pH 6.8 (ml)	1.26
ddH_2O (ml)	6.8
10% SDS (ml)	0.1
10% APS (ml)	0.1
TEMED (ml)	0.01
TOTAL (ml)	10

7.3 Immunoblot (IB)

Desired amounts of proteins were loaded onto 1-1.5 mm thick SDS-PAGE gels for electrophoresis (Biorad). Proteins were transferred in immune transfer tanks (Biorad) to nitrocellulose (Schleicher and Schnell) in 1X transfer buffer (supplemented with 20% methanol) at 30 V overnight or at 100 V for 1 h. Alternatively fast transfer (Trans-Blot® Turbo™ from Biorad) with polyvinylidene fluoride (PVDF) or nitrocellulose membranes from Biorad was used. Efficiency of protein transfer was determined by ponceau staining. Membranes were blocked for 1 h (or overnight) in 5% milk or BSA in TBS supplemented with 0.1% Tween (TBS-T). After blocking, membranes were incubated with the primary antibody for 1 h at RT, diluted in 5% milk or BSA in TBS-T, followed by three washes with TBS-T 10 min each. Membranes were then incubated for 30 min with the appropriate horseradish peroxidase-conjugated secondary antibody diluted in TBS-T. After 3 washes with TBS-T (10 min each), the bound secondary antibody was revealed using the ECL method (Amersham) and detected with ChemiDoc™ XRS+ System (Biorad).

7.4 Anti-ubiquitin immunoblot

Proteins were transferred on a PVDF membrane (Immobilion P, Millipore), previously activated by incubation in 100% MeOH for 5 min at RT. After transfer, membranes were incubated for 20 min at 4°C in denaturing solution. This treatment denatures ubiquitin and facilitates the recognition of latent ubiquitin epitopes by anti-ubiquitin antibody. After extensive washes in TBS-T buffer, membranes were blocked overnight at 4ºC in 5% BSA (dissolved in TBS-T). Membranes were incubated for 1 h at RT with antibodies against ubiquitin diluted in 5% BSA dissolved in TBS-T, followed by 3 washes (10 min each) with TBS-T. Anti-mouse horseradish peroxidase-conjugated secondary antibody was diluted in TBS-T and incubated for 30 min at RT. After 3 washes with TBS-T (10 min each), the bound secondary antibody was revealed using the ECL method (Amersham) and detected with ChemiDoc™ XRS+ System (Biorad).

Denaturing solution

Guanidinium Chloride	6 M
TRIS, pH 7.4	20 mM
PMSF (freshly added)	1 mM
β-Mercaptoethanol (freshly added)	5 mM

7.5 Immmunoprecipitation

For co-immunoprecipitation (co-IP) experiments lysates were prepared in non-denaturing conditions in JS buffer. For immunoprecipitation (IP) experiments lysates were prepared in denaturing conditions in RIPA buffer, in order to avoid co-immunoprecipitating proteins. Lysates were incubated in the presence of specific antibodies for 2 h at 4ºC while rotating. Protein G Sepharose beads (Zymed) were added and samples were shaked for an additional h at 4ºC. For IP of GFP-USP25 20µl GFP-beads (MBL) per mg lysate were used and

incubated for 2 h at 4ºC while rotating. Immunoprecipitates were then washed 4 times in JS or RIPA buffer. To detect ubiquitination of EGFR, EGFR was immunoprecipitated from 300 µg RIPA lysate using an anti-EGFR antibody produced in-house (anti-EGFR 317, 10 µg/mg). For co-IP experiments 1.5 mg of fresh lysates in JS buffer were used.

8 DUB library screening

A list of 92 genes corresponding to DUBs in human genome was compiled by manual curation of literature and protein databases. A DUB siRNA library consisting of a pool of two stealth oligos per DUB gene target was purchased from Invitrogen. Transfections were performed using RNAi Max (Invitrogen) and 10 nM RNAi pools. Cells were subjected to double transfection, 'reverse' (cells in suspension) on day 1 and 'forward' (adherent cells) on day 2. Cells were then processed 48–72 h after second transfection. After an overnight starvation, cells were stimulated with 100 ng/ml of EGF for 10, 60, 90 and 120 min at 37°C. Cell lysis was performed in RIPA buffer (50 mM Tris-HCl, 150 mM NaCl, 1 mM EDTA, 1% Triton X-100, 1% Sodium deoxycholate, 0.1% SDS) supplemented with a protease inhibitor cocktail (CALBIOCHEM) and NEM (N-ethylmaleimide) 5 mM.

9 Protein production and purification

9.1 GST-fusion protein production

Rosetta cells transformed with the indicated GST-fusion construct were used to inoculate 50 ml LB (containing appropriate antibiotics and chloramphenicol at 34 ug/ml). Cultures were grown overnight at 37°C. The 50 ml overnight culture was diluted in 1 litre of LB and grown until an OD of approximately 0.6 was reached. 1 mM IPTG was added and the culture was grown either at 37°C for 3 h or at 18°C overnight. Cells were pelleted at 4000 x g for 10 min at 4°C and pellets were resuspended in GST-lysis buffer (20 ml/liter of bacteria). Samples were sonicated 5 times 20 s each on ice and centrifuged at 14000 x g for

30 min at 4°C. 600 - 1000 µl of Glutathione Sepharose 4B (GE Healthcare) beads (1:1 slurry), previously washed 3 times with PBS and once with GST-lysis buffer, were added to the supernatant and samples were incubated for either 4 h (GST-AMSH and GST) or overnight (GST-USP25) at 4°C while rocking. Beads were washed once in PBS containing 1% triton, followed by 2 times in PBS alone and one time in GST-maintenance buffer. Beads were finally resuspended in 1:1 volume of GST-maintenance buffer and kept at -80°C.

GST-lysis buffer

HEPES pH 7.5	50 mM
NaCl	200 mM
EDTA	1 mM
Glycerol	5%
NP-40	0.1%
Protease Inhibitors (Calbiochem)	1:500

GST-maintenance buffer

Tris pH 7.4	50 mM
NaCl	100 mM
EDTA	1 mM
Glycerol	10%
DTT	1 mM
Protease Inhibitors (Calbiochem)	1:500

List of the GST-proteins used:

- USP25 full length (*Homo sapiens*)
- AMSH full length (*Homo sapiens*)

9.2 GST pull-down

GST-proteins were incubated with 2 mg JS HeLa cell lysates for 2h at 4°C. Beads were washed 4 times with JS buffer plus proteases and/or phosphatases inhibitors.

10 Assays with ^{125}I-EGF and ^{125}I-Tf

10.1 Receptor internalization assays with ^{125}I-EGF and ^{125}I-Tf

HeLa cells were plated in triplicate for each time point (plus one well for the unspecific binding) into 24 well plates in order to reach 90% confluence the following day. Cells were serum starved for at least 4 h and then incubated at 37°C in the presence of ^{125}I-EGF in binding buffer (MEM, BSA 0.1%, Hepes pH 7.4 20 mM). The concentration of radiolabelled EGF used in the assays was the following:

Low Dose EGF internalization	^{125}I-EGF: 1 ng/ml
High Dose EGF internalization	^{125}I-EGF: 20 ng/ml
Tf internalization	^{125}I-Tf: 1µg/ml

After 3, 5 and 7 min or 3 and 6 min of EGF treatment respectively, cells were washed 3 times in PBS, and then incubated for 5 min at 4°C in 300 µl of acid wash solution, pH 2.5 (acetic acid 0.2 M, NaCl 0.5 M). The solution was collected and the present radioactivity was measured. These samples represent the amount of ^{125}I-EGF/Tf bound to the receptor on the cell surface. Cells were lysed with 300 µl 1 M NaOH. These samples represent the amount of internalized ^{125}I-EGF/Tf. The unspecific binding was measured at each time point in the presence of an excess of non-radioactive EGF/Tf (300X/500X). After

correction for non-specific binding, the ratio between internalized and surface-bound radioactivity was determined for each time point. These data were used to obtain the internalization curves (x-axis time in min, y-axis ^{125}I-EGF internalized/bound). Internalization rate constants (K_e) were extrapolated from the internalization curves and correspond to slopes of the best-fitting curves (Wiley and Cunningham, 1982).

10.2 Measurement of the number of EGF/Tf receptors at the cell surface by saturation binding with ^{125}I-EGF and ^{125}I-Tf

The number of surface receptors was assessed as described previously (Tosoni et al., 2005). HeLa cells were plated in triplicate (plus one well for the unspecific binding) into 24 well plates in order to reach 90% confluence the following day. Cells were serum starved in binding buffer (MEM, BSA 0.1%, Hepes pH 7.4 20 mM) for at least 4 h and then incubated in the presence of 5 ng/ml of ^{125}I-EGF or 0.5 µg/ml ^{125}I-Tf, respectively. Unlabelled EGF and Tf was added to the mix to a final concentration of 50 ng/ml for EGF and 2 µg/ml for Tf. Samples were cooled on ice and incubated with the mix for 6 h at 4°C. Afterwards cells were washed 3 times with PBS and subsequently lysed with 300 µl 1 M NaOH. These samples represent the amount of ^{125}I-EGF/^{125}I-Tf bound at equilibrium, dependent on the number of receptors on the cell surface. The unspecific binding was measured for each condition in the presence of an excess of non-radioactive EGF/Tf (300X/500X). After correction for non-specific binding, the assay provides the quantitative measurement of the number of EGFRs/TfRs for each well. By counting the number of cells plated in each well, this assay allows the determination of the number of surface receptors per cell.

11 EGFR signalling and degradation

Cells were plated on six 10 cm cell culture dishes in order to reach 70% confluence the following day. Cells were serum starved for 16 h and each plate was stimulated with high dose EGF [100 ng/ml] or with the indicated concentration for one of the indicated time points. Either SDS-PAGE or ELISA (see section 13) was performed with total cell lysates. 10 µg lysate was loaded on SDS polyacrylamide gels to investigate EGFR degradation. To monitor downstream signalling at least 30 µg of total cell lysate was loaded and immunoblots were performed as described in section 7.3.

12 Immunofluorescence studies

Cells were plated on glass coverslips. For internalization assay cells were serum starved for at least 4 h and incubated with Alexa488-EGF, Alexa555-EGF or Alexa647-EGF [40 ng/ml] and/or 13A9 antibody [20 µg/ml] for 1h a 4°C and shifted to 37°C for various time points to allow internalization. Cells were fixed with 4% paraformaldehyde (PFA) in PIPES buffer (0.2% BSA, 0.1% Triton X-100, 1x PBS) for 10 min at RT. PFA fixed cells were permeabilized with 0.1% Triton X-100 in 1X PBS for 5 min at RT. For EEA1 and LAMP1 detection cells were permabilized with 0.1% saponine solution. For anti-USP25 stainings cells were fixed with cooled MeOH for 15 min at -20°C and afterwards washed with PBS. To prevent non-specific binding of the antibodies, cells were incubated with 2% BSA in 1x PBS for 30 min at RT. Next, cells were incubated for 1 h with primary antibody in 1X PBS in presence of 0.2% BSA, washed 3 times with 1X PBS and incubated for 30 min with fluorescently labelled secondary antibodies (Amersham). After 3 washes with PBS, nuclei were DAPI-stained for 5 min and washed again 3 times with 1X PBS. Coverslips were immediately mounted with either moviol and examined under a wide-field fluorescence microscope (Olympus) or glycerol and examined under a confocal

microscope. Images were further processed with the ImageJ software. To detect only surface EGFR (anti-EGFR Ab-1, Calbiochem) permeabilization step was avoided.

13 ELISA-based DELFIA assay

For the ELISA-based assay, the DELFIA (Dissociation Enhanced Lanthanide Fluoroimmunoassay) technology from Perkin Elmer was used (Sigismund et al., 2013). It is based on sandwich-recognition of a target protein by a capture antibody and a detection antibody. The capture antibody is immobilized on a solid surface (microwells) directly through non-covalent bonds. After the addition of the analyte (appropriate cellular lysate), the detection of signals relies on a lanthanide (Europium)-conjugated antibody that is able to produce a fluorescent signal upon enhancement with acidic enhancement buffer. Lanthanide ions are released in solution at low pH and they rapidly form new, highly stable fluorescent chelates. The fluorescence of the lanthanide chelate is amplified 1-10 million times by this enhancement step and it develops a signal in 5 minutes that is stable for up to 8 hours. For the assay microwell plates were coated with the capturing antibody (home-made polyclonal directed against aa 1172-1186 of human EGFR, 5μg/ml). Lysates were prepared in RIPA/1% SDS buffer and diluted to 0.2% SDS before incubation step. Blocking was performed for 2 h with BSA 2% in PBS. 25 μg (for EGFR degradation) or 50 μg (for EGFR ubiquitination) of lysates from HeLa cells, stimulated with the indicated concentration of EGF, were incubated overnight at 4ºC for the ubiquitination detection or 1h at RT for total EGFR detection. After three washes, wells were incubated with primary antibodies (either the anti-Ub FK2, or the anti-EGFR monoclonal m108 diluted at 1 μg/ml in assay buffer), for 1 h at RT. After three washes, anti-mouse or rabbit Europium-labelled secondary antibodies (1 μg/ml in assay buffer) were added for an additional hour. After three washes and treatment with enhancement solution, fluorescence was measured with EnVision instrument (excitation at 340 nm and emission at 615 nm).

14 Densitometry and statistical analysis

Quantification of immunoblots was performed with ImageJ or ImageLab software version 4.1 (Biorad). Average results from at least three independent experiments are shown. Error bars in the plots represent the standard deviation of the mean. All statistical analyses were performed using Excel. The statistical significance was obtained applying *t*-test.

RESULTS

1 Genome-wide small interfering RNA screen identified novel DUBs controlling EGFR turnover

To identify DUBs altering EGFR degradation, a genome-wide small interfering RNA (siRNA) screen targeting all known active DUBs was previously undertook in the lab. A list of 92 active deubiquitinating genes present in the human genome was compiled. Based on this gene list a siRNA library that contained a pool of two stealth oligos per gene target was designed and synthetized. These pools were transfected in HeLa cells and after EGF stimulation [100 ng/ml] EGFR degradation kinetics were determined with two approaches: (i) quantitation of EGFR levels in immunoblots (IB), and (ii) ELISA assay based on DELFIA technology (PerkinElmer), recently established in our lab (Sigismund et al., 2013) and described in detail in the methods section. Data from DUB KDs were summarized in **Figure 11**, where quantification of the immunoblots (**Figure 11A**) and ELISA values (**Figure 11B**) of total EGFR were hierarchically clustered using GeneCluster program and displayed using JavaTreeView software (analyses were performed by Michol Savio). Three main categories of EGFR degradation kinetics were observed: DUBs whose downregulation result in (i) EGFR degradation rates similar to control, (ii) slower EGFR degradation rates and (iii) faster EGFR degradation rates with respect to control (**Figure 11**). Of note, the relative variation in EGFR degradation kinetics upon knock-down of AMSH, USP8 (UBPY), USP2 and OTUD7B reflected previously published data (Liu et al., 2012; McCullough et al., 2004; Pareja et al., 2011; Row et al., 2006), supporting the reliability of our screen (**Figure 11**).

After validation (partially performed by me, see Appendix), we identified twelve novel DUBs affecting EGFR (Savio et al., manuscript in preparation)

Figure 11: Hierarchical clustering of EGFR degradation kinetics.

HeLa cells were transfected with a pool of two oligos for the indicated DUB targets or with a scrambled oligo (Control). Cells were stimulated with EGF [100 ng/ml] for the indicated time points. Total cell lysates were subjected to immunoblot (IB, **A**) and DELFIA (**B**) analyses. Values of EGFR were plotted as percentage of total EGFR at different time points against unstimulated condition. Normalized values were hierarchically clustered using GeneCluster program and displayed with JavaTreeView program. The black-to-white colour bar represents low to high log ratios of the signals associated to each sample. 24 DUBs that were selected for further validation by deconvolution experiments are highlighted in bold. These analyses were performed by Michol Savio.

2 Knock-down of USP25 impacts on EGFR fate

2.1 EGFR is degraded faster upon USP25 knock-down

Among the validated DUBs (see also Appendix), USP25 KD displayed one of the strongest effects (**Figure 11**). As for the other twenty-four DUBs, deconvolution experiments were performed in HeLa cells with two siRNA oligos (USP25 S1 and USP25 S2) used as a pool in the screen (**Figure 12**). Cells were stimulated with EGF [100 ng/ml] for different time points (from 0 min to 120 min). Effects on degradation kinetics were measured in immunoblot (**Figure 12A**) as well as in DELFIA (**Figure 12C**). EGFR levels detected in immunoblot were quantified and normalized to the amount of EGFR in the unstimulated condition and to the loading control (**Figure 12B**).

DELFIA and immunoblot analyses revealed an enhanced degradation rate of EGFR, detectable already at early time points like 30 minutes post-EGF as well as upon prolonged stimulation (120 min) (**Figure 12B,C**). While in control conditions typically ~40% of the initial amount of EGFR remained after two hours of EGF induction, only 20-30% was still present upon USP25 KD (**Figure 12B,C**). Overall, KD efficiency was slightly better with oligo S1 compared to oligo S2, therefore USP25 S1 siRNA was mainly used for further investigations.

It is well known that various cell types show differences in EGFR internalization pathways and kinetics. To validate that the observed effects are not only restricted to HeLa cells, we examined alterations of EGFR degradation upon USP25 depletion in different cell lines (**Figure 12D**). The metastatic human breast cancer cell line MDA-MB231 and the HeLa cells used in our lab (HeLa Milan) possess both EGFR internalization pathways, CME and NCE. HeLa-Oslo cells instead were characterized for the absence of NCE (Kazazic et al., 2006; Sigismund et al., 2013). EGFR degradation kinetics was measured in immunoblot upon KD of USP25 in HeLa-Oslo and MDA-MB231 cells. For both cell lines a faster EGFR degradation was assessed in cells depleted for USP25 (**Figure 12D**), which is in line with previous data obtained in HeLa Milan (**Figure 12A-C**).

In sum, we confirmed the initial data from the screening, showing that depletion of USP25 caused enhanced degradation of EGFR, for both siRNAs individually tested. Furthermore, effects of USP25 KD were substantiated in different cell lines.

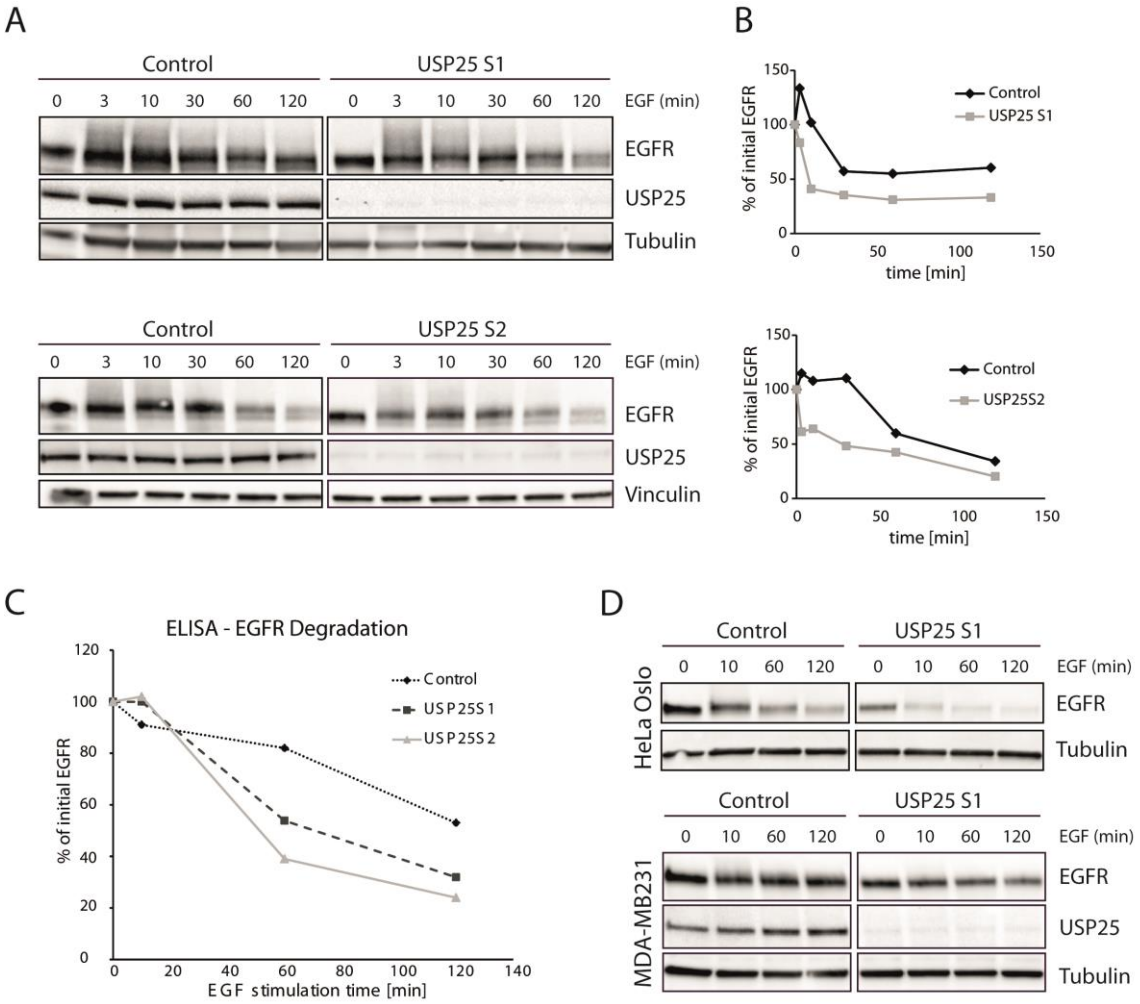

Figure 12: EGFR degradation kinetics measured after USP25 knock-down.

HeLa cells (Milan) were transfected with different siRNAs targeting USP25 (USP25 S1 and USP25 S2) (**A-C**), MDA-MB231 cells or HeLa Oslo cells were transfected with USP25 S1 (**D**), scrambled oligo was used as control (**A-D**). After serum deprivation cells were stimulated with EGF [100 ng/ml] for the indicated time points. Total cell lysates were analysed by IB with the indicated antibodies (**A** and **D**) or subjected to DELFIA (**C**) to determine EGFR degradation. Graphs in panel **B** show the quantification of EGFR degradation in IB. EGFR levels were normalized to the amount of EGFR in the unstimulated condition and to the loading control.

2.2 EGFR downstream signalling is affected in USP25 knock-down cells

Activation of EGFR mediates the intracellular signal transduction through phosphorylation of downstream signalling proteins (**Figure 7**). Following activation by EGF, the EGFR is rapidly routed to the lysosome for degradation in an ubiquitination-dependent fashion. This pathway represents the major mechanism of signalling attenuation. Therefore, alterations in EGFR degradation are predicted to have an impact on the signalling cascade (Mosesson, Nat. Rev Cancer, 2008).

This prompted us to investigate whether depletion of USP25 affects downstream signalling of EGFR. HeLa control and USP25 KD cells were stimulated with high dose of EGF [100 ng/ml], subsequently phosphorylation status of different signalling and adaptor molecules (Akt, MAPK and Hrs) was assessed in IB (**Figure 13**). No significant difference was scored for MAPK, neither in protein levels, nor in the phosphorylation status. In accordance with a faster degradation and consequently signalling attenuation (Sigismund et al., 2008), a decreased phosphorylation of Akt was observed in USP25 KD cells (**Figure 13**). Furthermore, the phosphorylation of Hrs was increased and anticipated in cells depleted for USP25. The phosphorylation peak of Hrs was shifted from ten minutes in control cells to three minutes post EGF in USP25 KD cells (**Figure 13**). It needs to be mentioned that there is less total Hrs at early time points in control conditions compared to USP25 KD cells. This might be probably caused by stripping of the immunoblot, since an anticipation of the phosphorylation of Hrs upon USP25 KD was observed in several independent experiments.

Hrs is an endocytic adaptor protein essential for endosomal sorting of growth factor receptors to the lysosomal degradation pathway. It is known that Hrs phosphorylation occurs upon interaction with ubiquitinated EGFR (Stern et al., 2007). As such Hrs phosphorylation can be used to monitor the trafficking of activated and ubiquitinated

EGFR. Thus, alterations in Akt and Hrs phosphorylation suggest a faster trafficking of EGFR.

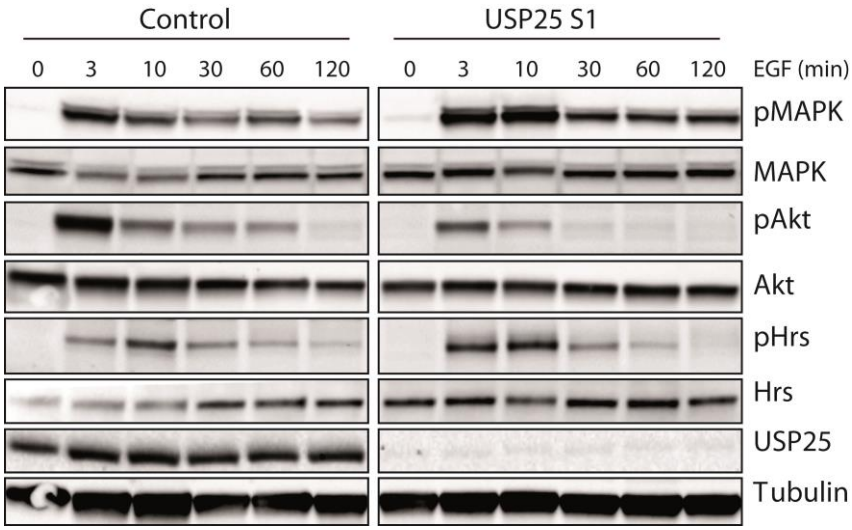

Figure 13: EGFR downstream signalling is affected in USP25 knock-down cells.

HeLa cells were transfected with siRNA targeting USP25 or with a scrambled oligo (Control). Cells were stimulated with EGF [100 ng/ml] for the indicated time points and effects on EGFR downstream signalling were revealed by IB with the indicated antibodies.

3 Internalization defects of EGFR in cells depleted for USP25

3.1 Faster trafficking of EGFR upon USP25 knock-down

On the basis of the anticipated phosphorylation of Hrs in conjunction with the accelerated EGFR degradation, we assumed a faster trafficking of EGFR upon USP25 KD.

To test this hypothesis, we examined EGFR endocytosis in immunofluorescence-based internalization assays at single cell level. AMSH and USP8 (UBPY) were used as positive controls, since it is already described that their depletion affects EGFR trafficking (McCullough et al., 2004; Row et al., 2006) (and chapter 2.2.4 introduction). HeLa cells were pre-incubated with EGF coupled to a fluorescence dye (Alexa-EGF) and an EGFR antibody (13A9 from Genentech) at 4°C, where no endocytosis takes place. The 13A9 EGFR antibody recognizes the extracellular part of EGFR but does not interfere with its

internalization and trafficking (Winkler et al., 1989). Cells were shifted to 37 °C allowing endocytosis and subsequently fixed at different time points. At the early three minutes time point the majority of the EGFR-EGF complexes resided at the plasma membrane in control cells, while in USP25 KD cells a substantial portion was already internalized (**Figure 14A**). Two hours post stimulation EGFR was fully degraded and not more detectable in control cells. In USP8 KD cells instead, a major fraction of EGFR was still present, and both receptor and ligand appeared to be stuck into endocytic compartments (Row et al., 2006) **(Figure 14A**). USP25 KD cells showed the opposite behaviour: at later time points, as 30, 60 and 120 minutes, less EGF-EGFR signal was observed in USP25 KD cells compared to control cells (**Figure 14A**). In particular at 30 minutes, this phenotype appeared to be even stronger compared to the one of ASMH KD (McCullough et al., 2004).

We decided to extend our analyses and to monitor the subcellular distribution and the itinerary of the EGF receptor in more detail. Antibodies against EEA1 (early endosomes) and LAMP1 (late endosomes/lysosomes) served as endocytic markers for tracking the route of internalized EGFR. At three minutes, the EGF signal resided still at the plasma membrane in control cells. In cells depleted for USP25, a partial co-localization of EEA1 with ALEXA-EGF was already observed at the same time point (**Figure 14B**). At ten minutes post EGF there was almost 100% co-localization of EGF and EEA1 in control cells, whereas in USP25 KD cells only partial co-localization between EEA1 and EGF was observed (**Figure 14B**). Analogous results were obtained with LAMP1, where co-localization between LAMP1 and EGF was anticipated after USP25 KD. In contrast to control cells, co-localization of LAMP1 and EGF was already detected ten minutes post EGF in USP25 KD cells (**Figure 14C**). At 30 minutes instead fewer dots for EGF were detected in the USP25KD. Possibly as a consequence, the merge of LAMP1 and EGF was less evident compared to control cells.

The sum of these results indicates that lack of USP25 leads to a faster internalization of EGFR and a general acceleration in the kinetics of EGFR trafficking from the early endocytic compartment to lysosomes.

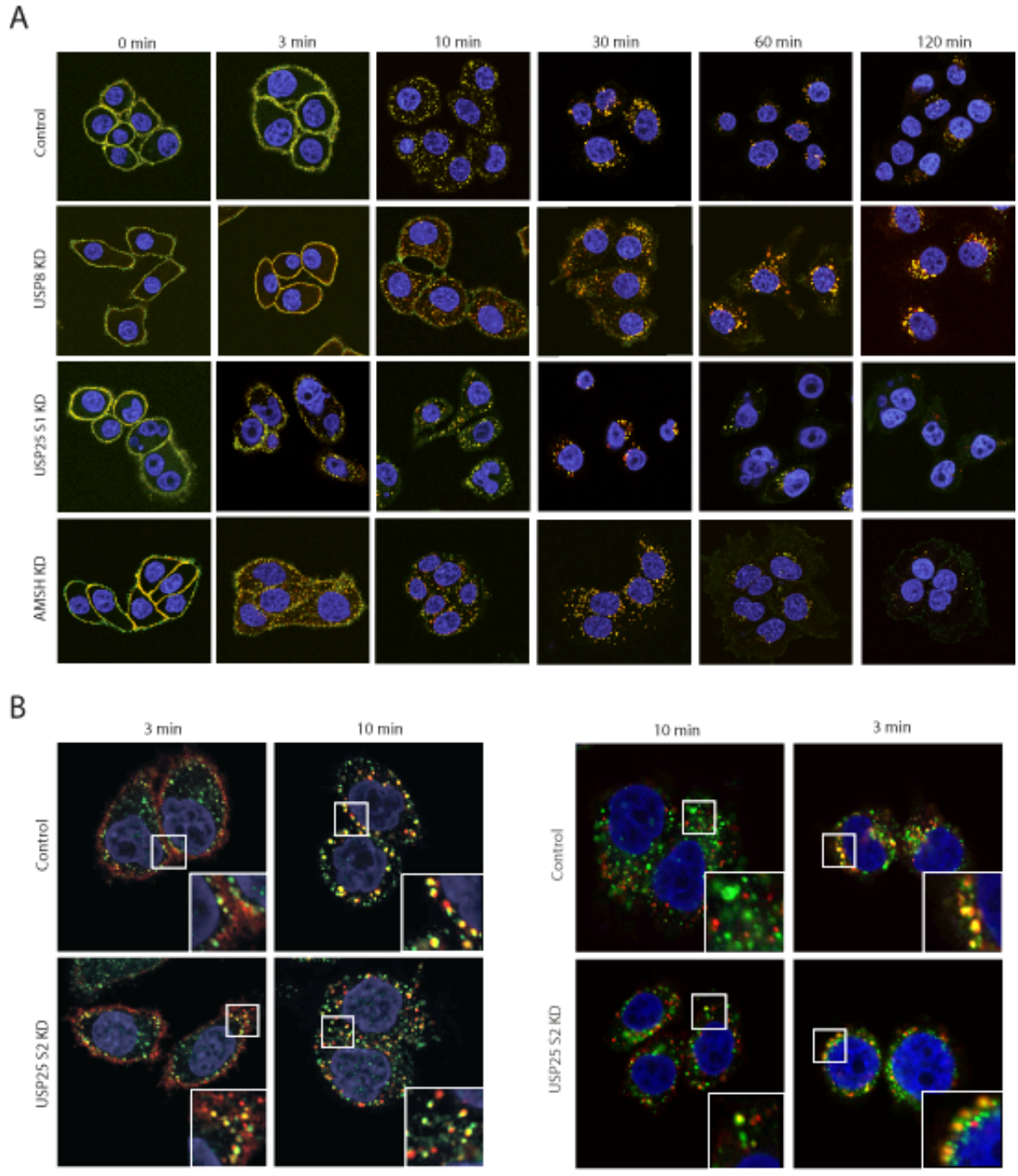

Figure 14: Depletion of USP25 alters EGFR trafficking.

HeLa cells were transfected with siRNA targeting USP25, AMSH, USP8 and with a scrambled oligo (Control) as indicated. KD cells were serum starved and incubated for one hour at 4°C in the presence of an EGFR antibody recognizing the extracellular part of

EGFR (13A9, green) (**A**) and/or Alexa555-EGF [40 ng/ml, red] (**A-C**). After washing, cells were shifted to 37°C for the indicated time points. Cells were fixed and stained with an EEA1 (green) (**B**) or LAMP1 antibody (green) (**C**), respectively. Blue, DAPI staining.

3.2 USP25 overexpression inhibits EGFR internalization

These results prompted us to assess if also the overexpression of USP25 might have an impact on EGFR endocytosis. Therefore we performed internalization assays as described in chapter 3.1, but this time in cells overexpressing either a GFP-tagged USP25wt construct or a catalytically inactive mutant USP25C178A, where the active site Cys was replaced by alanine (**Figure 15**). We observed a reduction in EGF-positive vesicles after ten minutes of EGF-stimulation in GFP-positive cells ectopically expressing USP25wt. Notably, in these cells a large amount of EGF signal was still present at the plasma membrane (**Figure 15** left panel), suggesting impairment in EGFR internalization. Moreover, the partial inhibition of EGFR internalization depends on the catalytic activity of USP25, since no effect was visible upon overexpression of the catalytic inactive mutant USP25C178A (**Figure 15** right panel).

These experiments establish that overexpression of USP25wt shows the reverse phenotype to the one observed in USP25 KD cells. GFP-USP25wt caused a delay in EGFR internalization; overexpression of a catalytically inactive mutant instead had no detectable effect on EGFR endocytosis, indicating that USP25 activity is essential for the assessed internalization defects.

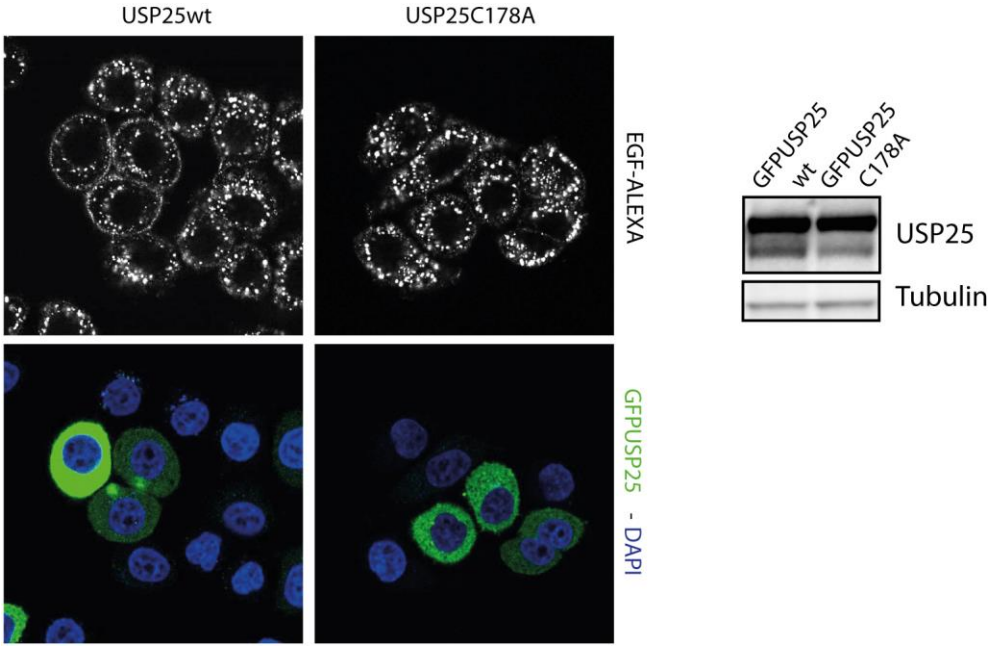

Figure 15: EGFR internalization defects upon USP25 overexpression.
HeLa cells were transfected with GFP -USP25wt or GFP-USP25C178A. After 48 hours cells were serum starved and then stimulated for ten minutes with EGF-ALEXA [40 ng/ml] at 37 °C. GFP-USP25wt causes a delay in EGFR internalization, GFP-USP25C178A does not. IB shows levels of endogenous USP25 and overexpressed GFP-USP25 proteins.

Encouraged by these results we decided to perform functional studies in cells overexpressing USP25. By transient transfection, we could not reach effectual transfection levels and only a few cells expressed USP25 constructs (**Figure 15**). To overcome this problem we took advantage of a doxycycline-inducible lentiviral system (Shin et al., 2006) and we generated stable cell lines in which USP25 overexpression could be induced.

To reach homogenous expression levels, HeLa cells were infected with lentivirus containing either pSLIK HA-USP25wt or HA-USP25C178A constructs. After the selection of infected cells with neomycin [400 µg/ml], HA-USP25wt and HA-USP25C178A expression was induced with [1 µg/ml] of doxycycline for 48 hours. Cells were serum starved and stimulated with high dose of EGF [100 ng/ml] for different time points up to 120 minutes. The impact of USP25 overexpression on EGFR degradation kinetics was assessed in IB with an EGFR antibody.

No significant change of EGFR degradation could be detected, neither in the HA-USP25wt nor in the HA-USP25C178A cell line compared to cells infected with pSLIK vector (e.v.) (**Figure 16A**). The lack of phenotype might be due to low USP25 protein levels. Indeed, only a slight increase in expression of USP25 upon doxycycline treatment was revealed with an USP25 antibody (**Figure 16A**). To check expression levels of USP25 constructs and infection efficiency of the lentiviral system, immunofluorescence analysis were performed. Staining with a HA antibody revealed that similar to transient transfection only a few cells expressed HA-USP25 at a detectable level (**Figure 16B** images left), suggesting that the remaining cells were not infected. To investigate the reason of this poor expression, stable cell lines were treated with the proteasome inhibitor MG132. After blocking proteasomal protein degradation nearly all cells showed a positive HA-signal, indicating that cells indeed do express USP25 ectopically (**Figure 16B** images right). Thus, at least artificially increased protein levels of tagged USP25 appeared to be toxic for cells that respond degrading the DUB in a proteasome-dependent manner. However we do not know what happens to endogenous USP25 and the observed effect might be simply caused by the protein-tag. Unfortunately this counter selectivity makes the execution of functional investigations impossible.

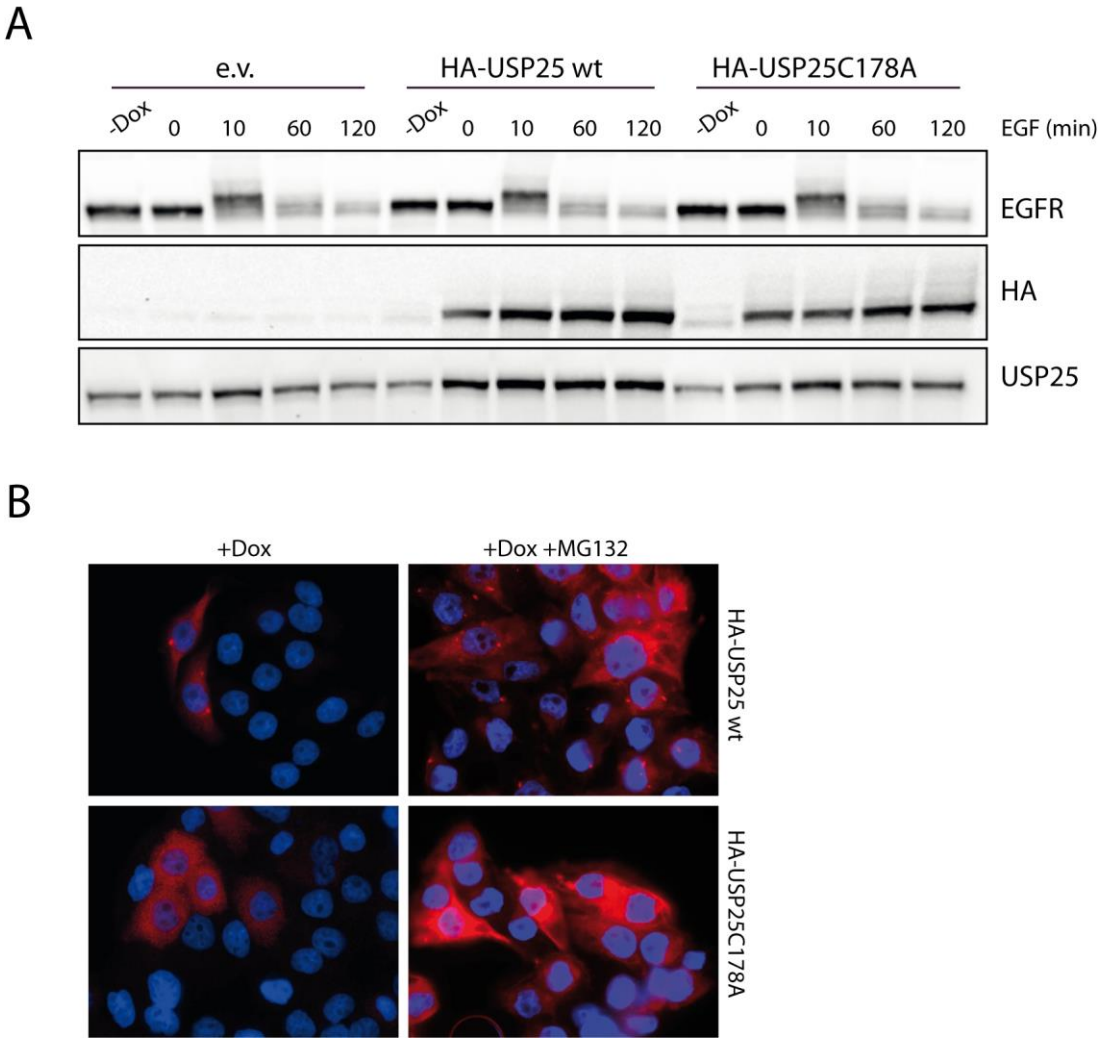

Figure 16: Stable cell lines inducible for USP25 and USP25C178A overexpression

HeLa cells transduced with pSLIK lentivirus expressing HA-USP25wt, HA-USP25C178A or pSLIK empty vector (e.v.) were grown for 48 hours in the presence or absence of doxycycline [1 µg/ml] (**A and B**). Cells were serum starved for 16 hours and then stimulated with EGF [100 ng/ml] for the indicated time points. Total cell lysates were analysed by IB with the indicated antibodies (**A)**. For immunofluorescence cells were treated with 5 µM MG132 overnight. After fixation cells were stained with HA antibody (**B**).

3.3 EGFR internalization rates upon USP25 knock-down

Our collected data indicate that USP25 has a direct impact on EGFR endocytosis. Immunofluorescence analyses in USP25 KD cells and in cells overexpressing GFP-USP25wt suggested that already the internalization of EGFR was affected by USP25. However, methods applied so far allowed only qualitative observations of the internalization process. Thus, we decided to use a quantitative assay to monitor EGFR internalization with the radioactively labelled ligand ^{125}I-EGF. This assay is well established in our lab (Sigismund et al., 2005) and enables the calculation of the internalization rate K_e, which describes the probability of an activated receptor to be internalized in one minute at 37 °C (Wiley & Cunningham, 1982).

HeLa cells transiently depleted for USP25 and control cells were plated into 24 well plates. Cells were serum starved for four hours and then incubated with ^{125}I-EGF [20 ng/ml] for three, five and seven minutes at 37°C. After extensive washes on ice the ^{125}I-EGF bound on the cell surface was removed by acid wash and the internalized ligand was collected through cell lysis. The unspecific binding was measured at each time point in the presence of non-radioactive EGF in excess (300X). After correction for non-specific binding, the ratio between internalized and surface-bound ^{125}I-EGF was determined for each time point. These data were used to obtain the internalization curves. Internalization rate constants were extrapolated from the internalization curves and correspond to slopes of the best-fitting curves (**Figure 17 A,B** right panel). Strikingly, the average of five independent experiments revealed that upon USP25 KD the K_e at high dose of EGF [20 ng/ml] was nearly twofold increased (**Figure 17A** left panel), confirming initial observations from immunofluorescence experiments (**Figure 14**).

All previously discussed experiments, as well as the genome-wide siRNA screen were performed in cells stimulated with high dose of EGF. In this condition, both the classical ubiquitin-independent CME as well as the NCE pathway are active (Sigismund et

al., 2008; Sorkin & von Zastrow, 2009). To gain insights into the role of USP25 in the clathrin-dependent internalization pathway, which is predominantly coupled with receptor recycling and signalling (Sigismund et al., 2008), quantitative internalization assays at low dose of EGF [1 ng/ml] were performed. We observed that even under these conditions the internalization rate was slightly but still significantly increased from 0.30 min^{-1} in control cells to 0.36 min^{-1} upon USP25 KD, as the average of seven independent experiments demonstrated (**Figure 17B** left panel).

As next we examined if the steady state levels of EGFR on the cell surface were affected in the absence of USP25. A saturation binding assay with radioactively labelled ligand enables the assessment of EGF receptors on the cell surface per cell. HeLa cells depleted for USP25 and control cells were incubated with ^{125}I-EGF for six hours on ice. After several washes cells were lysed. The measured radioactivity represents the amount of ^{125}I-EGF bound at equilibrium. After correction for non-specific binding, the assay provides the number of EGFR for each well. By counting the cells plated in each well, the amount of surface receptors per cell was determined. The average of four independent experiments revealed that EGFR surface levels are moderately decreased upon USP25 KD; from around 270.000 receptors per cell in control conditions to approximately 200.000 receptors per cell in the absence of USP25 (**Figure 17C**).

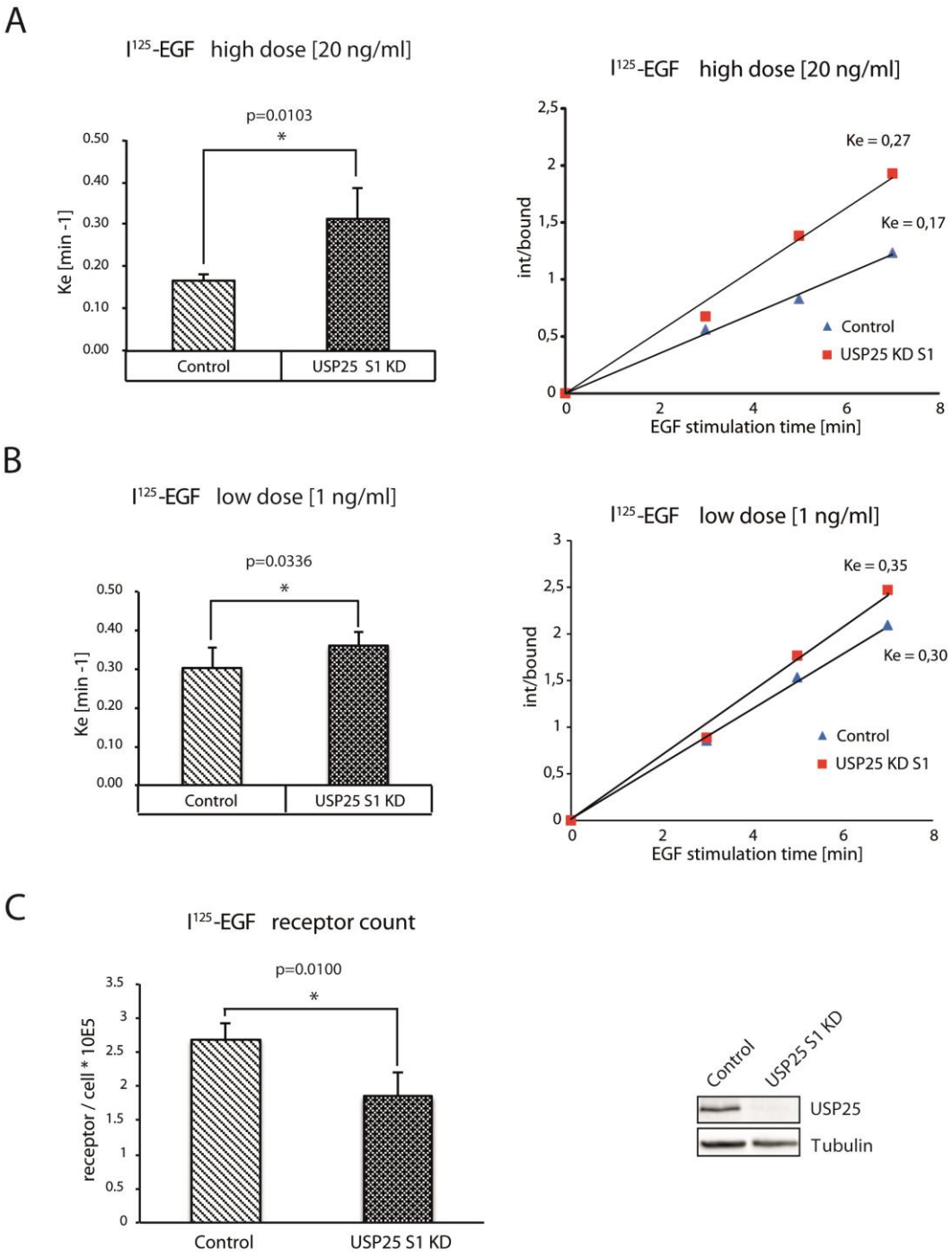

Figure 17: Knock-down of USP25 causes increased internalization of EGFR.

HeLa cells were either transfected with siRNA targeting USP25 or with a scrambled oligo (Control), as indicated. EGFR internalization at high [20 ng/ml] (**A**) and low [1 ng/ml] doses (**B**) of EGF ligand was followed at early time points (0-7 min) using a radiolabeled ligand binding assay and I^{125}-EGF. Results are expressed as a ratio between internalized ligand and bound ligand. The average of triplicates is shown (**A, B right graph**). K_e for high dose of EGF [20 ng/ml] is the average of five independent experiments (**A left graph**). K_e for low dose of EGF [1 ng/ml] is the average of seven independent experiments (**B left graph**). The number of EGFRs on the cell surface was measured by saturation

binding with I^{125}-EGF (**C**)**.** Results are average of four independent experiments. IB anti-USP25 is reported to show KD efficiency (**C**)**.**

To substantiate the impact of USP25 on EGFR endocytosis we decided to generate stable cell lines in which KD of USP25 can be induced by stimulation with doxycycline. HeLa cells were infected with a lentiviral-system (pSLIK) containing miR-shRNAs targeting different sequences compared to the siRNAs (USP25 S1 and S2) previously used. miR-shRNAs were designed to target a sequence within the open reading frame (ORF; sh2962) or in the untranslated region (3'UTR; sh3746) of the USP25 mRNA (**Figure 18A**). After selection, infected cells were treated with doxycycline and quantitative internalization assays were performed similar to transient KD conditions (see chapter 3.2). No significant changes upon doxycycline treatment were observed in cells infected with viruses that did not contain miR-shRNAs targeting USP25. This demonstrates that doxycycline on its own did not affect EGFR internalization. Induction of USP25 KD upon doxycycline treatment caused in both cell lines (sh2962 and sh3746) enhanced EGFR internalization (**Figure 18B,C**). However, the observed increase of the K_e at low [1 ng/ml] as well as at high dose [20 ng/ml] of EGF was less prominent compared to the results obtained in transient KD cells (**Figure 17A,B**) This is in agreement with a less efficient downregulation of USP25 in the inducible KD compared to transient USP25 KD, as shown by immunoblots in **Figure 18B** and **Figure 17C**. Therefore we decided to select clones from the bulk population in order to obtain a stronger KD of USP25 upon induction (**Figure 19A**).

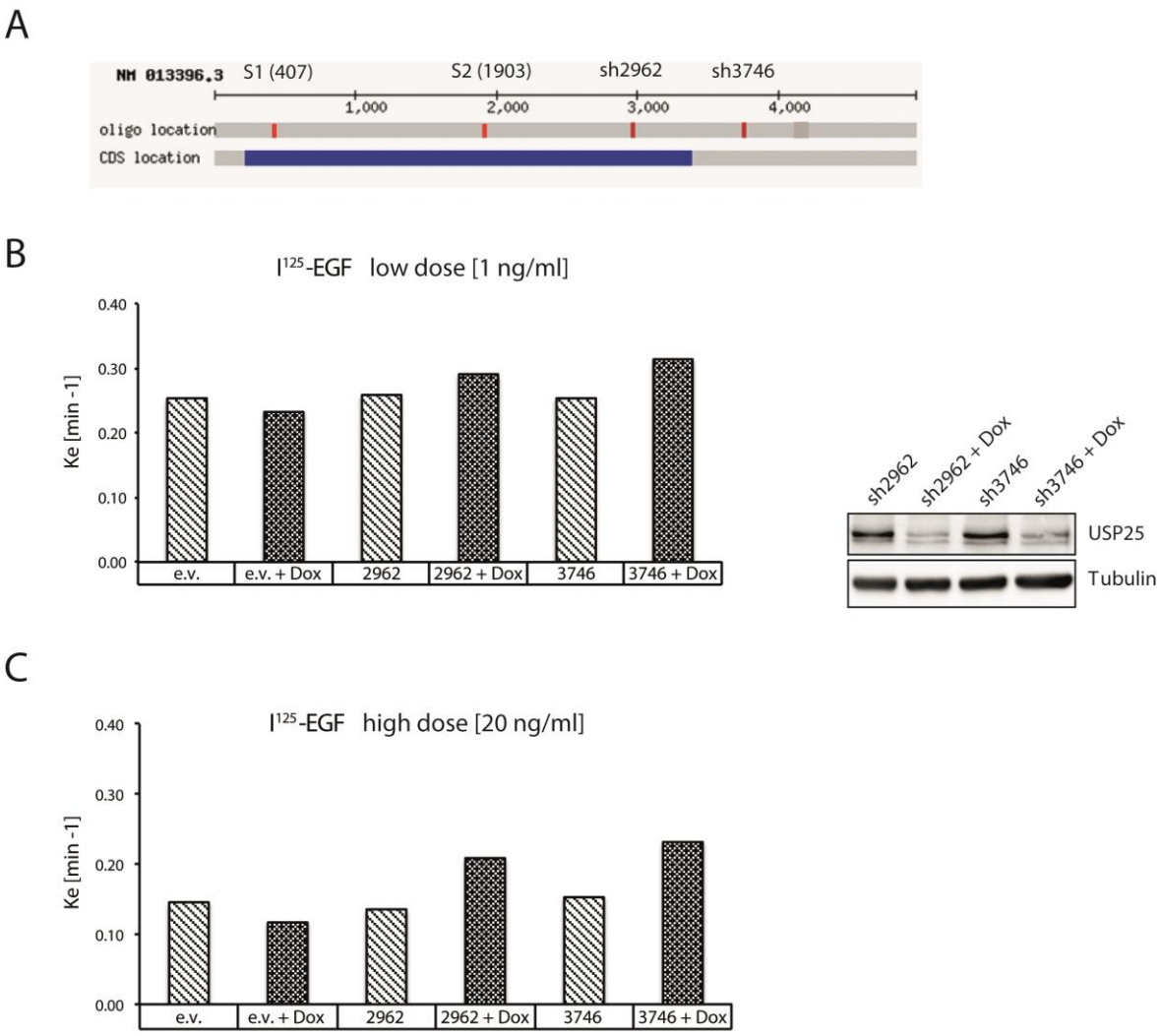

Figure 18: EGFR internalization in stable inducible USP25 knock-down cell lines.

Schematic representation of miR-shRNA locations targeting USP25 mRNA. ORF of USP25 is depicted as blue bar, positions of siRNAs and shRNAs are highlighted in red (**A**). Stable cell lines were stimulated with doxycycline [0.5 µg/ml] for 96 hours to induce USP25 depletion. EGFR internalization at low [1 ng/ml] (**B**) and high [20 ng/ml] (**C**) doses of EGF ligand was followed at early time points (0-7 min) using a radiolabeled ligand binding assay and I^{125}-EGF. Internalization constants (K_e) were extrapolated from the internalization curves and correspond to the slopes of the best-fitting curves. Immunoblots shown in **B** were performed to show KD efficiency.

25 clones were generated from the bulk populations by limiting dilution procedure for each cell line. **Figure 19** shows examples of the analysed clones. USP25 expression levels in all clones were revealed in the presence or absence of doxycycline treatment

using a USP25 antibody. Clones with a good level of USP25 depletion were selected for further investigations (**Figure 19A,** red rectangle). Clones 2_5 and 2_11 targeting USP25 mRNA within the ORF and clones 3_5 and 3_7 targeting USP25 mRNA in the 3'UTR were selected and quantitative internalization assays were performed. At high dose of EGF [20 ng/ml] an almost twofold increase of the internalization constant was observed for all selected clones (**Figure 19B**). This proves the hypothesis that the level of depletion is responsible for the observed differences in the K_e between transient KD and the bulk population of the stable KD cell lines. Therefore all further experiments were performed with the selected clones or upon transient KD of USP25.

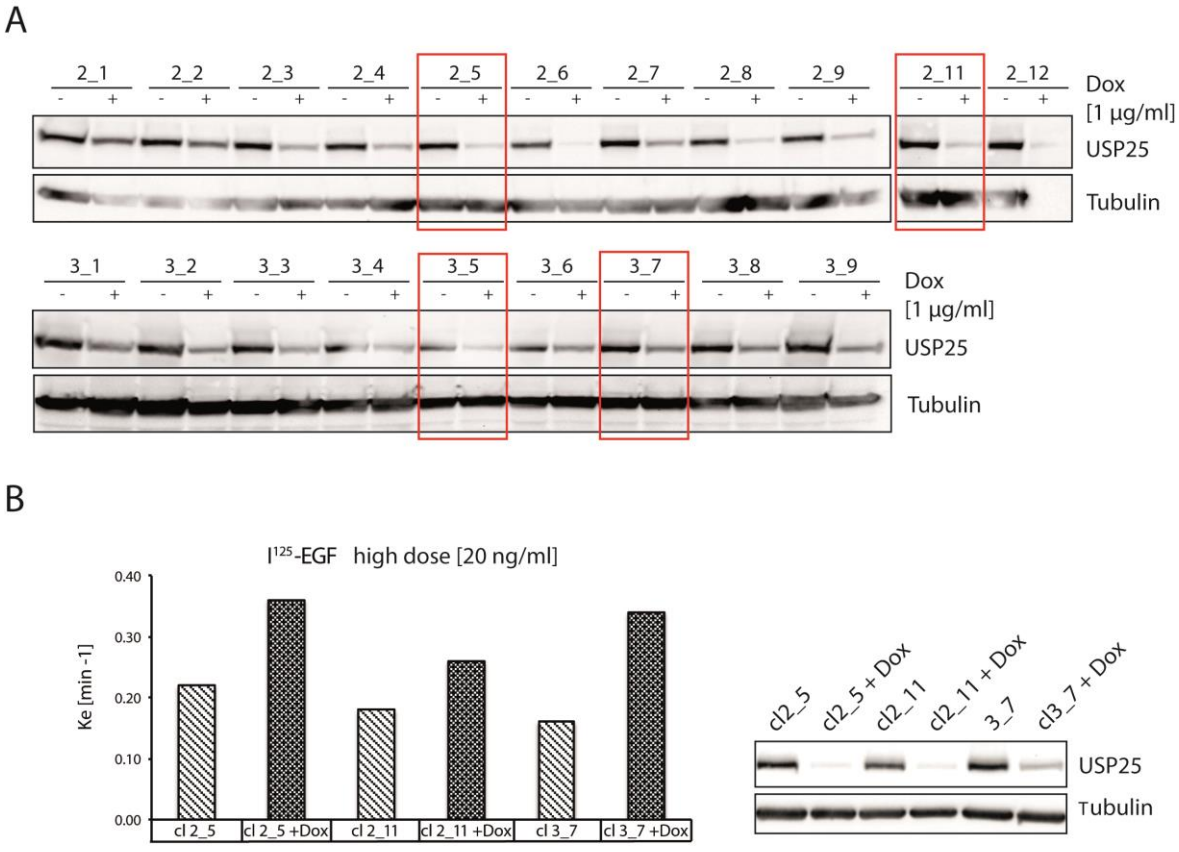

Figure 19: Selection and characterization of stable USP25 knock-down clones.

HeLa clones were treated for 96 hours with doxycycline [0.5 µg/ml]. Level of USP25 depletion was revealed by immunoblotting with an USP25 antibody (**A**). Tubulin was used as protein loading control. Selected clones are marked with a red rectangle (**A**). EGFR internalization at high dose of EGF ligand [20 ng/ml] was followed in selected HeLa

clones at early time points (0-7 min) using a radiolabeled ligand binding assay and I^{125}-EGF (**B**). Internalization constants (K_e) were extrapolated from the internalization curves and correspond to the slopes of the best-fitting curves. KD efficiency was revealed by IB (**B**).

4 Dissection of endocytic pathways affected by USP25

4.1 Role of USP25 in CME and NCE of EGFR

As described in the introduction, EGFR can be internalized via different entry routes; depending on ligand concentration and cell type. We were seeking to unravel the impact of USP25 on distinct endocytic pathways using a genetic approach. To distinguish between NCE and CME, different siRNAs were used to switch off one of the two entry routes. In particular we employed clathrin KD for CME and reticulon KD for NCE inhibition, since reticulon was recently found by our collaborator to be essential for endocytosis via the NCE pathway (Sara Sigismund, unpublished data). Quantitative internalization assays were performed in cells depleted for USP25 alone or in combination with reticulon or clathrin KD, respectively. KD cells were stimulated with high dose of EGF [20 ng/ml], a condition where both internalization pathways are active. In accordance with already published (Sigismund et al., 2013) and unpublished data, ablation of clathrin as well as of reticulon led to a fractional inhibition of the EGF internalization at high dose (**Figure 20A**). Notably, KD of clathrin or reticulon in USP25 KD cells was not sufficient to fully reverse the USP25 KD phenotype. The internalization rate was significantly increased in both double KDs compared to clathrin or reticulon KD alone (**Figure 20A**). Similar results were obtained at low dose [1 ng/ml] under conditions were only CME takes place. The simultaneous interference of clathrin and USP25 led only to a partial rescue in the increase of the internalization rate (**Figure 20B**).

The fact that neither clathrin KD nor the depletion of reticulon could completely restore alterations in EGFR internalization rates in cells depleted of USP25 suggests that USP25 plays a role in the clathrin-mediated as well as in the clathrin-independent endocytosis of EGFR.

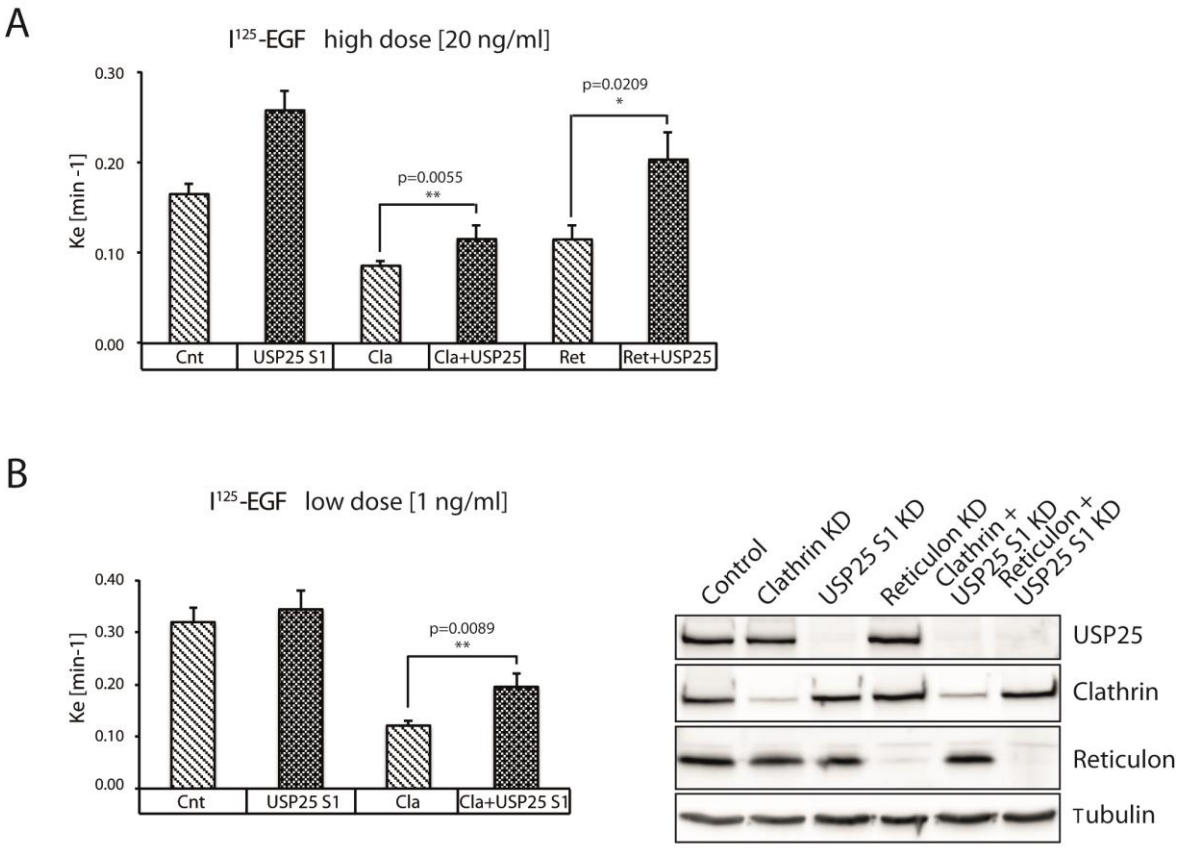

Figure 20: Impact of USP25 knock-down on different EGFR entry routes.

HeLa cells were transfected with siRNA targeting USP25, clathrin, reticulon or with a scrambled oligo (Control) as indicated. EGFR internalization was followed for early time points (0-7 min) at high [20 ng/ml] (**A**) and low [1 ng/ml] (**B**) doses of EGF ligand by using a radiolabeled ligand binding assay (I^{125}-EGF). Internalization constants (K_e) were extrapolated from the internalization curves and correspond to the slopes of the best-fitting curves. K_e for high [20 ng/ml] and low [1 ng/ml] doses of EGF are average of three independent experiments (**A** and **B**). Immunoblots shown in **B** were performed to show KD efficiency, respectively.

4.2 Transferrin as model substrate for CME

The Transferrin receptor (TfR) is one of the best-studied endocytic cargoes and exclusively internalized through the clathrin-dependent pathway (see also chapter 1.3 introduction). Therefore we decided to use the Transferrin receptor as a tool, to further analyse the role of USP25 in CME.

Quantitative internalization assays with radioactively labelled Tf (I^{125}-Tf) were performed to examine the early internalization rates of TfR. Cells were either transiently depleted for USP25, or stable cell lines were treated with doxycycline to induce USP25 KD. The average of three independent experiments revealed that the K_e for TfR internalization is strongly increased following USP25 depletion (**Figure 21A**). Consistent with previous data on EGFR, we assessed at least a twofold increase in the endocytic rate in both conditions, stably inducible and transient ablation of USP25 (**Figure 21A**).

Next, we investigated if also the basal surface level of TfR was affected in USP25 KD cells. Tf receptor numbers at the cell surface were quantified in KD cells using the I^{125}-Tf saturation-binding assay. Silencing of USP25 had a strong effect on the cell surface number of TfR. Approximately 1.5*10E6 receptors per cell were detected in HeLa e.v. and untreated cl3_7 cells (**Figure 21B**). When USP25 was depleted in cl3_7 cells, the number of surface receptors per cell dropped to 2.5*10E5. Thus, in USP25 KD cells less than 20% of TfR was present on the cell surface compared to control conditions (**Figure 21B**).

Transferrin is constitutively internalized therefore it was expected that also the basal level of TfR is affected. However, the strong decrease in surface receptors led us to hypothesize a possible transcriptional effect on TfR mRNA levels upon USP25 KD. mRNA levels of TfR and EGFR were assessed by qRT-PCR in two stable KD clones (cl 2_5 and cl 3_5) treated with doxycycline. The measured Ct-values were normalized to the housekeeping genes GAPDH or 18S. Depletion of USP25 caused in both cell lines a

reduction of TfR mRNA levels of 70-80% compared to untreated cells. On the contrary, transcriptional levels of EGFR were not affected (**Figure 21C**).

These results show that KD of USP25 has a strong effect on TfR homeostasis. The transcriptional defect might at least partially account for the reduced numbers of TfRs measured on the surface of USP25 KD cells. Moreover, we cannot exclude that the differences on receptor surface levels might also distort the measurement of the internalization rate in quantitative assays.

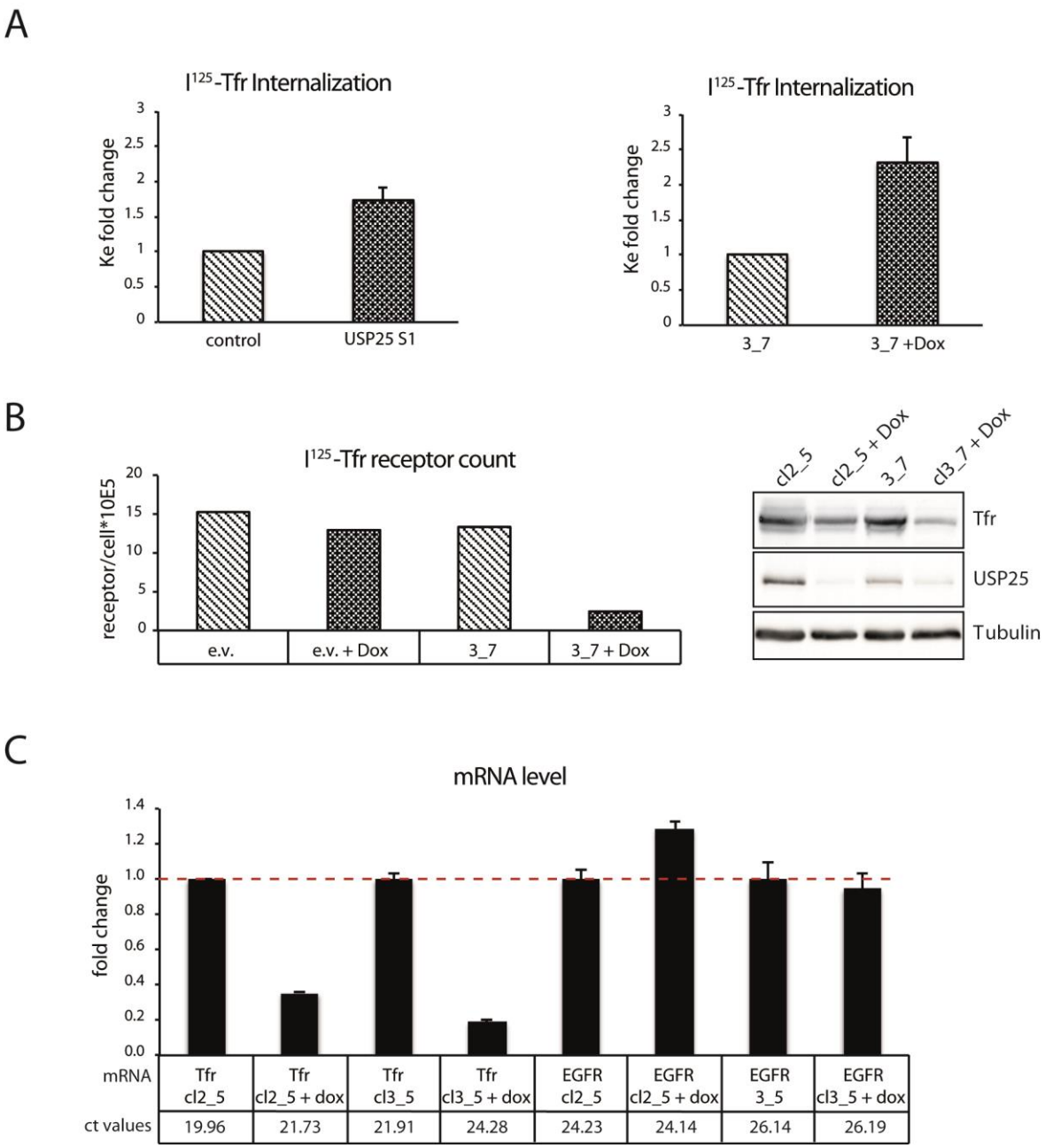

Figure 21: Effects of USP25 knock-down on Transferrin receptor endocytosis and homeostasis.

HeLa cells were transfected with siRNA targeting USP25 and a scrambled oligo (Control) as indicated (**A left graph**). Stable cell lines were stimulated with doxycycline [0.5 μg/ml] for 96 hours to induce USP25 KD (**A right graph**, **B,C**). TfR internalization rates upon stimulation with I^{125}-Tf [1 μg/ml] were followed at early time points (0-7 min) by using a radiolabeled ligand binding assay. Results are expressed as fold change of the internalization rate K_e compared to control conditions and are average of three independent experiments (**A**). The number of TfRs on the cell surface was measured by saturation binding with I^{125}-Tf (**B**)**.** IB anti-USP25 was performed to show KD efficiency (**B**). Expression levels of TfR and EGFR mRNA were assessed by qRT-PCR analysis and

normalized to the housekeeping genes 18S or GAPDH, respectively (**C**). Ct-values and fold changes in respect to control conditions are reported.

4.3 Investigation of CME- and NCE-independent EGFR internalization

Depletion of clathrin as well as depletion of reticulon could only partially reverse the increased internalization rate of EGFR caused by USP25 KD (see chapter 4.1). This raises the possibility that the measured alterations in EGFR uptake might be due to a possible third EGFR internalization pathway stimulated upon KD of USP25.

NCE as well as CME are both dynamin-dependent, while other described internalization pathways are dynamin-independent (Howes et al., 2010). To investigate the impact of an alternative entry route, quantitative internalization assays were performed in cells depleted of dynamin. KD of USP25 was induced by treating cl3_7 cells with doxycycline and transient KD for dynaminI and dynaminII was carried out simultaneously. The internalization constant was determined after stimulation with high dose of EGF [20 ng/ml]. The measured K_e of 0.04 min^{-1} for EGFR uptake in cells only depleted for dynamin reflects background level caused by unspecific binding of the radioactive ligand (**Figure 22A**). However depletion of dynamin in USP25 KD cells could not fully reverse the increased EGFR internalization generated by the lack of USP25 (**Figure 22A**). This suggests that the measured EGFR internalization rate upon USP25 KD depends on a third, dynamin-independent pathway.

To further substantiate this hypothesis, EGFR internalization was followed in HeLa cells in which both pathways, CME and NCE, were switched off. For this, cells were simultaneously depleted for USP25, clathrin and reticulon, eliminating CME as well as NCE pathway. Similar to dynamin depletion, there was still an increase of the internalization rate in triple KD compared to double KD of reticulon and clathrin alone in

cells stimulated with high dose of EGF [20 ng/ml] (**Figure 22B**). Again, the observed effect was less prominent compared to the one upon dynamin ablation.

Taken together these data open the possibility that the observed increase in EGFR internalization is neither based on CME nor on NCE but is caused by a dynamin-independent internalization pathway of EGFR. Transferrin internalization would have been a proper control to exclude that the increased internalization rate in double KD conditions is caused by residual CME activity. Therefore additional studies are needed in future to investigate the hypothesis of a potential third EGFR internalization pathway, activated in cells depleted for USP25.

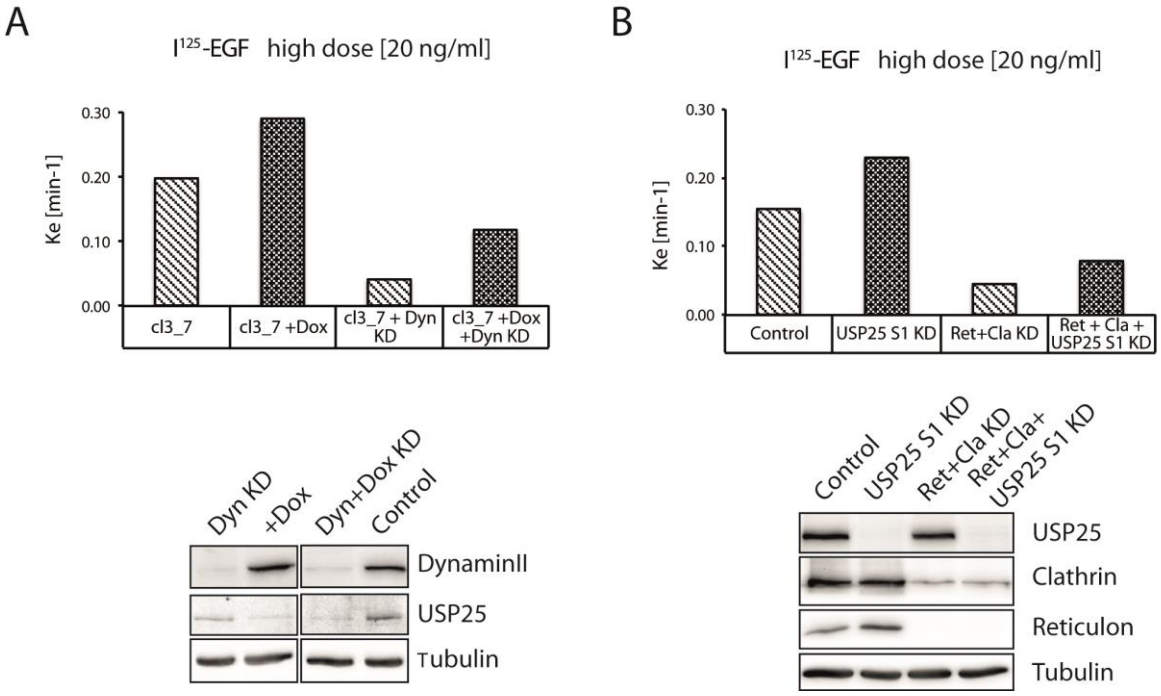

Figure 22: Characterization of EGFR internalization upon USP25 knock-down

HeLa cl3_7 cells were treated with doxycycline [0.5 µg/ml] and transiently transfected with siRNA targeting dynaminI and dynaminII as indicated (**A**). HeLa cells were transfected with siRNA targeting USP25, clathrin, reticulon or with a scrambled oligo (Control) as indicated (**B**). After 72 hours EGFR internalization was followed for early time points (0-7 min) at high dose of EGF ligand [20 ng/ml] by using a radiolabeled ligand binding assay and I^{125}-EGF. Internalization constants (K_e) were extrapolated from the internalization curves and correspond to the slopes of the best-fitting curves. KD efficiency was revealed by the indicated antibodies (**A,B**).

5 Investigation of USP25 substrate/s

5.1 Endocytic proteins involved in EGFR endocytosis

To elucidate the observed alterations in EGFR endocytosis, we were seeking for substrates of USP25. There are multiple steps of the endocytic process regulated via ubiquitination (see chapter 2.1 introduction). Since USP25 already impinges on internalization of EGFR, we focused our attention on proteins involved in early steps of endocytosis.

Endocytic adaptor proteins are known to be monoubiquitinated upon EGF stimulation (Katz et al., 2002; Polo et al., 2002). To test whether USP25 could reverse this type of modification, we examined protein levels and posttranslational modifications of Eps15 and Epsin1 and 2 in cells stimulated for different time points with high dose of EGF [100 ng/ml]. We could not assess any differences in USP25 KD cells compared to control cells for all tested adaptor proteins (**Figure 23A**). Note that the decrease in Epsin 1 and 2 at later time points in USP25 KD cells is probably based on loading problems and was not observed in other immunoblot analyses.

Overall our data are also compatible with a model in which USP25 regulates the protein stability of an unknown positive factor. This protein has to be a limiting factor in EGFR internalization. Depletion of USP25 would increase protein levels and therefore enhance the internalization of EGFR. The most obvious candidates are E3 ligases known to be involved in EGFR endocytosis. The E3 ligase c-Cbl directly ubiquitinates several RTKs including EGFR and is indeed a limiting factor, at least in the NCE pathway (Sigismund et al., 2013). NEDD4 is indirectly involved in EGFR endocytosis by regulating ubiquitination status and stability of several endocytic adaptor and trafficking proteins (Woelk et al., 2006).

Protein levels of c-Cbl and NEDD4 were assessed in USP25 KD cells stimulated with high dose of EGF [100 ng/ml]. Again, we could not score any major differences in

expression levels or posttranslational modifications compared to control conditions (**Figure 23B,C**).

In sum, our data show that depletion of USP25 does neither affect known endocytic adaptor proteins, nor E3 ubiquitin ligases important in EGFR endocytosis.

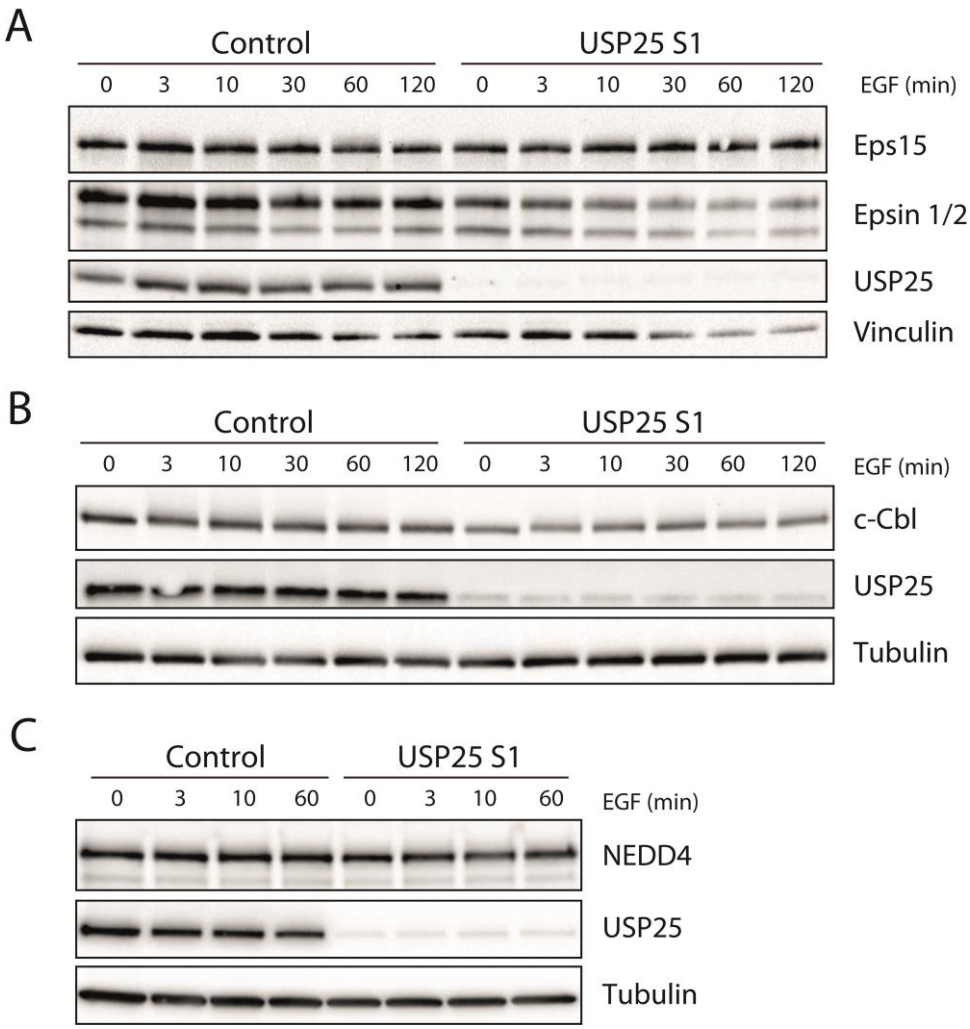

Figure 23: Characterization of endocytic proteins upon USP25 knock-down.

HeLa cells were transfected with siRNA targeting USP25 or with a scrambled oligo (Control) as indicated. After 72 hours cells were stimulated with EGF [100 ng/ml] for the indicated time points. Effects on endocytic proteins were revealed by immunoblot on total cell lysate with the indicated antibodies (**A-C**).

5.2 USP25 has a direct effect on the ubiquitination levels of EGFR

A manifest target for a DUB whose depletion increases EGFR degradation, is the receptor itself. To test if KD of USP25 has a direct effect on the ubiquitination of EGFR, we performed immunoprecipitation experiments in control and USP25 KD cells, stimulated with high dose of EGF [100 ng/ml] for different time points. Ubiquitination levels were determined by immunoblot using an ubiquitin antibody. A general increase in the ubiquitination of EGFR was observed in USP25 KD, as indicated by the normalized ubiquitin to EGFR ratio in (**Figure 24A**). The most striking increase in the ubiquitination level of EGFR was observed at three minutes post EGF (**Figure 24A**). Results were confirmed with different siRNAs in DELFIA approach, with an EGFR antibody for coating and anti-ubiquitin (FK2) as revealing antibody (**Figure 24B**). To reinforce this observation the ubiquitination status of EGFR was also assessed in selected clones of the two stable KD cell lines. A remarkable increase in EGFR ubiquitination was scored in all tested HeLa clones treated with doxycycline compared to untreated cells after three minutes of EGF stimulation (**Figure 24C**).

Furthermore, EGFR ubiquitination was assessed at different EGF concentrations. HeLa cells transiently depleted for USP25 were stimulated with increasing dose of EGF from 0.3 ng/ml up to 30 ng/ml. EGFR was immunoprecipitated and ubiquitination levels were revealed by immunoblot using an ubiquitin antibody. For all tested EGF concentration an increased number of EGFR modified with ubiquitin was observed in USP25 KD cells compared to control cells (**Figure 24D**).

Taken together our data show that depletion of USP25 causes higher ubiquitination levels of EGFR suggesting that the receptor is a direct target of USP25. Increased ubiquitination of EGFR was already scored three minutes post EGF at low and high doses of ligand concentrations.

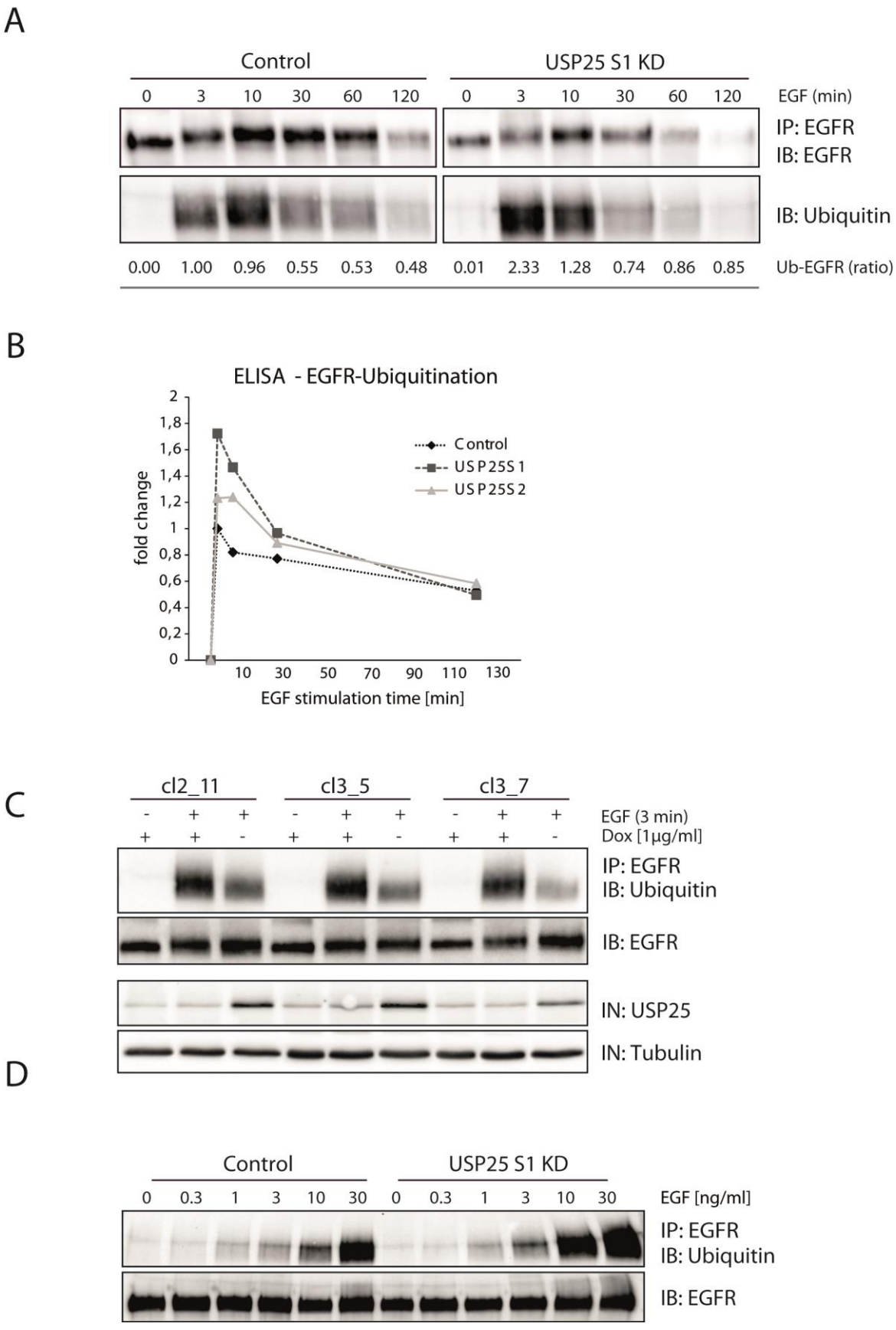

Figure 24: Ubiquitination of EGFR is increased upon USP25 knock-down.

HeLa cells were either transfected with siRNA targeting USP25 or a scrambled oligo (Control) as indicated (**A,B,D**). Stable cell lines were stimulated with doxycycline [0.5 μg/ml] to induce USP25 KD (**C**). After 72 hours cells were stimulated with high dose of EGF [100 ng/ml] (**A-C**) or with increasing EGF concentrations [0.3 – 30 ng/ml] (**D**) for the indicated time points. EGFR was immunoprecipitated using protein specific antibody and the ubiquitination status was revealed with an ubiquitin antibody (**A,C,D**). Normalization of ubiquitinated receptor versus total receptor illustrates an increase in ubiquitination upon USP25 KD as shown by numbers of ubiquitin to EGFR ratio (**A**) Alternatively, lysates were subjected to DELFIA with an EGFR antibody for coating and anti-ubiquitin as revealing antibody (**B**).

5.3 Interaction of USP25 and EGFR

To verify that EGFR is a direct substrate of USP25, we investigated a possible interaction between the two proteins in co-immunoprecipitation experiments. HeLa cells were transfected with GFP-tagged constructs, either USP25wt, the catalytically inactive mutant USP25C178A or with GFP alone as control. To induce EGFR ubiquitination, which might be essential for the interaction, cells were stimulated for three minutes with high dose of EGF [100 ng/ml]. EGFR was immunoprecipitated with a specific antibody from cell lysates. Co-immunoprecipitation was assessed either with anti-GFP or anti-USP25 antibodies (**Figure 25A,B**). For none of the tested conditions a significant binding was detected.

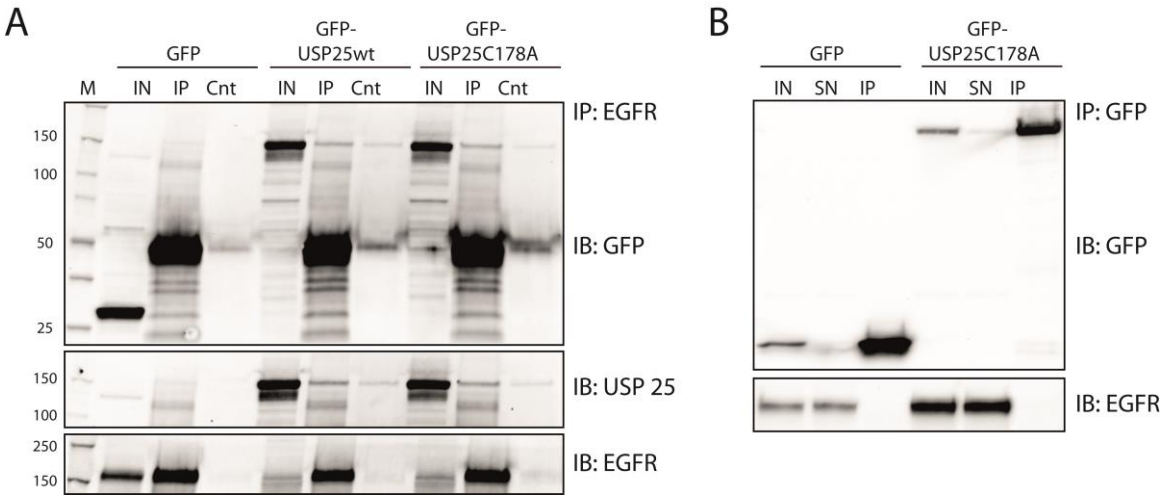

Figure 25: Co-immunoprecipitation experiments of USP25 and EGFR.

HeLa cells were transfected with GFP-USP25wt, GFP-USP25C178A or GFP, respectively. After 24 hours cells were serum starved overnight and stimulated with high dose of EGF [100 ng/ml]. Lysates were subjected to anti-EGFR (**A**) or anti-GFP (**B**) immunoprecipitation, respectively. Co-immunoprecipitation was revealed by the indicated antibodies (**A,B**).

These negative outcomes prompted us to investigate USP25 and EGFR in immunofluorescence studies. Due to the lack of an antibody suitable for immunofluorescence, we decided to generate a polyclonal anti-USP25 antibody. The antibody was produced against GST-USP25 full length protein in rabbits. Two different bleedings were tested for the specificity to detect USP25 in immunoblot analyses (data not shown). The one that gave better response was purified against the antigen and tested in control cells and USP25 KD cells in immunofluorescence experiments. To better visualize antibody specificity, USP25 KD and control cells were mixed 1:1 and seeded on coverslips. Methanol- or paraformaldehyde-fixed cells were stained with different concentrations of USP25 antibody. **Figure 26A** shows that the purified USP25 antibody specifically recognizes USP25, since HeLa control cells and cells which were depleted from USP25 are clearly distinguishable. The signal to noise ratio appeared to be better in methanol fixed cells compared to fixation with 4% PFA (**Figure 26A**). Our analyses revealed a predominantly cytoplasmic localization of USP25 in HeLa cells.

To investigate an interaction between USP25 and EGFR, internalization assays with Alexa-EGF were performed. Due to the fact that EGFR internalization is affected in USP25 KD cells and an increased EGFR ubiquitination was already observed three minutes post EGF, we assumed that an interaction between USP25 and EGFR would take place at very early time points post EGF stimulation. Hence HeLa cells were stimulated for two and three minutes with Alexa-EGF after four hours of serum deprivation. Cells were subsequently fixed with methanol and stained with USP25 antibody. Subcellular distribution of USP25 was revealed with confocal microscopy. We could not detect any changes in USP25 localization between cells stimulated with EGF and serum starved conditions (**Figure 26B**). Moreover, USP25 signal appears to be highly diffused, therefore no clear co-localization between USP25 and Alexa-EGF could be observed (**Figure 26B**).

In our analyses we were not able to establish an interaction between USP25 and EGFR. However substrate-enzyme interactions are very transient and therefore difficult to detect. The phenotype in the internalization assay suggested that USP25 and EGFR may interact at a very early time point, maybe only seconds after EGF stimulation. Thus, future experiments will entail proximity ligation and total internal reflection fluorescence (TIRF) assays.

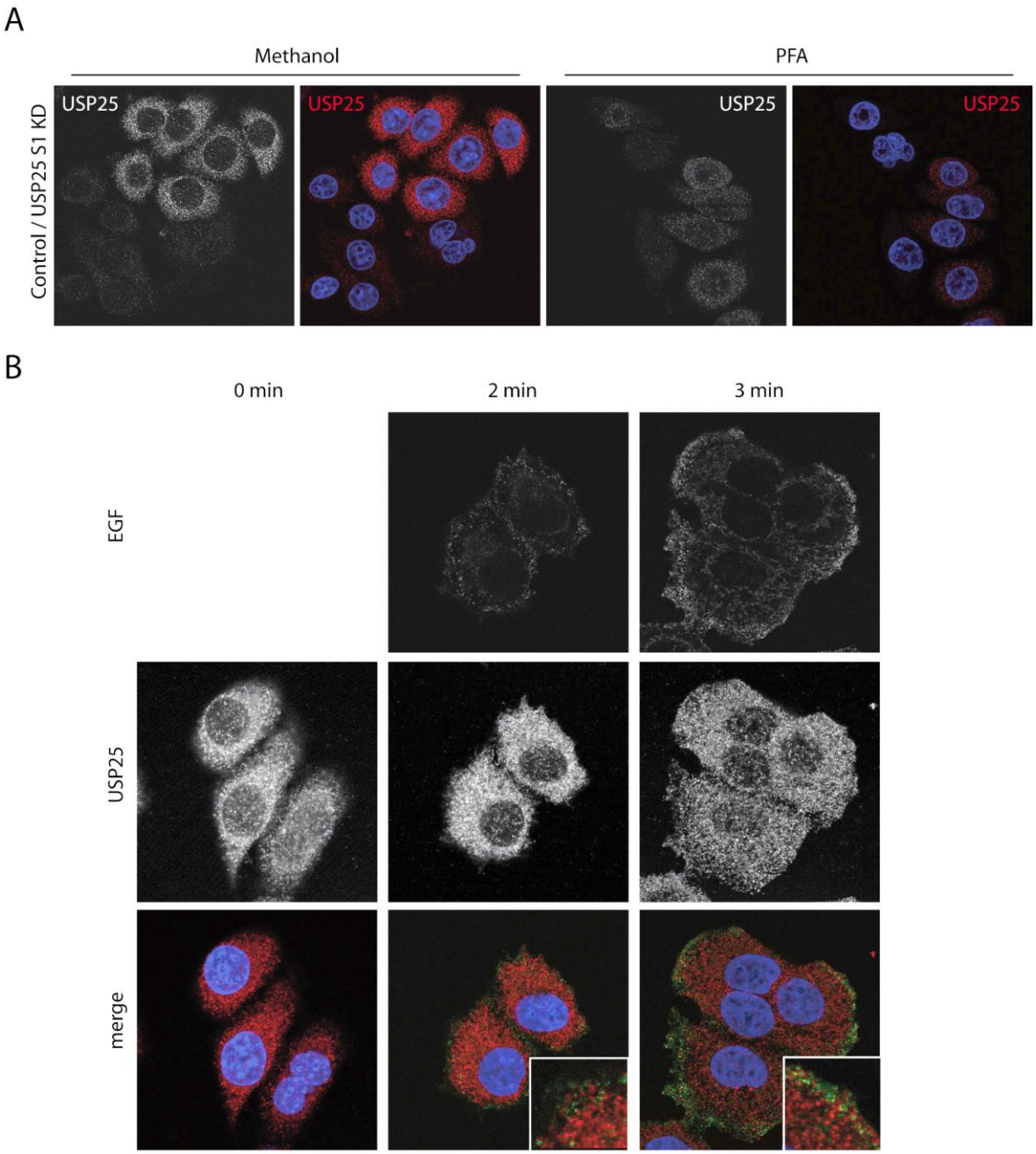

Figure 26: Subcellular localization of USP25.

HeLa cells were transfected with siRNA targeting USP25 and with a scrambled oligo (Control). KD and control cells were mixed 1:1 and seeded on coverslips. Cells were fixed with Methanol (MeOH) or with 4% paraformaldehyde (PFA) and stained with an USP25 antibody (**A**). HeLa cells were serum starved for four hours and stimulated with Alexa555-EGF [40 ng/ml, green] for the indicated time points. Cells were fixed with MeOH and stained with an USP25 antibody (red) (**B**). Blue, DAPI staining.

6 USP25 and Cullin 3

6.1 USP25 binds preferentially the neddylated form of Cullin 3

For a better understanding of the functional regulation and relevance of USP25 in EGFR endocytosis, we looked at already described substrates/interaction partners in literature. Previously, a global proteomic analysis of the DUB protein families was performed with the help of a Comparative Proteomic Analysis Software Suite (CompPASS), to identify stably associated interacting proteins (Sowa et al., 2009). One of the high-confidence candidate interacting proteins (HCIPs) identified for USP25 was the E3 ubiquitin ligase component Cullin 3 (CUL3) (**Figure 27A**). Strikingly the HCIPs comprise not only CUL3 but also four BTB domain-containing proteins which serve as substrate adaptors in the CUL3 complexes (**Figure 27A** red rectangle). Furthermore, CUL3 was recently described to be involved in EGFR endocytosis and trafficking (Huotari et al., 2012). Based on all these indications we hypothesized that USP25 deubiquitinating activity and ligase activity of the CUL3 complex could counteract each other.

As first we sought to verify the interaction between USP25 and CUL3 in GST pull-down experiments. HeLa cells were transfected with HA-CUL3, or with HA-CUL1 as negative control. To ensure that the interaction is specific for USP25, GST-tagged AMSH, a DUB known to be involved in EGFR endocytosis, was used as additional control. GST-proteins were incubated with cell lysates and binding was revealed with a HA antibody (**Figure 27B**). Strikingly, pull-down experiments revealed not only that USP25 specifically binds CUL3, but that it has a preference for the active neddylated form of CUL3 (**Figure 27B**).

A

	Z_Score	%AP_MS/MS	Ratio	WD^N_Score	Symbol
1.	146.82	1.80	3/167	39.67	USP25
2.	12.88	0.60	1/167	6.56	KCTD13
3.	12.88	0.60	1/167	6.56	USP28
4.	12.30	1.80	3/167	5.79	LOC124220
5.	7.97	2.40	4/167	2.32	BTBD9
6.	6.73	4.20	7/167	2.20	KCTD10
7.	2.67	4.80	8/167	1.93	KLHL9
8.	8.74	5.40	9/167	1.88	ANXA1
9.	5.47	9.60	16/167	1.50	KRT4
10.	7.65	3.60	6/167	1.34	WRNIP1
11.	2.52	3.00	5/167	1.31	MYO6
12.	1.63	26.90	45/167	1.08	CUL3

B

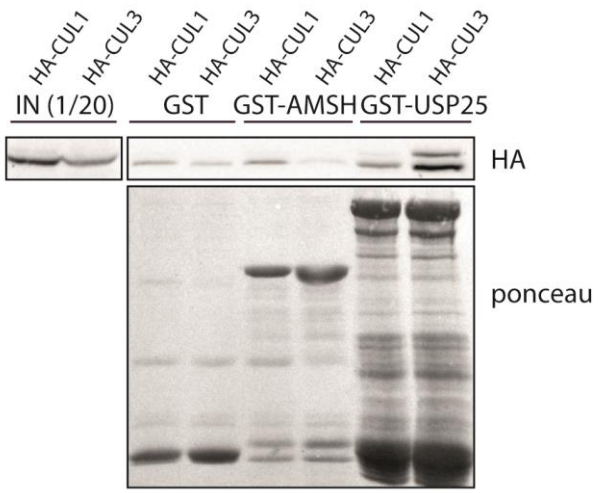

Figure 27: USP25 binds preferentially neddylated CUL3.

The twelve best hits (HCIPs) of the CompPASS DATA for USP25 published by the Harper laboratory are shown in table **A** (taken from: https://harper.hms.harvard.edu/). HeLa cells were transfected with HA-CUL3 or HA-CUL1 as negative control (**B**). The indicated GST-tagged proteins were incubated with HeLa cell lysate. GST was used as a negative control. The extent of interaction was evaluated trough IB analysis, using a specific HA antibody (**B**). Results are representative of three independent experiments.

6.2 Internalization defects upon Cullin 3 knock-down

This result prompted us to investigate if there might be a functional relationship between USP25 and CUL3, relevant in EGFR endocytosis. We performed quantitative internalization assays with iodinated ligand in cells either depleted for USP25, CUL3 or both. Internalization rates were quantified in three independent experiments in cells stimulated with high [20 ng/ml] and low dose [1 ng/ml] of EGF. The K_e was about 50% reduced in CUL3 KD cells compared to control conditions, while KD of USP25 caused an increase in EGFR internalization (**Figure 28A**), as already previously assessed (see chapter 3.3). Interestingly, depletion of CUL3 and USP25 compensate for each other, since in the double KD the measured K_e of 0.13 min^{-1} is comparable to the one in control cells (0.16 min^{-1}) (**Figure 28A**). Similar results were obtained in cells stimulated with low dose of

EGF [1 ng/ml], where only clathrin-mediated endocytosis occurs (**Figure 28B**). Of note, also the internalization of Transferrin is affected by CUL3. The endocytic rate quantified in internalization assays with I^{125}-Tf behaved analogous to the one measured for EGFR. Depletion of CUL3 caused a decrease, and USP25 KD an increase in TfR internalization, while the observed phenotypes were fully reversed in the double KD (**Figure 28C**). Moreover, immunoblot analyses revealed that downmodulation of one of the two proteins reciprocally caused an increase in the protein level of the other one, as exemplified in **Figure 28D**.

Taken together the described results show that: (i) ablation of USP25 and CUL3 have opposite effects on EGFR internalization; (ii) the observed phenotypes compensate each other in double KD; (iii) there is a transregulation between USP25 and CUL3.

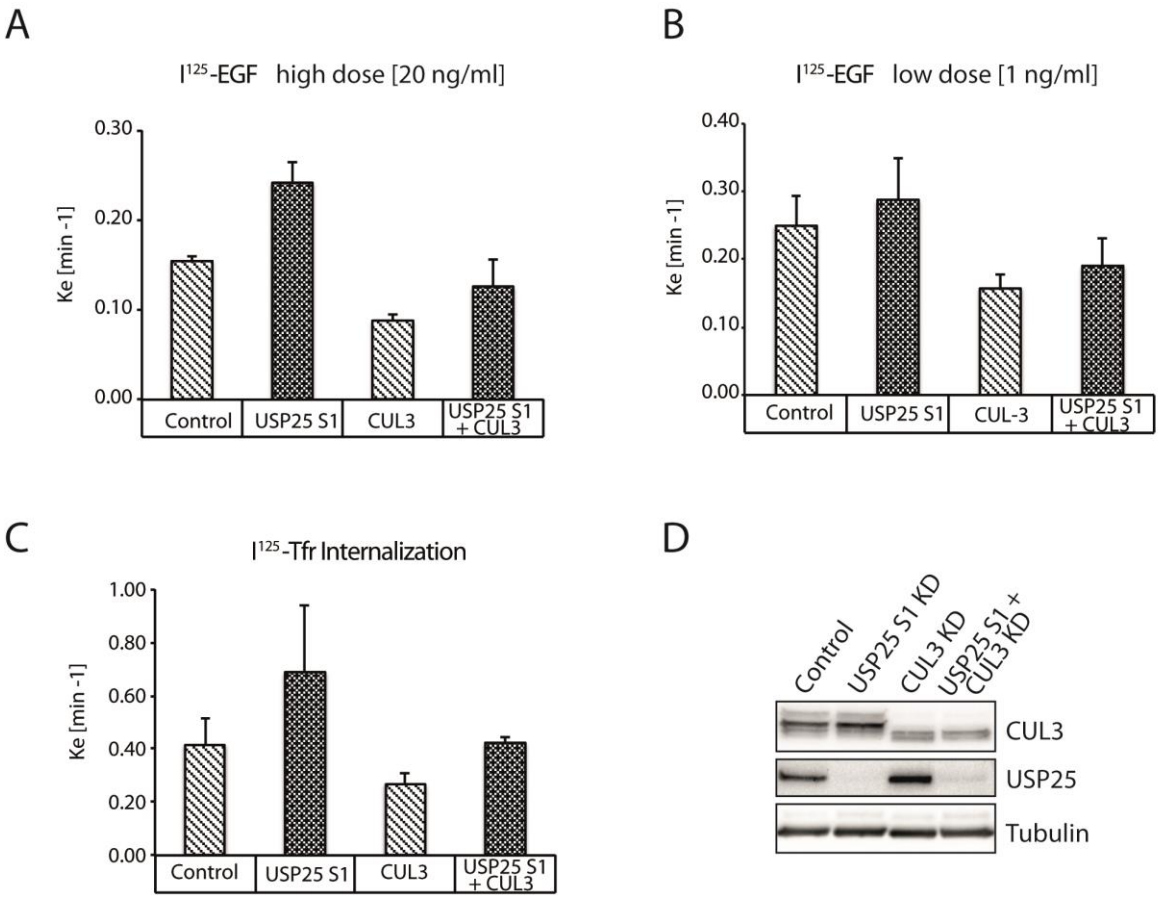

Figure 28: Altered internalization rates upon CUL3 knock-down.

HeLa cells were either transfected with siRNA targeting USP25, CUL3 or with a scrambled oligo (Control) as indicated. EGFR internalization at high [20 ng/ml] (**A**) and low [1 ng/ml] (**B**) doses of EGF ligand was followed at early time points (0-7 min) using a radiolabeled ligand binding assay and I^{125}-EGF. TfR internalization rates upon stimulation with I^{125}-Tf [1 µg/ml] were followed at early time points (0-7 min) by using a radiolabeled ligand binding assay (**C**). Internalization rates are average of three independent experiments (**A-C**). IB analyses were performed to show KD efficiency (**D**).

6.3 EGFR ubiquitination in Cullin 3 depleted cells

DUBs are often found to be associated with ubiquitin ligases (Wilkinson, 2009). Based on prior results, one could speculate that also USP25 and CUL3 are together in a complex, with opposing activity on EGFR ubiquitination. Whether the observed alterations in EGFR internalization upon CUL3 KD and USP25/CUL3 double KD cells might be caused by differences in EGFR ubiquitination levels, needs to be tested.

To induce EGFR ubiquitination, HeLa cells transiently depleted for USP25 and/or CUL3 were stimulated for three and ten minutes with high dose EGF [100 ng/ml]. Differences in EGFR protein levels and posttranslational modifications were first assessed in immunoblot analyses with an EGFR antibody. Silencing of CUL3 with two different siRNAs (CUL3 D2 and CUL3 5) caused an increase in total EGFR (**Figure 29A**), as it was already reported by the Peter laboratory (Huotari et al., 2012). We also noticed opposite effects of CUL3 and USP25 depletion on the smear towards higher molecular weight of the EGFR band upon EGF stimulation. This smear is determined by both phosphorylation and ubiquitination of the activated EGFR. In particular, less "high molecular weight smear" was observed in CUL3 KD cells suggesting a decrease in EGFR ubiquitination and/or phosphorylation (**Figure 29A**). To verify this observation EGFR was immunoprecipitated from different KD lysates stimulated for three minutes with high dose of EGF [100 ng/ml]. Modifications of EGFR with ubiquitin were assessed by blotting with

an ubiquitin antibody. IP experiments could confirm IB analyses, that EGFR is less ubiquitinated in CUL3 KD cells (**Figure 29B**). For the USP25 CUL3 double KD no clear result was obtained (**Figure 29B**).

To collect more quantitative information on EGFR ubiquitination we decided to perform DELFIA experiments. All lysates were quantified in a parallel DELFIA assay with anti-EGFR and anti-ubiquitin antibodies. Values of EGFR ubiquitination were normalized to the amount of EGFR receptors present at 0 time point (see chapter 13 in methods for details). We scored a reduction in EGFR ubiquitination of almost 50% in cells depleted for CUL3 (**Figure 29C**), confirming previously collected data (**Figure 29A,B**). A twofold increase of EGFR ubiquitination three minutes post EGF was measured in USP25 KD cells, but also upon CUL3 USP25 double KD (**Figure 29C**).

In sum data indicate that KD of CUL3 caused a decrease of EGFR ubiquitination. The fact that EGFR ubiquitination in single and double KD behaved in the same way does not confirm the initial assumption that the observed compensatory effects of USP25 and CUL3 in EGFR internalization are caused by opposing activities on EGFR ubiquitination. While these preliminary data on EGFR ubiquitination need to be repeated together with the analysis of the phosphorylation status of the EGFR, we can conclude that CUL3 has an impact on EGFR behaviour already at three minutes upon stimulation and affects receptor internalization.

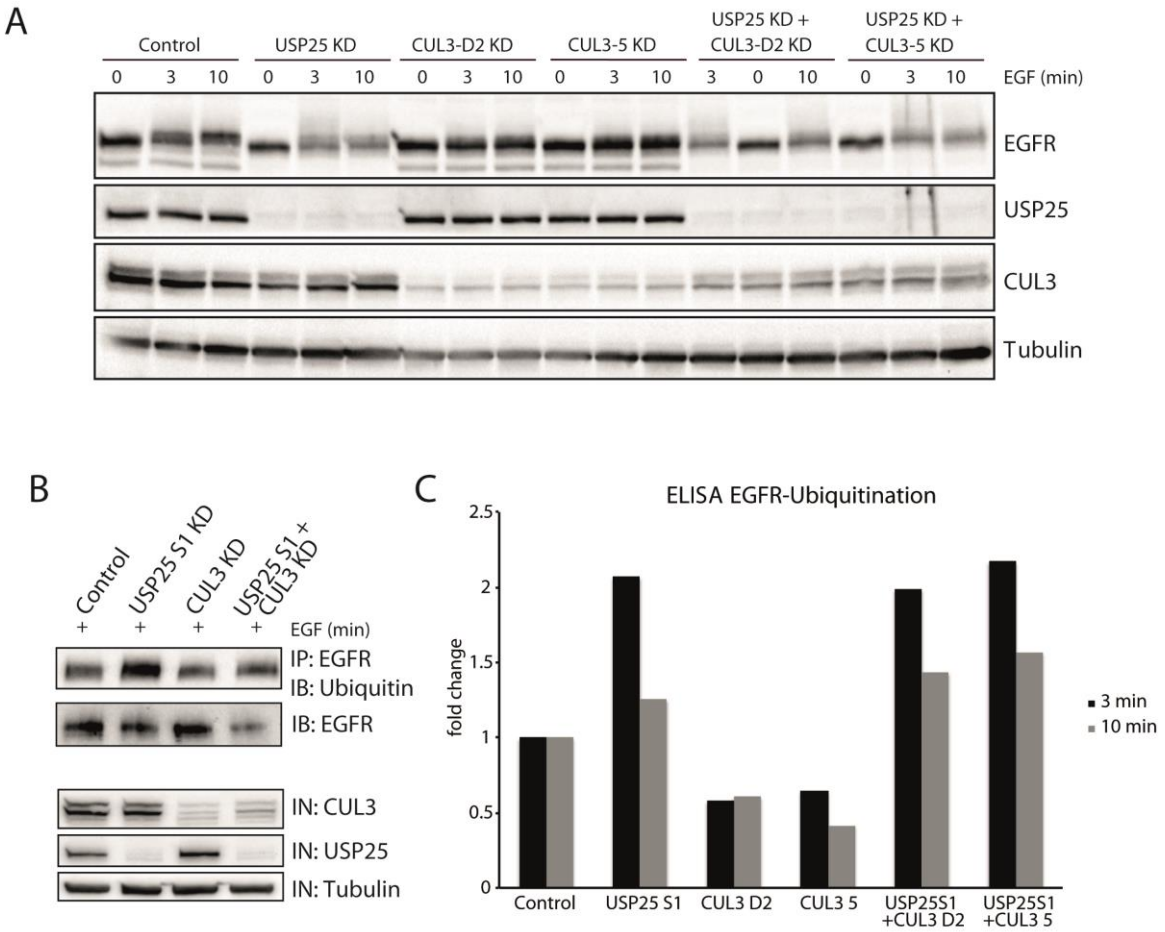

Figure 29: Impact of CUL3 depletion on EGFR ubiquitination.

HeLa cells were transfected with siRNAs targeting USP25 (S1), CUL3 (5 and D2) or with a scrambled oligo (Control) as indicated. After serum starvation overnight, cells were stimulated with EGF [100 ng/ml] for the indicated time points. Total cell lysates were analysed by IB with the indicated antibodies (**A**) or subjected to DELFIA (**C**). To determine EGFR ubiquitination, anti-EGFR antibody was used for coating and anti-ubiquitin as revealing antibody. Results are normalized to serum starved conditions and expressed as fold change in respect to control cells (**C**). Results are representative of two independent experiments. EGFR was immunoprecipitated from total cell lysates stimulated for three minutes with high dose of EGF [100 ng/ml] using protein specific antibody. The EGFR ubiquitination status was revealed with an ubiquitin antibody (**B**).

DISCUSSION

1 Screening for novel DUBs involved in EGFR endocytosis

Ubiquitination plays a fundamental role in the regulation of EGFR endocytosis. EGFR was one of the first endocytic cargo which was described to be modified with ubiquitin (Galcheva-Gargova et al., 1995). Upon binding of its cognate ligands EGFR is ubiquitinated by Cbl E3 ligases. For the early internalization steps, ubiquitination of the receptor appears to be either essential (Sigismund et al., 2005) or sufficient but not required (Goh et al., 2010), depending on the endocytic pathway. By contrast, sorting and trafficking of the internalized receptor into the lysosomal degradation pathway is clearly ubiquitin-dependent (Huang et al., 2006; Huang et al., 2013). This last step promotes downmodulation of the receptor and is crucial for signal attenuation and the maintenance of normal cell physiology. Moreover, various adaptor proteins along the endocytic route are known to be a target of ubiquitin modification upon ligand stimulation. In the regulation of these proteins and throughout the endocytic steps of the EGFR, DUB-mediated removal of ubiquitin plays an important role. Until now, we have few clues regarding the identity and exact functions of DUBs involved in the endocytic process. This work represents a contribution to the investigations of DUB-mediated regulation of endocytic processes upon EGFR activation. In a genome-wide siRNA screen targeting all known active DUBs, we found twelve DUBs affecting EGFR degradation kinetic, which were not described yet (**Figure 11**). This number of identified enzymes is not surprising in light of the complexity of EGFR regulation. Similar to the results of our screen, for the HGF-Receptor (Met) up to 12 DUBs have been identified to orchestrate multiple steps of the Met activation response (Buus et al., 2009).

DUBs may affect EGFR fate either directly, acting at the various step of the endocytic pathways or indirectly, impinging on feedback regulatory loops active on the EGFR pathway (Avraham & Yarden, 2011). In this context it needs to be mentioned that

the screen reported here did not consider the requirement of the catalytic activity of the DUBs. Therefore it is conceivable that some of the measured alterations in EGFR degradation kinetics are independent of deubiquitinating activity and might be due to scaffolding or other catalytic independent functions of DUBs. One example for a catalytically independent function of a DUB is given by USP13. It was demonstrated that USP13 inhibits the activity of the E3 ligase Siah2. This effect depends on the UBDs of USP13 but is independent of its deubiquitinating activity (Scortegagna et al., 2011).

Nowadays siRNA screens in mammalian cells are a common tool for "loss of function" studies. Indeed other groups have performed similar siRNA-based DUB screens. A screen conducted by the Urbe' laboratory investigated the effects of DUB KDs on steady state levels of ErbB2 through immunoblots (Liu et al., 2009). After the validation procedure a single enzyme, the proteasome-associated POH1, was confirmed to influence ErbB2 levels. Duex and Sorkin reported a screen in which not only DUBs but also other genes related to deubiquitination were included (Duex & Sorkin, 2009). They assessed EGFR levels present on the cell surface at a single time point post EGF in immunofluorescence experiments. This screen identified USP18 as an EGF-independent regulator of EGFR biosynthesis based on its role in EGFR mRNA translation (Duex & Sorkin, 2009). The rather high number of DUBs identified in our screen might be based in a different design of the assay. Instead of only steady state levels we monitored EGFR degradation kinetics, which led us to unravel DUBs involved in several ligand-dependent endocytic steps of EGFR. In addition to immunoblot experiments our screen was accomplished by a second approach, DELFIA analyses that allowed us to quantify EGFR degradation kinetics in a more precise way (**Figure 11B**). In this sense it appears to be more complete of one generated by Pareja et al. in which the authors assessed EGFR degradation kinetics upon stimulation with EGF in a similar way to our screen and

identified Cezanne-1 (OTUD7B) as negative regulator of EGFR turnover (Pareja et al., 2012).

The relative small numbers of DUBs and the fact that they are suitable "druggable" targets makes them to eligible subjects of genome-wide siRNA screens. Nevertheless the usage of siRNAs has a number of limitations. One problem is the transient inhibition of gene expression due to the unstable nature of siRNAs. We tried to overcome this by employing stealth siRNAs from Invitrogen. These oligos are chemically modified resulting in increased longevity and stability in cells. To ensure optimal KD efficiency we performed two consecutive rounds of transfection. The major concern when conducting siRNAs in particular in large scale is the risk of unspecific off-target effects. Therefore an extensive validation procedure was included in the screen. The initial data-set of IB quantifications and ELISA values revealed that 24 of the 82 screened enzymes influenced EGFR degradation kinetics (**Figure 11**). As a first validation step deconvolution experiments were performed (**Appendix Figure 1**) and KD efficiency was assessed by qRT-PCR (**Table 1**). Both approaches are compulsory to rule out off-target effects. Indeed almost ten of the positive hits from the initial screen could not be confirmed. This was either based on differences in the behaviour of the two siRNAs revealed in the deconvolution or on unspecific effects in the absence of a good level of protein depletion.

Ubiquitination events are involved in a broad spectrum of processes; therefore not only protein stability but also transcriptional and translational activity can be affected by knocking down DUBs, as it was described for USP18 (Duex & Sorkin, 2009). Therefore, we included an additional qRT-PCR screen looking directly on EGFR transcription upon DUB KD. Indeed, 4 out of 24 DUBs showed strong alteration in EGFR transcription that need be further investigated at the single DUB level.

Ultimately 15 out of 82 passed all validation steps confirming that they have an impact on EGFR turnover upon EGF stimulation. Beside the identification of yet unknown

DUBs, we were able to confirm previously published data, including AMSH and USP8, as well as USP2 and Cezanne-1 (Liu et al., 2013; McCullough et al., 2004; Pareja et al., 2012; Row et al., 2006), corroborating the reliability of the methods chosen for the screen and the validation procedure. Thus our screen represents a valuable source for future in-depth studies on specific DUBs to dissect their specific functions in EGFR endocytosis as we already started it in the case of USP25 and USP10 (see the Appendix).

2 USP25 a new DUB controlling EGFR turnover

2.1 Knock-down of USP25 enhances EGFR degradation kinetics

Based on the results of the siRNA screen and the validation procedure in which USP25 KD significantly enhanced EGFR degradation kinetics, we decided to further characterize the function of USP25 in EGFR endocytosis. Quantitative analyses of DELFIA and immunoblot experiments unravelled that there is an enhanced EGFR degradation rate, which is already detectable at early time points post EGF stimulation (like 10 and 30 minutes). Furthermore an increase in the total amount of EGFR degradation as exemplified at later time points (60 and 120 minutes) was assessed (**Figure 12**). In control cells approximately 40% of the initial amount of EGFR remained intact after 120 minutes of EGF induction, whereas in USP25 KD cells only 20-30% of EGFR was present at the same time point. If USP25 has also an effect on the EGFR net degradation would need further studies with later time points, in order to reach the steady state level of EGFR degradation.

Internalized receptors can be either recycled back to the PM or are degraded in lysosomes. The major signal for sorting into the lysosomal degradation pathway is the attachment of ubiquitin to the cargo. Therefore an increase in the net degradation could be caused by increased ubiquitination. Indeed, we found that upon USP25 KD EGFR is more ubiquitinated compared to control cells (**Figure 24**), which probably accounts for the

higher amount of degraded EGFR. Furthermore, we found that also the internalization of EGFR is affected upon USP25 KD. Quantitative radioactive internalization assays and immunofluorescence analyses revealed that we have an increased internalization rate but also a faster trafficking of EGFR in cells depleted for USP25 (**Figure 14** and **Figure 17**). Endocytic adaptor proteins involved in early internalization steps of EGFR, like Eps15, Epsin1 and Epsin2, are located at the PM. Via their intrinsic UIMs (Polo et al., 2002) they undergo coupled monoubiquitination (Woelk et al., 2006), a process that is needed for EGFR internalization (Savio et al., manuscript in preparation). We did not observe any increased monoubiquitination upon USP25 KD, disproving the hypothesis that this DUB may work directly on such substrates. Nonetheless, Eps15, Epsin1 and Epsin2 bind to ubiquitinated EGFR, facilitating its internalization (Sigismund et al., 2005). It is reasonable to assume that an increased ubiquitination of EGFR results in an increased internalization rate based on an augmented association between the receptor and the endocytic adaptor proteins. Whether this explanation accounts also for the faster trafficking and degradation of EGFR or if those are uncoupled events, needs to be further tested. To gain insight into this issue one possibility is to perform trafficking and/or degradation experiments only with a pool of already internalized receptors. After a pulse of labelled EGF, residual ligands are removed from the medium and only the internalized receptor-ligand complexes are further monitored. These conditions compensate for alterations in the internalization, and should give an answer if the different alterations in EGFR internalization, trafficking and degradation upon USP25 are causative or uncoupled events.

2.2 USP25: a novel DUB at the plasma membrane?

The overexpression of USP25 displayed the reverse phenotype observed under KD conditions and EGFR internalization is delayed in cells overexpressing USP25wt at early time points (**Figure 15**). Based on this result we assumed that USP25 is involved in early

steps of EGFR internalization. Moreover, the most remarkable increase in EGFR ubiquitination could be observed already three minutes post EGF stimulation (**Figure 24**). In line with this observation the phosphorylation peak of Hrs is anticipated in USP25 KD cells (**Figure 13**). Taken together our data indicate that USP25 should work at the PM, or it might be recruited to the PM upon EGFR activation. In an attempt to investigate whether USP25 is active at the PM, we immunoprecipitated EGFR from cells depleted for USP25 alone, or in combination with KD of dynamin (data not shown). Ablation of dynamin blocks the EGFR internalization, thus the comparison of the EGFR ubiquitination levels should allow to define whether USP25 deubiquitinates EGFR already at the PM. Unfortunately these experiments were not conclusive due to technical difficulties. As next we raised a polyclonal antibody against USP25 in rabbits, to visualize the localization of endogenous USP25 in cells unstimulated or stimulated with EGF at different time points. Unfortunately we could not score any clear staining of USP25 at the PM or relocalization upon EGF stimulation (**Figure 26**). One technical problem which might prevent the detection of co-localization events between USP25 and Alexa-EGF could be the fixation with MeOH. We found that for our USP25 antibody the signal to noise ratio in immunofluorescence is much better in cells fixed with MeOH compared to paraformaldehyde-fixation. However MeOH destroys the native conformation of proteins which results in a decreased signal of fluorescent dyes as it happened in the case of Alexa-EGF at least for the early time points. Another issue in the assessment of co-localization between USP25 and EGFR in immunofluorescence-based internalization assays might be poor level of USP25 expression. Global mRNA and protein abundance analyses in 3T3 cells suggest that USP25 is one of the low abundant DUBs with only a few hundred copy numbers per cell (Schwanhausser et al., 2011). Low protein levels of USP25 might complicate the detection of USP25. To overcome the described difficulties we are planning proximity ligation assays (PLA) (Leuchowius et al., 2009) with antibodies against USP25

in endogenous condition or anti-tag in the overexpressed condition in combination with anti-phospho-EGFR to localize activated receptors. Based on signal amplification PLA is a very sensitive method, which enables the detection of transient interactions as it is the case for the binding of enzymes to their substrates.

To prove the specificity of the phenotypes mediated by the used siRNAs and to rule out off-target effects, rescue experiments, in which USP25 expression is re-introduced after depletion, are needed. For this purpose we engineered a stable cell line in which the expression of USP25wt or the catalytic inactive mutant USP25C178A can be induced. Unfortunately, high protein levels of USP25 caused lethality, as we observed in cells transiently or stably expressing tagged-USP25 constructs. The treatment of the stable cell lines with the proteasome inhibitor MG132 revealed that the expression of USP25 is prevented by proteasomal degradation of exogenous USP25 (**Figure 16B**). Taken together these results suggest that aberrant protein levels of USP25 are harmful for cells.

Although rescue experiments are missing so far, the wealth of the collected data consistently indicates that the observed phenotypes upon USP25 KD are due to the lack of USP25 protein. All key experiments like the assessment of the internalization rate or the ubiquitination level of EGFR in USP25 KD cells were confirmed with four distinct siRNAs, targeting different sequences of the USP25 mRNA (**Figure 17**, **Figure 18** and **Figure 24**).

2.3 Dissection of EGFR internalization pathways affected upon USP25 knock-down

There are multiple ways to endocytose activated EGFR. In the past our group discovered a clathrin-independent internalization pathway (NCE) for the EGFR that is activated after stimulation with high dose of EGF (Sigismund et al., 2005). Our quantitative internalization assays revealed that ablation of USP25 leads to an almost twofold increase of the EGFR internalization rate at high dose of EGF [20 ng/ml], in conditions in which

both internalization pathways (NCE and CME) are known to be active. Also at low dose [1 ng/ml], in which endocytosis occurs only through CME (Sigismund et al., 2008; Sigismund et al., 2005), the observed internalization rate of EGFR is less pronounced but still significantly increased. At first glance this seems to suggest that USP25 plays a role in both, CME and in NCE pathway.

CME is typically faster than NCE with a measured rate constant (K_e) of about 0.3 min^{-1} in HeLa cells (Sigismund et al., 2005). Kinetic analysis of EGFR endocytosis suggested that CME is saturated when a large number of surface EGFRs are activated by EGF, and the contribution of the slower NCE pathway leads to a reduction in the apparent internalization rate (Wiley, 1988). Our data are consistent with the idea that the increased internalization rate measured upon KD of USP25 is due to an increased capacity of the CME pathway. As a consequence the K_e at high dose of EGF would also be increased. In cells stimulated with high dose of EGF, a condition where many receptors are activated, about 60% of the internalized EGFR occurs via CME. The remaining 40% is accomplished by the NCE pathway. A shift in this contribution towards CME would result in an increased K_e at high dose, with values typically measured at low dose, where only CME is active. In this case USP25 would regulate the protein stability of an unknown positive factor essential for clathrin-mediated endocytosis. This protein has to be a limiting factor in EGFR internalization via CME. Depletion of USP25 would increase the protein level thus enhancing the internalization rate of EGFR. One obvious candidate would be Cbl. This E3 ligase is indeed a limiting factor for EGFR ubiquitination (Sigismund et al., 2013) and is indeed ubiquitinated and degraded at later time points (Magnifico et al., 2003). However, no obvious difference in the level of Cbl expression was seen upon USP25 KD (**Figure 23B**).

To further dissect the impact of USP25 in different endocytic routes, we switched off either NCE or CME pathway separately, through siRNA-mediated ablation of essential

components of the clathrin-dependent and -independent internalization of EGFR (CHC and Reticulon3, respectively). Neither clathrin ablation nor Reticulon3 depletion is able to completely reverse the increased K_e measured upon USP25 KD. Based on these results we can envision two possible scenarios. In the first one, USP25 impinges on both CME and NCE pathways. In the second one USP25 is involved in a third pathway that is hyperactivated in its absence. To better discriminate between these two possibilities, we knocked-down dynamin. The GTPase dynamin is an essential component for both CME and NCE, while other described internalization pathways are dynamin independent (Howes et al., 2010). To switch off NCE and CME at the same time, we performed quantitative internalization assays with cells depleted for dynamin and USP25. In addition, we defined the internalization rate in HeLa cells triple KD for USP25, clathrin and reticulon. Also in this case CME and NCE should be abrogated at the same time. In both approaches the increased internalization rate upon USP25 KD was not fully reversed by the simultaneous interference with dynamin or clathrin and reticulon, respectively (**Figure 22**). This suggests that the measured alterations of EGFR internalization in cells silenced for USP25 are indeed caused by the presence of a third dynamin-independent endocytic route for EGFR. It seems that this pathway is only activated upon USP25 inactivation. According to the literature there are several dynamin-independent internalization pathways, including the CLIC/GEEK-, flotillin-, and the Arf6-mediated pathway (Kumari et al., 2010). To verify the hypothesis of dynamin-independent EGFR internalization upon depletion of USP25, it should be examined if inhibition of the aforementioned pathways has an effect on EGFR endocytosis in USP25 KD cells.

It needs to be point out that all experiments are based on siRNA-mediated depletion of proteins to inhibit CME and/or NCE. Although this is a potent tool to downregulate endogenous protein levels, protein depletion never reached 100% efficiency. In immunoblot analyses small amounts of remaining protein upon siRNA treatment were

observed. Furthermore the simultaneous interference of two or more proteins is often less efficient compared to single KD. Thus we cannot exclude that the residual protein levels are sufficient to support the observed EGFR internalization. One possibility to overcome this problem would be complementary studies using chemical inhibitors, e.g. dynasore is a potent inhibitor of dynamin I and II (Macia et al., 2006). In addition to the above discussed difficulties in protein depletion via siRNA it needs to be mentioned that in general the observed effects on EGFR internalization in low dose conditions, where only CME is active, are rather small compared to the assessed alterations at high dose. That it might be still possible that USP25 is only working in the NCE of EGFR. Consistent with this is that ubiquitination of EGFR is crucial in this pathway while it is not essential for EGFR uptake via CME (Sigismund, et al., 2005). Therefore one can assume that USP25 impinges mainly in the NCE pathway since a proper regulation of DUB activity might be more critical in the non-clathrin endocytosis of EGFR.

2.4 USP25 and the Transferrin receptor

The Transferrin receptor (TfR) is one of the best described cargoes and exclusively internalized via CME (Pearse & Robinson, 1990). This makes the TfR to a well-established tool to examine alterations in clathrin-mediated endocytosis. Here we were using radioactively labelled Transferrin (I^{125}-Tf) to control the impact of USP25 on the CME pathway. We observed that similar to EGFR also the internalization rate of TfR was about twofold increased in cells depleted for USP25 compared to control conditions (**Figure 21A**). However saturation binding assays as well as immunofluorescence analyses (data not shown) revealed that the cell surface levels of TfR are tremendously decreased in cells depleted for USP25 (**Figure 21B**). By inhibiting the proteasome and/or lysosomal degradation in USP25KD cells, we were not able to restore TfR proteins to normal cellular levels (data not shown). On the other hand, qRT-PCR analyses revealed that the lower TfR

protein expression might be rather due to alterations in the TfR transcription than to an increased degradation and/or a failure in recycling of TfR (**Figure 21C**). This low number of TfR at the plasma membrane has to be considered once discussing its altered internalization rate. Although the K_e is independent of receptor affinity and cell surface number, one crucial point is that the quantity of surface-bound ligand must remain approximately constant during the experimental measurement (Wiley & Cunningham, 1982). This condition is presumably not given in USP25 KD cells where less than 20% of Transferrin receptors are present on the cell surface in cells depleted of USP25 compared to control cells (**Figure 21B**) and saturating conditions might be reached. Thus, we cannot exclude that the changes in TfR internalization rates upon USP25 KD are due to different starting numbers of surface TfRs. Consequently we could not use TfR internalization to get a final conclusion about a general role of USP25 in clathrin-mediated endocytosis.

The number of DUBs is greatly outnumbered by the E3 ligases. This suggests that each DUB has multiple targets and might be involved in the regulation of multiple different processes. Therefore, we can conclude that alterations in EGFR and TfR turnover presumably originate from dissimilar cellular roles exerted by USP25 on these different receptors. It would be interesting to test whether KD of USP25 would lead to enhanced internalization of other receptors such as the insulin-like growth factor 1 receptor (IGF-1R) (Backer et al., 1991; Prager et al., 1994) or FGFR and VEGFR (Haugsten et al., 2011; Lanahan et al., 2010) for which alternative pathways and sensitivity to ligand concentration has been demonstrated.

2.5 Ubiquitin and USP25 and their role in EGFR endocytosis

The role of ubiquitin in EGFR endocytosis is object of a long-standing debate. Although c-Cbl activity, the major E3-ligase of EGFR, seems to be necessary for EGFR internalization, is it not clear whether this is based on a direct ubiquitination of EGFR or

rather on adaptor functions executed by c-Cbl in the endocytic process of EGFR (Huang et al., 2006; Levkowitz et al., 1999; Zeng et al., 2005). Indeed it was demonstrated that a 16KR mutant of EGFR, in which 15 Lys residues within the kinase domain were mutated to Arginine, is only marginally ubiquitinated but internalized at a normal rate (Huang et al., 2007). By using an in-frame fusion of ubiquitin to EGFR, other studies could show that monoubiquitination of EGFR appears to be sufficient to induce its internalization. This EGFR chimera was constitutively internalized and resulted in an enhanced degradation (Haglund et al., 2003; Mosesson et al., 2003). At first glance these findings seem to be contradictory, but might be indicative of the presence of multiple redundant mechanisms (Acconcia et al., 2009). In the case of EGFR endocytosis, this includes ubiquitination of Lys residues in the intracellular kinase domain of the receptor, but also the interaction of the receptor with the AP2 complex and with the adaptor protein Grb2, as well as acetylation of C-terminal Lys residues (Goh et al., 2010). It is likely that not all mechanisms are simultaneously activated and that certain mechanisms are preferentially engaged under physiological conditions. Therefore the relative contribution might vary depending on the cell type, on the utilized internalization pathway and on different stimuli, e.g. type and concentration of ligands.

In the present study we demonstrate that depletion of USP25 results in increased EGFR ubiquitination, suggesting that the receptor itself is a direct target of USP25 deubiquitinating activity (**Figure 24**). Moreover we found that this correlates with an increased internalization rate at high but also at low dose of EGF stimulation and that CME and NCE are not directly implicated. It is likely that the detected increase of EGFR ubiquitination and the increased internalization rate of EGFR are not only correlative but causative. This is also supported by the observation of increased EGFR ubiquitination levels at lower EGF concentrations in cells depleted for USP25 compared to control cells (**Figure 24D**).

EGFR ubiquitination is a signal for downregulation via lysosomal degradation (Acconcia et al., 2009). KD of USP25 results not only in an increased internalization but also in an increased degradation of EGFR. Together with the higher EGFR ubiquitination levels assessed in USP25 KD cells, it seems to be plausible that depletion of USP25 orchestrates the ratio of receptor recycling and receptor degradation. Our data indicate, that based on higher ubiquitination levels of EGFR upon USP25 KD, more receptors are shuttled to lysosomes and are subsequently degraded. It would be interesting to know whether this is also true for cells stimulated with low dose of EGFR, where under normal conditions only a small portion of EGFR is degraded.

An increase in EGFR ubiquitination can be either accomplished by an increased activity of E3 ligases or by a diminished deubiquitination of the receptor. None of the tested E3 ligases described to be involved in EGFR endocytosis displayed major changes upon USP25 KD (**Figure 23B,C**). Thus, we think that EGFR is indeed a direct target of USP25 and that the lack of USP25 results in higher EGFR ubiquitination levels. Another theoretical possibility would be that USP25 regulates the stability of an alternative DUB of EGFR. Depletion of USP25 would result in enhanced degradation of this hypothetical enzyme and consequently in increased EGFR ubiquitination. Although we have not formally tested this possibility we think that this is rather unlikely.

Overall DUB activity can have different functions: they (i) process ubiquitin precursors, (ii) rescue substrates from degradation, (iii) recycle ubiquitin from cargoes destined for proteasomal or lysosomal degradation (iv) but their function is also essential in the editing of polyubiquitin chains (Reyes-Turcu et al., 2009). Mass spectrometry analyses revealed that EGFR is monoubiquitinated at multiple Lys residues within the kinase domain but also polyubiquitinated with Lys63-linked chains (Huang et al., 2006). As typical for E3 ligases of the RING-type also Cbl proteins seem to be rather linkage unspecific. Furthermore the mechanism how Cbl E3 ligases mediate mono- rather than

polyubiquitination is not defined yet. Thus it seems to be likely that DUBs are involved in the trimming of polyubiquitin chains to monoubiquitin and/or selectively remove polyubiquitin chains with other linkages than Lys63. USP25 can cleave both Lys63 and Lys48 chains (Zhong et al., 2013b) and it was suggested that the UBDs of USP25 preferentially bind to Lys48 linked polyubiquitin chains (Nathan et al., 2013), supporting a model in which USP25 modifies the ubiquitin signals on EGFR. In this case the lack of USP25 would result in increased ubiquitination levels of EGFR with a specific linkage type. To test this hypothesis we need to compare the abundance of differently linked polyubiquitin chains on EGFR in USP25 KD and control cells by either antibodies against specific chains (Lys63, Lys48 and Lys11, provided us by Genentech) or by mass spectrometry analyses using the AQUA methodology (Maspero et al., 2013).

The described hypothesis opens also the possibility that upon USP25 KD EGFR might be not exclusively degraded in lysosomes, as it is the rule under normal conditions. Due to "atypical" modifications with other polyubiquitin chains than Lys63, EGFR degradation might occur in an abnormal way in USP25 KD cells. Most of the available data indicate that EGFR degradation takes place in lysosomes. However, some studies have demonstrated that the inhibition of the proteasome blocks the degradation of the EGFR as well. Increased K48-linked polyubiquitination of EGFR at the plasma membrane may cause its extraction (possibly via p97 ATPase (Meyer et al., 2012)) and a temporal increase of internalized receptors that could account for the increased internalization rate observed in the absence of USP25. Indeed it is easy to envision a "quality control" mechanism at the plasma membrane similar to the one occurring at the ER (ERAD pathway reviewed in (Lemus & Goder, 2014)). To get insights in a possible role of a proteasomal degradation of EGFR upon KD of USP25, it would be interesting to investigate if the increased EGFR degradation in USP25 KD cells can be rescued by the treatment with lysosomal versus proteasomal inhibitors.

3 Cullin 3 and USP25: is there a functional relationship regulating EGFR endocytosis?

In search of potential interaction partners to further investigate the functional role of USP25 in cells, we got attracted by the CompPASS data of the Harper laboratory (Sowa et al., 2009). Almost half of the best hits (HCPIPs) comprehends Cullin 3 (CUL3) itself plus a number of BTB-containing proteins which serve as substrate adaptors in CUL3 E3 ligase complexes (**Figure 27A**). DUB function is in general opposing E3 ligase activity and these two types of enzymes are often found to be associated in complexes (Ventii & Wilkinson, 2008). Moreover, a recent publication describes a regulatory role of CUL3 in EGFR and influenza A virus (IAV) endocytosis (Huotari et al., 2012). In GST pull-down experiments we could verify that there is an interaction between USP25 and CUL3 (**Figure 27B**). Strikingly, USP25 binds the neddylated form of CUL3 preferentially. Conjugation of NEDD8 to Cullin complexes results in an activation of the E3 ligase due to conformational changes (Duda et al., 2008). Our data demonstrate that the binding of USP25 to the active form of CUL3 is specific and not only mediated by NEDD8 alone, since USP25 did not bind CUL1 even in its neddylated form (**Figure 27B**). Moreover USP25 was not able to bind free NEDD8 (data not shown).

We found that KD of CUL3 results in a decreased internalization rate of EGFR thus displaying the reverse effect on EGFR internalization to USP25 KD (**Figure 28**). The double KD of CUL3 and USP25 suggested that the two proteins possess opposing activity on EGFR internalization, since the quantified K_e was almost restored to control conditions at high but also at low dose of EGF stimulation (**Figure 28A,B**). Moreover immunoblot analyses revealed that depletion of one of the two proteins results in increased protein levels of the other, indicating a transregulation (**Figure 28D**). Of note, the assessed decreased internalization rate upon CUL3 KD is not in line to what was reported by Huotari et al. (Huotari et al., 2012). In this publication the depletion of CUL3 leads to

accumulation of EGFR in the late endocytic compartment, while the internalization of EGFR is not affected. Their proposed working model suggests a defect in endosome maturation in cells depleted for CUL3. The discrepancy to our results can be explained by the employment of different methods to unravel the impact on EGFR internalization. Huotari et al. performed immunofluorescence-based internalization assays to monitor EGFR fate. With this method only internalized receptors can be followed without considering the number of receptors on the cell surface bound to EGF. We instead employed radioactive labelled EGF to quantify the internalization rate of EGFR in CUL3 depleted cells (**Figure 28**). The internalization rate K_e is based on the ratio of surface bound EGF to internalized EGF, measured at early time points post EGF stimulation. This assay allows a more precise quantification of the endocytic internalization kinetics of EGFR. We indeed observed strong effects on the EGFR internalization already at three minutes post EGF, a condition that was not tested by Huotari et al..

Based on the interaction of CUL3 and USP25 and the observed defects in EGFR internalization, we assumed that USP25 and CUL3 might form a complex to regulate EGFR ubiquitination. In immunoblot as well as in DELFIA analyses we observed a decreased ubiquitination of EGFR in CUL3 KD cells, a reverse phenotype compared to cells depleted for USP25 (**Figure 29**). It needs to be mentioned that also these data are conflicting to immunoprecipitation experiments from Huotari et al., where no differences in EGFR ubiquitination upon CUL3 depletion were described. KD of CUL3 increases EGFR expression levels in cells, complicating the immunoprecipitation of equal protein amounts even under limiting conditions (**Figure 29B**) (Huotari et al., 2012). Therefore we applied DELFIA analyses in which the ubiquitination of the receptor was normalized to the number of EGFR present in the different KD lysates (**Figure 29C**).

Our assumption that CUL3 and USP25 possess opposing activity on the ubiquitination of EGFR implies that in double KD cells the ubiquitination of EGFR should

be restored to the levels in control conditions. Our data unfortunately did not confirm this idea. In the USP25 and CUL3 double KD, the ubiquitination of EGFR was elevated similar to USP25 KD alone (**Figure 29C**). We observed that KD of CUL3 appeared to be less efficient in double KD compared to the single KD, while we did not score any differences in USP25 protein levels for the two conditions (**Figure 29A**). The residual protein levels of CUL3 in double KD cells might be sufficient to increase EGFR ubiquitination. Overall it needs to be mentioned that depletion of CUL3 is always critical for cells homeostasis due to important regulatory functions exerted by CUL3 in cell cycle control (Sumara et al., 2008). Thus, we cannot exclude that the occurrence of alterations in EGFR endocytosis might be a secondary effect.

Another conclusive explanation which would explain the assessed alterations in EGFR internalization would be that USP25 is a target of a CUL3 based E3 ligase complex, controlling USP25 protein stability. As a result of the lack of CUL3 USP25 protein levels would be increased, resulting in a delayed EGFR internalization rate. Indeed we scored a decreased Ke for EGFR upon CUL3 KD (**Figure 28A,B**) and increase in USP25 protein levels in cells depleted of CUL3 (**Figure 28D**), supporting this possibility.

Another interesting hypothesis is that CUL3, being part of the "quality control" mechanism at the plasma membrane, may attach Lys48-linked chains to the EGFR. These signals can be then edited by USP25. In absence of USP25 higher presence of these chains could lead to proteasomal degradation of EGFR, as previously discussed.

Substrates modified by CUL3-based E3 ligases are almost invariably degraded by the proteasome. Evidence from *C. elegans* studies suggests that CUL3 plays a role in the membrane receptors turnover. It was shown that the $CUL3^{KEL8}$ E3 ligase complex is critical for degradation of the Glutamate receptor (Schaefer & Rongo, 2006). Our results on CUL3 are only preliminary and further investigations are needed to clarify the

functional relationship between USP25 and CUL3 to regulate EGFR endocytosis. Nonetheless, our data open an interesting and novel possible regulation of EGFR level.

4 USP25 as a promising target in cancer therapy

In a recent publication, USP25 mRNA and protein levels were found to be upregulated in NSCLC patients correlating with advanced clinical stage, histological grade, and lymph node metastasis (Li et al., 2014). Li and co-workers found that high levels of USP25 promote the epithelial to mesenchymal transition (EMT), a precondition of cancer cells allowing migration, invasion and metastasis. A general property induced by the transition is a change in cell morphology with the acquisition of spindle shape, loss of epithelial cell polarity and stress fibers redistribution. The possible targets of USP25 responsible for EMT were not identified yet. Many RTK signalling pathways play a role in EMT including EGFR but also c-met, PDGFR (Platelet Derived Growth Factor Receptor), NGFR (Nerve Growth Factor Receptor) and FGFR (Fibroblast Growth Factor Receptor) (Larue & Bellacosa, 2005). Therefore one interesting possibility is that the increased metastasis observed *in vitro* but also *in vivo* upon overexpression of USP25 is due to its role as a positive regulator of EGFR, and maybe also of other RTKs. Indeed we found a decrease in Akt signalling when USP25 was silenced (**Figure 13**), which could be a hint for the reverse effect upon USP25 overexpression. Therefore it would be worth to investigate if there is a connection between the reported upregulation of USP25 in EMT cells and the role of USP25 in rescuing EGFR from lysosomal degradation, as we described in the present study.

Deregulated EGFR signalling is a typical feature of numerous solid tumours including breast, ovarian, NSCLC, prostate, head and neck cancers and others (Salomon et al., 1995). EGFR signalling activates cell proliferation, angiogenesis, metastasis and is anti-apoptotic, thus providing the basis for cell transformation and tumour progression

(Hanahan & Weinberg, 2000). This makes the EGF receptor a prominent drug target and several strategies have been developed to block EGFR mediated oncogenic signalling. Monoclonal antibodies specific for the extracellular part of EGFR and small molecule tyrosine kinase inhibitors, targeting the kinase activity of EGFR, are already approved in clinics. However in many cases cancer cells were able to acquire resistance to this drugs resulting in tumour relapse (Cheng & Chen, 2014). Another promising anticancer strategy would be forcing EGFR downregulation and consequently compelling signal attenuation. Ubiquitination of EGFR plays a key role in this process, regulating receptor internalization, trafficking and degradation (Roepstorff et al., 2008). Therefore possible strategies to increase receptor ubiquitination are enhancing E3 ligases activity or alternatively inhibiting DUBs activity. In this context the latter one appears to be more practicable for clinical purposes.

In recent years there was a massive effort in screening for and developing of small compound inhibitors. Targeting the ubiquitin-proteasome system for cancer therapy is an emerging field. Since cancer cells are more sensitive for altered protein homeostasis compared to normal cells, many compounds were developed for blocking the proteasome. The most clinically successful is bortezomib an inhibitor of the 26S proteasome, used for the treatment of myeloma and mantle cell lymphoma (Adams, 2004). A problem of this anticancer therapeutics is that a complete inhibition of the proteasomal degradation has also tremendous effects to normal cells and goes along with serious side-effects. Targeting DUBs is more specific and a promising future direction. The mechanisms of action of proteases and the presence of distinct catalytically active residues facilitate the development of specific inhibitors. Their unique biochemical structures and the fact that they are rather substrate- than linkage-specific, makes DUBs of the USP-type to ideal “druggable” targets (Pal et al., 2014). Up to date about 30 USPs have been described to be directly or indirectly involved in cancer (Pal et al., 2014). With the exception of CYLD,

DUBs are not frequently mutated in tumours (Bignell et al., 2000). Upregulated transcript levels of several USPs have been found in certain cancer types, including USP18 (Liu et al., 1999), USP9X (Schwickart et al., 2010) and also for USP25 in NSCLC (Li et al., 2014). Moreover numerous USP-type DUBs are described to be a regulator of cancer-associated pathways. As it is the case for USP4, USP11and USP15 in the TGF-β signalling pathway (Aggarwal & Massague, 2012) or as it was recently suggested for USP2a and Cezanne in the EGFR signalling pathway (Liu et al., 2013; Pareja et al., 2012). Our study added USP25 to this growing list.

Based on our data, blocking of USP25 activity would result in increased ubiquitination of EGFR. As a consequence EGFR is degraded in lysosomes and excessive oncogenic EGFR signalling would be shut off. This is in particular interesting for cancer types in which EGFR signalling is upregulated due to increased protein levels. Recently a novel mechanism of DUB inhibition was reported. Small molecules which are capable of generating ROS, resulting in a selective and nonreversible oxidation of the catalytic Cys residue were identified (Ohayon et al., 2014). Previously USP25 was shown to be sensitive for oxidative inhibition (Lee et al., 2013). Exploiting USP25 inhibition for cancer therapy might open up a promising direction for future investigations.

APPENDIX: Additional USPs implicated in the EGFR pathway

Starting from our siRNA screen targeting all known active DUBs we selected sixteen USPs that displayed major alterations in EGFR degradation kinetics for further validation. The two oligos of the initial pool were individually tested for each of the selected DUBs (**Appendix Figure 1**) and the efficiency of the knock-down was assessed by quantitative RT-PCR (**Table 1**). Eleven out of sixteen USPs confirmed previous results (**Appendix Figure 1A**). The remaining DUBs were not validated and displayed discrepancies between the phenotypes observed for the two single oligos or affected EGFR degradation kinetics in the absence of mRNA depletion, suggestive of an off-target effect (**Appendix Figure 1B**). USP6 and USP29 were discarded since they are apparently not expressed in HeLa cells (**Table 1**).

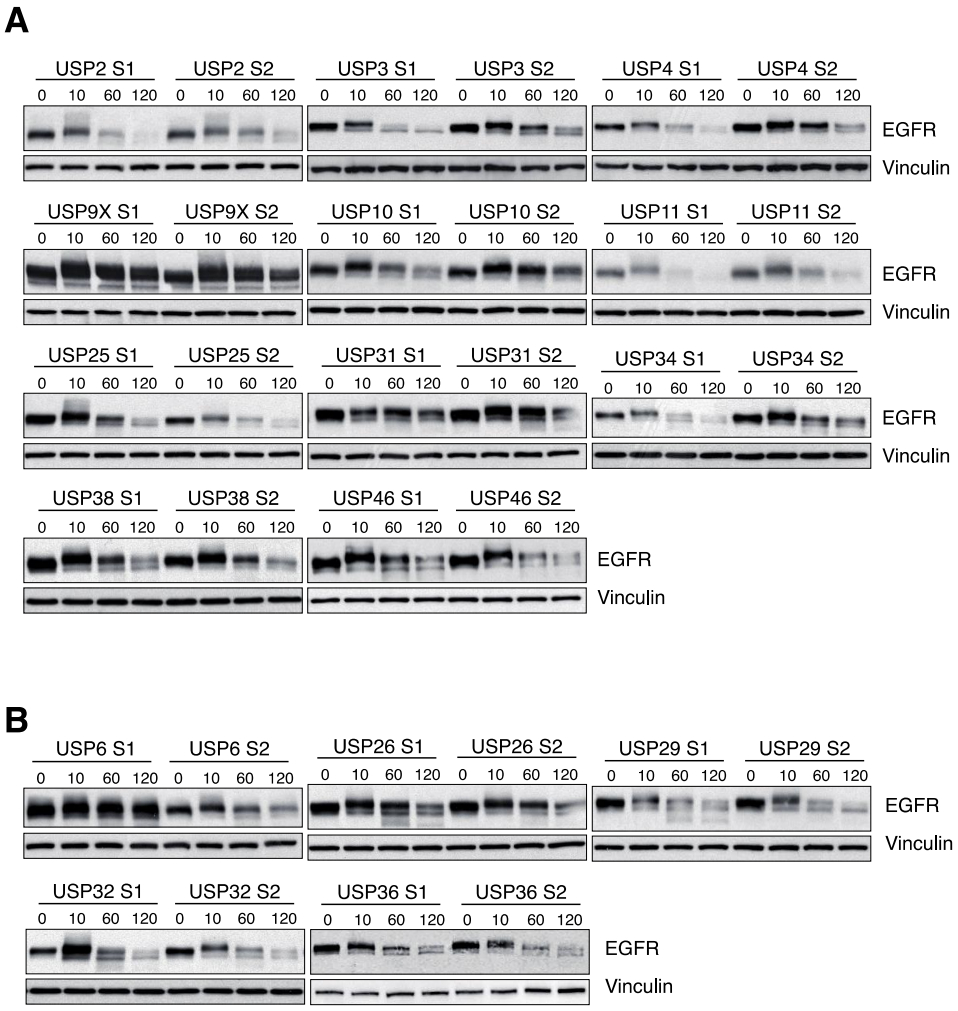

Appendix Figure 1: Deconvolution experiments of selected USPs.

HeLa cells have been separately transfected with either oligo S1 and S2, for the 16 selected USP-type DUBs. After serum starvation cells were stimulated with EGF [100 ng/ml] for the indicated time points. Total cell lysates were analysed by IB with an EGFR antibody. Eleven USP KDs displayed the same EGFR degradation kinetics between oligo S1 and S2 (**A**). Five USP KDs showed no phenotype or discrepancy between the two oligos or a phenotype in the absence of mRNA depletion (**B**).

Sample	USP2	Ct usp2	Ct 18S
USP2 s1	0.725	35.5	10.1
USP2 s2	0.140	37.6	9.9
Cnt	1.000	35.1	10.1
Sample	**USP3**	**Ct usp3**	**Ct 18S**
USP3 s1	0.188	28.8	9.7
USP3 s2	0.253	28.7	10.1
Cnt	1.000	26.3	9.7
Sample	**USP4**	**Ct usp4**	**Ct GAPDH**
USP4 s1	0.311	28.4	19.0
USP4 s2	0.358	27.9	18.8
Cnt	1.000	26.7	19.1
Sample	**USP6**	**Ct usp6**	**Ct GAPDH**
USP6 s1	1.073	33.9	20.4
USP6 s2	0.810	33.5	19.5
Cnt	1.000	32.8	19.2
Sample	**USP9X**	**Ct usp9X**	**Ct GAPDH**
USP9X s1	0.063	32.1	18.1
USP9X s2	0.070	32.1	18.2
Cnt	1.000	28.1	18.1
Sample	**USP10**	**Ct usp10**	**Ct 18S**
USP10 s1	0.093	28.9	10.4
USP10 s2	0.097	29.6	11.2
Cnt	1.000	25.3	10.1
Sample	**USP11**	**Ct usp11**	**Ct 18S**
USP11 s1	0.048	30.9	9.7
USP11 s2	0.140	30.3	10.6
Cnt	1.000	27.0	10.1
Sample	**USP25**	**Ct usp25**	**Ct GAPDH**
USP25 s1	0.335	30.2	20.2
USP25 s2	0.506	29.5	20.2
Cnt	1.000	27.6	19.2
Sample	**USP26**	**Ct usp26**	**Ct GAPDH**
USP26 s1	not detectable	not detectable	19.2
USP26 s2	not detectable	not detectable	19.0
Cnt	not detectable	38.3	19.2
Sample	**USP29**	**Ct usp29**	**Ct GAPDH**
USP29 s1	not detectable	not detectable	20.3
USP29 s2	not detectable	not detectable	19.7
Cnt	not detectable	not detectable	19.2
Sample	**USP31**	**Ct usp31**	**Ct GAPDH**
USP31 s1	0.343	29.2	19.3
USP31 s2	0.363	28.9	19.0
Cnt	1.000	27.6	19.2
Sample	**USP32**	**Ct usp32**	**Ct 18S**
USP32 s1	0.190	29.6	10.0
USP32 s2	0.241	29.4	10.2
Cnt	1.000	26.9	9.7

Sample	USP34	Ct usp34	Ct GAPDH
USP34 s1	undetermined	35.7	24.8
USP34 s2	0.749	26.8	19.5
Cnt	1.000	25.6	18.8
Sample	**USP36**	**Ct usp36**	**Ct GAPDH**
USP36 s1	0.200	29.0	20.3
USP36 s2	0.212	28.7	20.0
Cnt	1.000	25.7	19.2
Sample	**USP38**	**Ct usp38**	**Ct 18S**
USP38 s1	0.076	31.7	10.1
USP38 s2	0.146	30.4	9.9
Cnt	1.000	27.5	9.7
Sample	**USP46**	**Ct usp46**	**Ct GAPDH**
USP46 s1	0.579	28.0	18.5
USP46 s2	0.294	29.1	18.7
Cnt	1.000	27.9	19.1

Table 1: Expression levels of USPs mRNA.

By qRT-PCR analyses mRNA expression levels of selected USPs were assessed and normalized to the housekeeping genes 18S or GAPDH. Ct-values and fold changes in respect to control conditions are reported.

Among the eleven validated DUBs we selected USP10, USP11 and USP31 for further analysis. EGFR degradation kinetics upon DUBs KD were tested by DELFIA assay (**Appendix Figure 2**).

While depletion of USP11 caused enhanced EGFR degradation kinetics, KD of USP10 and USP31 showed the opposite behaviour.

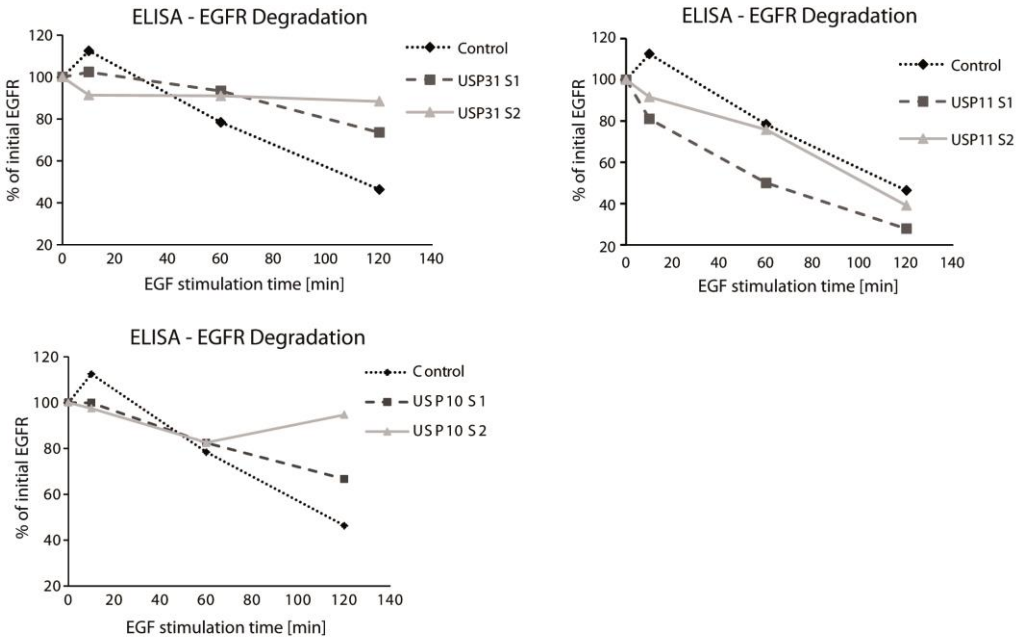

Appendix Figure 2: DELFIA analyses of selected USPs.

HeLa cells were transfected with different siRNAs targeting the indicated USPs or with a scrambled oligo (Control). Cells were serum starved and then stimulated with EGF [100 ng/ml] for the indicated time points. Total cell lysates were subjected to DELFIA analyses to determine EGFR degradation.

As a next step we decided to acquire information related to the ubiquitination status of EGFR upon depletion of the selected USPs. KD cells were stimulated with high dose of EGF [100 ng/ml] to induce EGFR ubiquitination. EGFR was immunoprecipitated from cell lysates and modifications with ubiquitin were revealed with an ubiquitin specific antibody (**Appendix Figure 3A**). This was complemented by DELFIA assay using an anti-ubiquitin (FK2) as revealing antibody (**Appendix Figure 3B**). Silencing of USP10, USP11 and USP31 caused a decreased ubiquitination of EGFR (**Appendix Figure 3**).

We also assessed possible transcriptional effects exerted by the KD on the EGFR transcript levels by qRT-PCR. Downregulation of the three DUBs showed no major changes in EGFR transcription (**Appendix Table 2**).

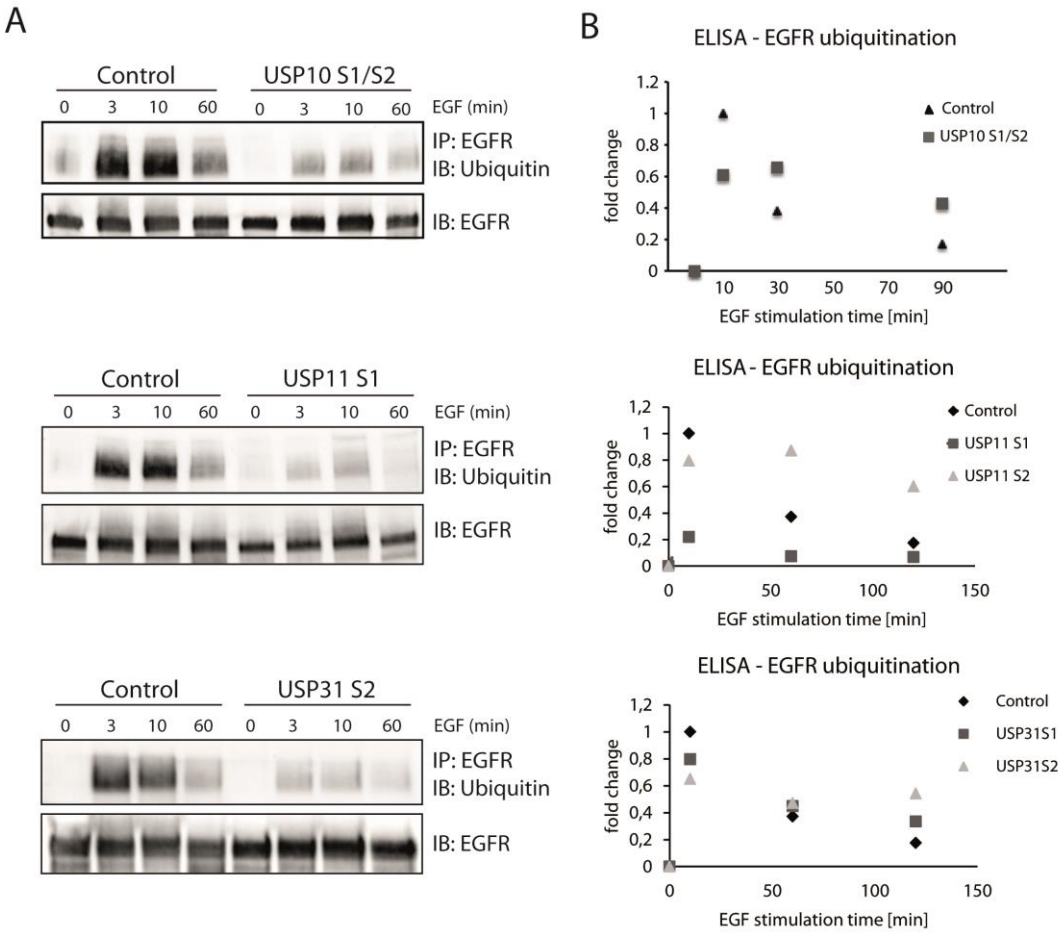

Appendix Figure 3: EGFR ubiquitination upon selected USP knock-downs.

HeLa cells were transfected with different siRNAs targeting the indicated USPs or with a scrambled oligo (Control). Cells were stimulated with high dose of EGF [100 ng/ml] for the indicated time points. EGFR was immunoprecipitated using protein specific antibody and its ubiquitination status was revealed with an ubiquitin antibody (**A**). Alternatively, lysates were subjected to DELFIA with an EGFR antibody for coating and anti-ubiquitin (FK2) as revealing antibody (**B**).

Sample	EGFR	USP10
USP10 s1	0,813	0,093
USP10 s2	0,875	0,097
Cnt	1,000	1
Sample	**EGFR**	**USP11**
USP11 s1	0,559	0,048
USP11 s2	0,717	0,140
Cnt	1,000	1,000
Sample	**EGFR**	**USP31**
USP31 s1	0,822	0,343
USP31 s2	1,068	0,363
Cnt	1,000	1,000

Table 2: Expression levels of EGFR und USPs mRNA.

By qRT-PCR analyses EGFR and USP mRNA expression levels were assessed upon DUB KD and normalized to the housekeeping genes 18S or GAPDH. Fold changes in respect to control conditions are reported.

4.1 EGFR is slower degraded in cells depleted for USP10

Depletion of USP10 caused one of the strongest effects on EGFR turnover with opposite outcome compared to KD of USP25. Therefore we decided to further characterize the impact of USP10 on EGFR endocytosis.

To gain additional information, the phosphorylation status of selected signalling and adaptor proteins upon USP10 KD was monitored by IB analyses (**Appendix Figure 4**). Specifically, MAPK and Akt were tested as downstream effectors of the signalling cascade and Hrs phosphorylation as a read-out for the trafficking of the activated EGFR. USP10 was transiently depleted in HeLa cells with siRNA-based oligos (USP10 S1 and USP10 S2), after serum deprivation overnight, cells were stimulated with high dose of EGF [100 ng/ml] for different time points from 0 to 120 minutes. In cells depleted for USP10 less Akt and Hrs phosphorylation was observed compared to that of control cells, while for MAPK no differences were scored (**Appendix Figure 4**).

In sum our analyses showed that EGFR degradation kinetics are decreased upon USP10 KD. The assessed phosphorylation level of Akt instead is not compatible with the simple model that a reduced degradation of the EGFR may cause a prolonged signalling of Akt (Sousa et al., 2012; Stern et al., 2007).

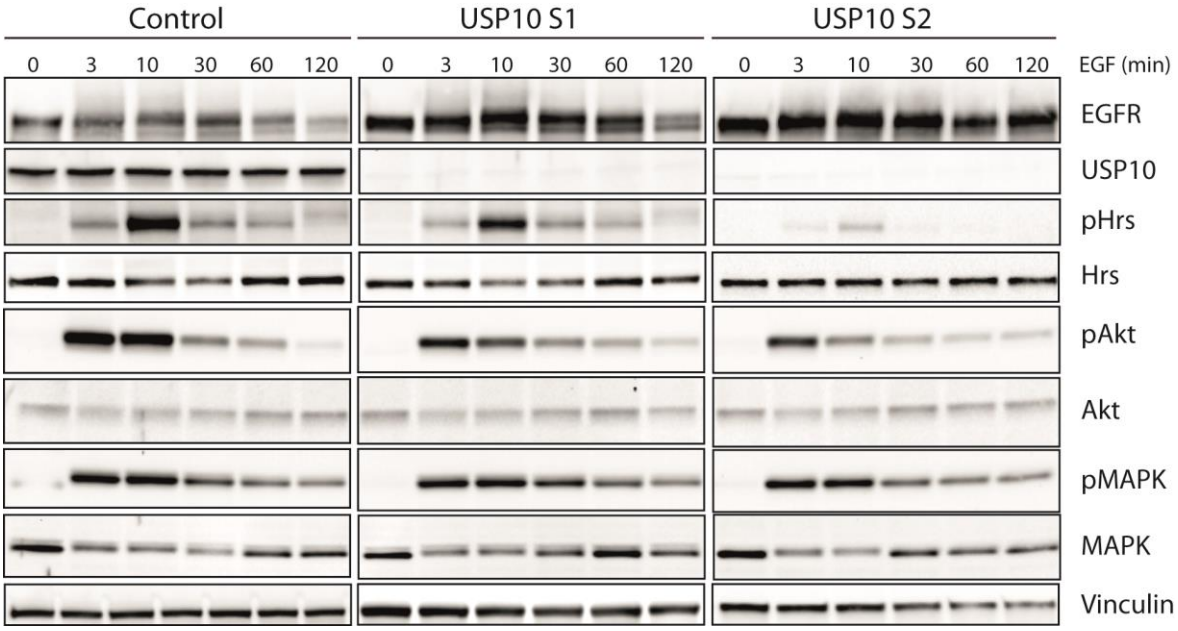

Appendix Figure 4: EGFR degradation kinetics and downstream signalling after USP10 knock-down.

HeLa cells were transfected with different siRNAs (USP10 S1 and USP10 S2) or with a scrambled oligo (Control) as indicated. Cells were serum starved and then stimulated with EGF [100 ng/ml] for the indicated time points. Total cell lysates were analysed by IB with the indicated antibodies.

4.2 Internalization and trafficking of EGFR in cells depleted of USP10

Next, we sought to visualize the effects of USP10 depletion on EGFR trafficking and degradation at single cell level. Therefore immunofluorescence based internalization assays were performed in HeLa control and USP10 KD cells (**Appendix Figure 5A**). After one hour incubation on ice with fluorescently labelled EGF, cells were shifted to 37°C allowing internalization of the EGF-EGFR complex for various time points. The fate of the receptor-ligand complex was visualized by confocal microscopy. EGFR was completely degraded 90 minutes post EGF stimulation, since no EGF signal was detectable in control cells at that time point. In USP10 KD cells instead a major fraction of the receptor was still present (**Appendix Figure 5A**).

This is in accordance with the previously observed slower degradation kinetics. Thus, in the absence of USP10, both receptor and ligand appear to be stuck into endocytic compartments inside the cells. To test this hypothesis we performed the same experiment but this time the trafficking route of the EGF-EGFR complex was observed in more detail by the help of endocytic markers. Co-staining with EEA1, associated with early endosomes, or LAMP1, known to be localized at the late endosomes/lysosomes were performed. At early time points the trafficking of EGF appeared to be normal in USP10 KD cells and no alterations compared to control conditions were detected (**Appendix Figure 5B**). At the 90 min time point a strong co-localization between EGF and LAMP1 was observed in USP10 KD cells, confirming the idea that upon USP10 KD the EGF-EGFR complex accumulates in the late endocytic compartment (**Appendix Figure 5B**).

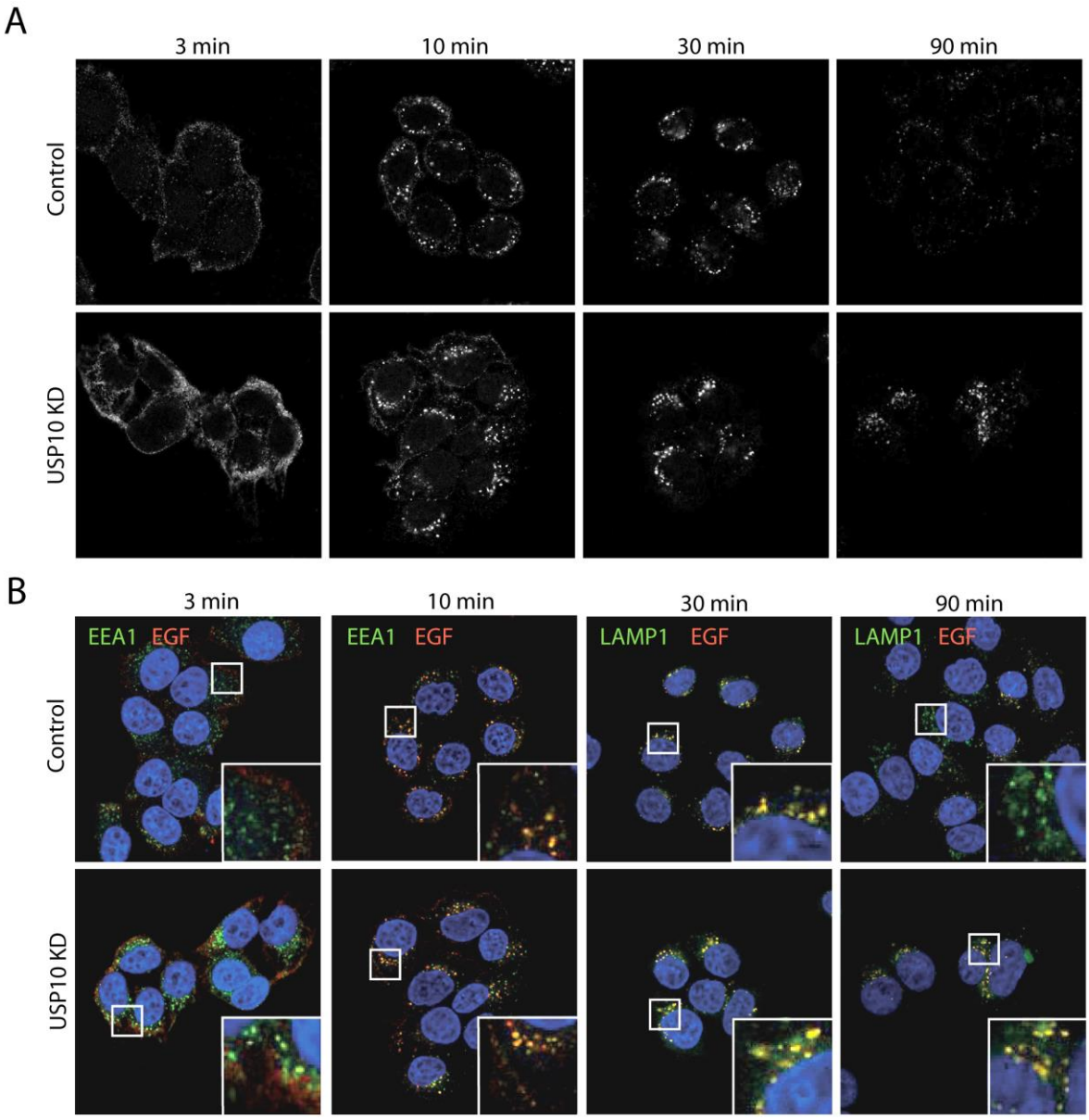

Appendix Figure 5: Internalization and trafficking of EGFR upon USP10 knock-down.

HeLa cells were transfected with siRNA targeting USP10 or with a scrambled oligo (Control) as indicated. Cells were serum starved for four hours and incubated for one hour at 4°C in the presence of Alexa555-EGF [40 ng/ml, red] (**A,B**). After washing, cells were shifted at 37°C for the indicated time points to allow internalization. Cells were subsequently fixed and stained with an EEA1 (green) or LAMP1 antibody (green) (**B**) as indicated. Blue, DAPI staining (**A,B**).

Although no internalization defects in cells depleted for USP10 were detected in immunofluorescence experiments, we decided to monitor EGFR internalization more accurate by quantitative analyses. Internalization assays with radioactively labelled EGF were performed at low [1 ng/ml] and high [20 ng/ml] doses. No significant differences of the internalization rates between KD and control cells were measured (**Appendix Figure 6**), affirming immunofluorescence analyses (**Appendix Figure 5**).

Taken together immunofluorescence experiments confirmed the initial observations that USP10 KD delays EGFR degradation. Co-staining with markers of the endocytic compartments unravelled that the non-degraded EGFR was trapped in the lysosomal compartment, while internalization of EGFR upon USP10 KD was not affected.

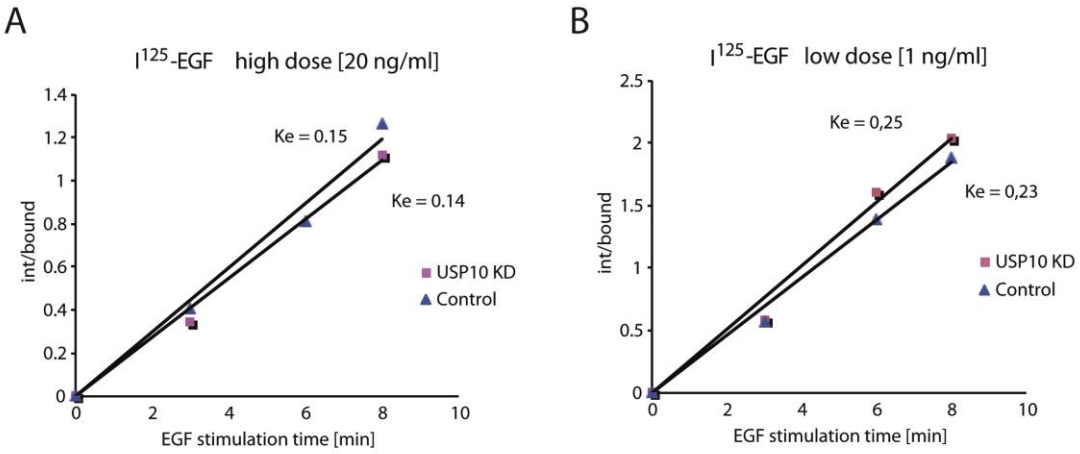

Appendix Figure 6: Effects on EGFR internalization upon USP10 knock-down.

HeLa cells were transfected with siRNAs targeting USP10 or with a scrambled oligo (Control) as indicated. EGFR internalization at high [20 ng/ml] (**A**) and low [1 ng/ml] (**B**) dose of EGF ligand was followed at early time points (0-7 min) using a radiolabeled ligand binding assay and I^{125}-EGF. Results are average of triplicates and expressed as a ratio between internalized and bound ligand. Internalization constants (K_e) were extrapolated from the internalization curves and correspond to the slopes of the best-fitting curves (**A,B**).

4.3 Effects on endocytic proteins and phosphorylation of EGFR in cells depleted of USP10

To gain a better understanding of the observed alterations in EGFR degradation, we were seeking for potential substrates of the deubiquitinating activity of USP10. As previously shown, a substantial decrease in EGFR ubiquitination was evident in both the anti-ubiquitin immunoblot and DELFIA analysis. To complete the picture we tested the behaviour of endocytic adaptor proteins in the absence of USP10. No changes in posttranslational modifications or protein levels of Eps15, Epsin1 and Epsin2 were discovered in IB analyses (**Appendix Figure 7A**).

The alteration of EGFR ubiquitination might be due to alterations in E3 ligase activity in cells depleted of USP10. Hence protein levels and possible changes in posttranslational modifications of the main E3 ligases involved in the EGFR internalization pathway (Levkowitz et al., 1999; Levkowitz et al., 1998; Woelk et al., 2006) were analysed in immunoblot. No significant differences were detectable for c-Cbl, Cbl-b and Nedd4 protein levels (**Appendix Figure 7B**).

Prior to EGFR ubiquitination, Cbl binds the regulatory region of EGFR either directly, or indirectly mediated by Grb2 (see chapter 3.3 introduction). For both interactions specific phosphorylation sites at the EGFR C-terminus are essential. A reduced Cbl activity and consequently decreased ubiquitination of EGFR can be also caused by a reduced phosphorylation of EGFR Tyr residues. We checked the presence of pTyr1045 (necessary for direct binding of Cbl) and pTyr1068 (necessary for the indirect binding via Grb2) in HeLa control and USP10 KD cells stimulated with EGF [100 ng/ml] in immunoblot (**Appendix Figure 7B**). We could not detect differences in the phosphorylation status of pTyr1068 between control and USP10 KD cells. However, there was significantly less pTyr1048 present in cells depleted of USP10 (**Appendix Figure 7B**).

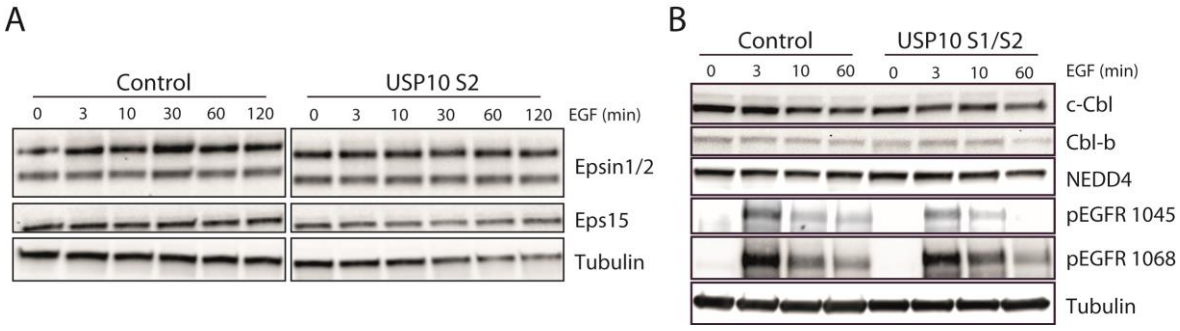

Appendix Figure 7: Characterization of endocytic proteins upon USP10 knock-down.
HeLa cells were transfected with siRNA targeting USP10 or with a scrambled oligo (Control) as indicated. After 72 hours cells were stimulated with EGF [100 ng/ml] for the indicated time points. Effects on endocytic proteins (**A**) or E3 ligases and phosphorylation of EGFR (**B**) were revealed in total cell lysates by immunoblot with the indicated antibodies.

Our data show that silencing of USP10 leads to a decrease in EGFR ubiquitination. This might be caused by a reduction in the phosphorylation of the Tyr residue (pTyr1048) essential for a direct Cbl EGFR interaction and consequently Cbl activity is diminished (Levkowitz et al., 1999). Whether this accounts for the alterations in EGFR trafficking and degradation could not be finally concluded and requires further investigations.

REFERENCES

Acconcia F, Sigismund S, Polo S (2009) Ubiquitin in trafficking: the network at work. *Experimental cell research* **315:** 1610-1618

Adams J (2004) The development of proteasome inhibitors as anticancer drugs. *Cancer cell* **5:** 417-421

Aggarwal K, Massague J (2012) Ubiquitin removal in the TGF-beta pathway. *Nature cell biology* **14:** 656-657

Al-Hakim A, Escribano-Diaz C, Landry MC, O'Donnell L, Panier S, Szilard RK, Durocher D (2010) The ubiquitous role of ubiquitin in the DNA damage response. *DNA repair* **9:** 1229-1240

Ambroggio XI, Rees DC, Deshaies RJ (2004) JAMM: a metalloprotease-like zinc site in the proteasome and signalosome. *PLoS biology* **2:** E2

Amerik AY, Li SJ, Hochstrasser M (2000) Analysis of the deubiquitinating enzymes of the yeast Saccharomyces cerevisiae. *Biological chemistry* **381:** 981-992

Anderson HA, Chen Y, Norkin LC (1996) Bound simian virus 40 translocates to caveolin-enriched membrane domains, and its entry is inhibited by drugs that selectively disrupt caveolae. *Molecular biology of the cell* **7:** 1825-1834

Ardley HC, Robinson PA (2005) E3 ubiquitin ligases. *Essays in biochemistry* **41:** 15-30

Avraham R, Yarden Y (2011) Feedback regulation of EGFR signalling: decision making by early and delayed loops. *Nature reviews Molecular cell biology* **12:** 104-117

Backer JM, Shoelson SE, Haring E, White MF (1991) Insulin receptors internalize by a rapid, saturable pathway requiring receptor autophosphorylation and an intact juxtamembrane region. *The Journal of cell biology* **115:** 1535-1545

Bailly M, Wyckoff J, Bouzahzah B, Hammerman R, Sylvestre V, Cammer M, Pestell R, Segall JE (2000) Epidermal growth factor receptor distribution during chemotactic responses. *Molecular biology of the cell* **11:** 3873-3883

Barriere H, Nemes C, Du K, Lukacs GL (2007) Plasticity of polyubiquitin recognition as lysosomal targeting signals by the endosomal sorting machinery. *Molecular biology of the cell* **18:** 3952-3965

Barriere H, Nemes C, Lechardeur D, Khan-Mohammad M, Fruh K, Lukacs GL (2006) Molecular basis of oligoubiquitin-dependent internalization of membrane proteins in Mammalian cells. *Traffic* **7:** 282-297

Bastiani M, Liu L, Hill MM, Jedrychowski MP, Nixon SJ, Lo HP, Abankwa D, Luetterforst R, Fernandez-Rojo M, Breen MR, Gygi SP, Vinten J, Walser PJ, North KN, Hancock JF, Pilch PF, Parton RG (2009) MURC/Cavin-4 and cavin family members form tissue-specific caveolar complexes. *The Journal of cell biology* **185:** 1259-1273

Berlin I, Schwartz H, Nash PD (2010) Regulation of epidermal growth factor receptor ubiquitination and trafficking by the USP8.STAM complex. *The Journal of biological chemistry* **285:** 34909-34921

Bignell GR, Warren W, Seal S, Takahashi M, Rapley E, Barfoot R, Green H, Brown C, Biggs PJ, Lakhani SR, Jones C, Hansen J, Blair E, Hofmann B, Siebert R, Turner G, Evans DG, Schrander-Stumpel C, Beemer FA, van Den Ouweland A, Halley D, Delpech B, Cleveland MG, Leigh I, Leisti J, Rasmussen S (2000) Identification of the familial cylindromatosis tumour-suppressor gene. *Nature genetics* **25:** 160-165

Bilodeau PS, Urbanowski JL, Winistorfer SC, Piper RC (2002) The Vps27p Hse1p complex binds ubiquitin and mediates endosomal protein sorting. *Nature cell biology* **4:** 534-539

Bjorge JD, Chan TO, Antczak M, Kung HJ, Fujita DJ (1990) Activated type I phosphatidylinositol kinase is associated with the epidermal growth factor (EGF) receptor following EGF stimulation. *Proceedings of the National Academy of Sciences of the United States of America* **87:** 3816-3820

Blount JR, Burr AA, Denuc A, Marfany G, Todi SV (2012) Ubiquitin-specific protease 25 functions in Endoplasmic Reticulum-associated degradation. *PloS one* **7:** e36542

Bomberger JM, Barnaby RL, Stanton BA (2010) The deubiquitinating enzyme USP10 regulates the endocytic recycling of CFTR in airway epithelial cells. *Channels* **4:** 150-154

Bosch-Comas A, Lindsten K, Gonzalez-Duarte R, Masucci MG, Marfany G (2006) The ubiquitin-specific protease USP25 interacts with three sarcomeric proteins. *Cellular and molecular life sciences : CMLS* **63:** 723-734

Boulkroun S, Ruffieux-Daidie D, Vitagliano JJ, Poirot O, Charles RP, Lagnaz D, Firsov D, Kellenberger S, Staub O (2008) Vasopressin-inducible ubiquitin-specific protease 10 increases ENaC cell surface expression by deubiquitylating and stabilizing sorting nexin 3. *American journal of physiology Renal physiology* **295:** F889-900

Bowers K, Piper SC, Edeling MA, Gray SR, Owen DJ, Lehner PJ, Luzio JP (2006) Degradation of endocytosed epidermal growth factor and virally ubiquitinated major histocompatibility complex class I is independent of mammalian ESCRTII. *The Journal of biological chemistry* **281:** 5094-5105

Burnett B, Li F, Pittman RN (2003) The polyglutamine neurodegenerative protein ataxin-3 binds polyubiquitylated proteins and has ubiquitin protease activity. *Human molecular genetics* **12:** 3195-3205

Buus R, Faronato M, Hammond DE, Urbe S, Clague MJ (2009) Deubiquitinase activities required for hepatocyte growth factor-induced scattering of epithelial cells. *Current biology : CB* **19:** 1463-1466

Cadavid AL, Ginzel A, Fischer JA (2000) The function of the Drosophila fat facets deubiquitinating enzyme in limiting photoreceptor cell number is intimately associated with endocytosis. *Development* **127:** 1727-1736

Canton I, Battaglia G (2012) Endocytosis at the nanoscale. *Chemical society reviews* **41**:2718-39

Carpenter G (2003) ErbB-4: mechanism of action and biology. *Experimental cell research* **284:** 66-77

Chau V, Tobias JW, Bachmair A, Marriott D, Ecker DJ, Gonda DK, Varshavsky A (1989) A multiubiquitin chain is confined to specific lysine in a targeted short-lived protein. *Science* **243:** 1576-1583

Chen H, Polo S, Di Fiore PP, De Camilli PV (2003) Rapid Ca2+-dependent decrease of protein ubiquitination at synapses. *Proceedings of the National Academy of Sciences of the United States of America* **100:** 14908-14913

Chen L, Davis NG (2002) Ubiquitin-independent entry into the yeast recycling pathway. *Traffic* **3:** 110-123

Chen X, Zhang B, Fischer JA (2002) A specific protein substrate for a deubiquitinating enzyme: Liquid facets is the substrate of Fat facets. *Genes & development* **16:** 289-294

Chen YG, Wang Z, Ma J, Zhang L, Lu Z (2007) Endofin, a FYVE domain protein, interacts with Smad4 and facilitates transforming growth factor-beta signaling. *The Journal of biological chemistry* **282:** 9688-9695

Cheng X, Chen H (2014) Tumor heterogeneity and resistance to EGFR-targeted therapy in advanced nonsmall cell lung cancer: challenges and perspectives. *OncoTargets and therapy* **7:** 1689-1704

Cholay M, Reverdy C, Benarous R, Colland F, Daviet L (2010) Functional interaction between the ubiquitin-specific protease 25 and the SYK tyrosine kinase. *Experimental cell research* **316:** 667-675

Citri A, Skaria KB, Yarden Y (2003) The deaf and the dumb: the biology of ErbB-2 and ErbB-3. *Experimental cell research* **284:** 54-65

Clague MJ, Barsukov I, Coulson JM, Liu H, Rigden DJ, Urbe S (2013) Deubiquitylases from genes to organism. *Physiological reviews* **93:** 1289-1315

Clague MJ, Liu H, Urbé S (2012) Governance of endocytic trafficking and signaling by reversible ubiquitylation. *Developmental cell* **23:** 457-467

Cohen M, Stutz F, Belgareh N, Haguenauer-Tsapis R, Dargemont C (2003a) Ubp3 requires a cofactor, Bre5, to specifically de-ubiquitinate the COPII protein, Sec23. *Nature cell biology* **5:** 661-667

Cohen M, Stutz F, Dargemont C (2003b) Deubiquitination, a new player in Golgi to endoplasmic reticulum retrograde transport. *The Journal of biological chemistry* **278:** 51989-51992

Cooper JA, Sefton BM, Hunter T (1984) Diverse mitogenic agents induce the phosphorylation of two related 42,000-dalton proteins on tyrosine in quiescent chick cells. *Molecular and cellular biology* **4:** 30-37

D'Souza-Schorey C, Chavrier P (2006) ARF proteins: roles in membrane traffic and beyond. *Nature reviews Molecular cell biology* **7:** 347-358

DeGraff JL, Gagnon AW, Benovic JL, Orsini MJ (1999) Role of arrestins in endocytosis and signaling of alpha2-adrenergic receptor subtypes. *The Journal of biological chemistry* **274:** 11253-11259

Deng S, Zhou H, Xiong R, Lu Y, Yan D, Xing T, Dong L, Tang E, Yang H (2007) Over-expression of genes and proteins of ubiquitin specific peptidases (USPs) and proteasome subunits (PSs) in breast cancer tissue observed by the methods of RFDD-PCR and proteomics. *Breast cancer research and treatment* **104:** 21-30

Denuc A, Bosch-Comas A, Gonzalez-Duarte R, Marfany G (2009) The UBA-UIM domains of the USP25 regulate the enzyme ubiquitination state and modulate substrate recognition. *PloS one* **4:** e5571

Di Guglielmo GM, Baass PC, Ou WJ, Posner BI, Bergeron JJ (1994) Compartmentalization of SHC, GRB2 and mSOS, and hyperphosphorylation of Raf-1 by EGF but not insulin in liver parenchyma. *The EMBO journal* **13:** 4269-4277

Di Guglielmo GM, Le Roy C, Goodfellow AF, Wrana JL (2003) Distinct endocytic pathways regulate TGF-beta receptor signalling and turnover. *Nature cell biology* **5:** 410-421

Dikic I, Wakatsuki S, Walters KJ (2009) Ubiquitin-binding domains - from structures to functions. *Nature reviews Molecular cell biology* **10:** 659-671

Doherty GJ, McMahon HT (2009) Mechanisms of endocytosis. *Annual review of biochemistry* **78:** 857-902

Dormann D, Weijer CJ (2003) Chemotactic cell movement during development. *Current opinion in genetics & development* **13:** 358-364

Duda DM, Borg LA, Scott DC, Hunt HW, Hammel M, Schulman BA (2008) Structural insights into NEDD8 activation of cullin-RING ligases: conformational control of conjugation. *Cell* **134:** 995-1006

Duex JE, Comeau L, Sorkin A, Purow B, Kefas B (2011) Usp18 regulates epidermal growth factor (EGF) receptor expression and cancer cell survival via microRNA-7. *The Journal of biological chemistry* **286:** 25377-25386

Duex JE, Sorkin A (2009) RNA interference screen identifies Usp18 as a regulator of epidermal growth factor receptor synthesis. *Molecular biology of the cell* **20:** 1833-1844

Edeling MA, Smith C, Owen D (2006) Life of a clathrin coat: insights from clathrin and AP structures. *Nature reviews Molecular cell biology* **7:** 32-44

Ellis S, Mellor H (2000) The novel Rho-family GTPase rif regulates coordinated actin-based membrane rearrangements. *Current biology : CB* **10:** 1387-1390

Fallon L, Belanger CM, Corera AT, Kontogiannea M, Regan-Klapisz E, Moreau F, Voortman J, Haber M, Rouleau G, Thorarinsdottir T, Brice A, van Bergen En Henegouwen PM, Fon EA (2006) A regulated interaction with the UIM protein Eps15 implicates parkin in EGF receptor trafficking and PI(3)K-Akt signalling. *Nature cell biology* **8:** 834-842

Fraile JM, Quesada V, Rodríguez D, Freije JM, López-Otín C. (2012) Deubiquitinases in cancer: new functions and therapeutic options. *Oncogene* **19:** 2373-2388

Funakoshi Y, Chou MM, Kanaho Y, Donaldson JG (2014) TRE17/USP6 regulates ubiquitination and trafficking of cargo proteins that enter cells by clathrin-independent endocytosis. *Journal of cell science*

Galan JM, Haguenauer-Tsapis R (1997) Ubiquitin lys63 is involved in ubiquitination of a yeast plasma membrane protein. *The EMBO journal* **16:** 5847-5854

Galcheva-Gargova Z, Theroux SJ, Davis RJ (1995) The epidermal growth factor receptor is covalently linked to ubiquitin. *Oncogene* **11:** 2649-2655

Galperin E, Sorkin A (2008) Endosomal targeting of MEK2 requires RAF, MEK kinase activity and clathrin-dependent endocytosis. *Traffic* **9:** 1776-1790

Genschik P, Sumara I, Lechner E (2013) The emerging family of CULLIN3-RING ubiquitin ligases (CRL3s): cellular functions and disease implications. *The EMBO journal* **32:** 2307-2320

Goffin JR, Zbuk K (2013) Epidermal growth factor receptor: pathway, therapies, and pipeline. *Clinical Therapeutics* **35:** 1282-1303

Goh LK, Huang F, Kim W, Gygi S, Sorkin A (2010) Multiple mechanisms collectively regulate clathrin-mediated endocytosis of the epidermal growth factor receptor. *The Journal of cell biology* **189:** 871-883

Gonnord P, Blouin CM, Lamaze C (2012) Membrane trafficking and signaling: two sides of the same coin. *Seminars in cell & developmental biology* **23:** 154-164

Goodrich JS, Clouse KN, Schupbach T (2004) Hrb27C, Sqd and Otu cooperatively regulate gurken RNA localization and mediate nurse cell chromosome dispersion in Drosophila oogenesis. *Development* **131:** 1949-1958

Grant BD, Donaldson JG (2009) Pathways and mechanisms of endocytic recycling. *Nature reviews Molecular cell biology* **10:** 597-608

Haglund K, Dikic I (2012) The role of ubiquitylation in receptor endocytosis and endosomal sorting. *Journal of cell science* **125:** 265-275

Haglund K, Sigismund S, Polo S, Szymkiewicz I, Di Fiore PP, Dikic I (2003) Multiple monoubiquitination of RTKs is sufficient for their endocytosis and degradation. *Nature cell biology* **5:** 461-466

Hanahan D, Weinberg RA (2000) The hallmarks of cancer. *Cell* **100:** 57-70

Hanson PI, Cashikar A (2012) Multivesicular body morphogenesis. *Annual review of cell and developmental biology* **28:** 337-362

Hassink GC, Zhao B, Sompallae R, Altun M, Gastaldello S, Zinin NV, Masucci MG, Lindsten K (2009) The ER-resident ubiquitin-specific protease 19 participates in the UPR and rescues ERAD substrates. *EMBO reports* **10:** 755-761

Haugh JM, Meyer T (2002) Active EGF receptors have limited access to PtdIns(4,5)P(2) in endosomes: implications for phospholipase C and PI 3-kinase signaling. *Journal of cell science* **115:** 303-310

Haugsten EM, Zakrzewska M, Brech A, Pust S, Olsnes S, Sandvig K, Wesche J (2011) Clathrin- and dynamin-independent endocytosis of FGFR3--implications for signalling. *PloS one* **6:** e21708

Hayashi T, Sakamoto S (1988) Radioimmunoassay of human epidermal growth factor--hEGF levels in human body fluids. *J Pharmacobiodyn* **11:** 146-151

Henley JR, Krueger EW, Oswald BJ, McNiven MA (1998) Dynamin-mediated internalization of caveolae. *The Journal of cell biology* **141:** 85-99

Hershko A, Ciechanover A (1998) The ubiquitin system. *Annual review of biochemistry* **67:** 425-479

Hicke L, Riezman H (1996) Ubiquitination of a yeast plasma membrane receptor signals its ligand-stimulated endocytosis. *Cell* **84:** 277-287

Hicke L, Schubert HL, Hill CP (2005) Ubiquitin-binding domains. *Nature reviews Molecular cell biology* **6:** 610-621

Higashiyama S, Lau K, Besner GE, Abraham JA, Klagsbrun M (1992) Structure of heparin-binding EGF-like growth factor. Multiple forms, primary structure, and glycosylation of the mature protein. *J Biol Chem* **267:** 6205-6212

Hoeller D, Crosetto N, Blagoev B, Raiborg C, Tikkanen R, Wagner S, Kowanetz K, Breitling R, Mann M, Stenmark H, Dikic I (2006) Regulation of ubiquitin-binding proteins by monoubiquitination. *Nature cell biology* **8:** 163-169

Howes MT, Mayor S, Parton RG (2010) Molecules, mechanisms, and cellular roles of clathrin-independent endocytosis. *Current opinion in cell biology* **22:** 519-527

Huang F, Goh LK, Sorkin A (2007) EGF receptor ubiquitination is not necessary for its internalization. *Proceedings of the National Academy of Sciences of the United States of America* **104:** 16904-16909

Huang F, Kirkpatrick D, Jiang X, Gygi S, Sorkin A (2006) Differential regulation of EGF receptor internalization and degradation by multiubiquitination within the kinase domain. *Molecular cell* **21:** 737-748

Huang F, Zeng X, Kim W, Balasubramani M, Fortian A, Gygi SP, Yates NA, Sorkin A (2013) Lysine 63-linked polyubiquitination is required for EGF receptor degradation.

Proceedings of the National Academy of Sciences of the United States of America **110:** 15722-15727

Huang TT, D'Andrea AD (2006) Regulation of DNA repair by ubiquitylation. *Nature reviews Molecular cell biology* **7:** 323-334

Huotari J, Meyer-Schaller N, Hubner M, Stauffer S, Katheder N, Horvath P, Mancini R, Helenius A, Peter M (2012) Cullin-3 regulates late endosome maturation. *Proceedings of the National Academy of Sciences of the United States of America* **109:** 823-828

Hupalowska A, Miaczynska M (2012) The new faces of endocytosis in signaling. *Traffic* **13:** 9-18

Hurley JH, Yang D (2008) MIT domainia. *Developmental cell* **14:** 6-8

Husnjak K, Dikic I (2012) Ubiquitin-binding proteins: decoders of ubiquitin-mediated cellular functions. *Annual review of biochemistry* **81:** 291-322

Jaworski J, de la Vega M, Fletcher SJ, McFarlane C, Greene MK, Smyth AW, Van Schaeybroeck S, Johnston JA, Scott CJ, Rappoport JZ, Burrows JF (2014) USP17 is required for clathrin mediated endocytosis of epidermal growth factor receptor. *Oncotarget* **5:** 6964-6975

Jiang X, Sorkin A (2003) Epidermal growth factor receptor internalization through clathrin-coated pits requires Cbl RING finger and proline-rich domains but not receptor polyubiquitylation. *Traffic* **4:** 529-543

Johannessen LE, Pedersen NM, Pedersen KW, Madshus IH, Stang E (2006) Activation of the epidermal growth factor (EGF) receptor induces formation of EGF receptor- and Grb2-containing clathrin-coated pits. *Molecular and cellular biology* **26:** 389-401

Johannessen LE, Ringerike T, Molnes J, Madshus IH (2000) Epidermal growth factor receptor efficiently activates mitogen-activated protein kinase in HeLa cells and Hep2 cells conditionally defective in clathrin-dependent endocytosis. *Experimental cell research* **260:** 136-145

Kaneko T, Kumasaka T, Ganbe T, Sato T, Miyazawa K, Kitamura N, Tanaka N (2003) Structural insight into modest binding of a non-PXXP ligand to the signal transducing adaptor molecule-2 Src homology 3 domain. *The Journal of biological chemistry* **278:** 48162-48168

Kato M, Miyazawa K, Kitamura N (2000) A deubiquitinating enzyme UBPY interacts with the Src homology 3 domain of Hrs-binding protein via a novel binding motif PX(V/I)(D/N)RXXKP. *The Journal of biological chemistry* **275:** 37481-37487

Katoh Y, Shiba Y, Mitsuhashi H, Yanagida Y, Takatsu H, Nakayama K (2004) Tollip and Tom1 form a complex and recruit ubiquitin-conjugated proteins onto early endosomes. *The Journal of biological chemistry* **279:** 24435-24443

Katz M, Shtiegman K, Tal-Or P, Yakir L, Mosesson Y, Harari D, Machluf Y, Asao H, Jovin T, Sugamura K, Yarden Y (2002) Ligand-independent degradation of epidermal

growth factor receptor involves receptor ubiquitylation and Hgs, an adaptor whose ubiquitin-interacting motif targets ubiquitylation by Nedd4. *Traffic* **3:** 740-751

Kazazic M, Roepstorff K, Johannessen LE, Pedersen NM, van Deurs B, Stang E, Madshus IH (2006) EGF-induced activation of the EGF receptor does not trigger mobilization of caveolae. *Traffic* **7:** 1518-1527

Kirkham M, Fujita A, Chadda R, Nixon SJ, Kurzchalia TV, Sharma DK, Pagano RE, Hancock JF, Mayor S, Parton RG (2005) Ultrastructural identification of uncoated caveolin-independent early endocytic vehicles. *The Journal of cell biology* **168:** 465-476

Kolling R, Hollenberg CP (1994) The ABC-transporter Ste6 accumulates in the plasma membrane in a ubiquitinated form in endocytosis mutants. *The EMBO journal* **13:** 3261-3271

Komander D, Barford D (2008) Structure of the A20 OTU domain and mechanistic insights into deubiquitination. *The Biochemical journal* **409:** 77-85

Komander D, Clague MJ, Urbe S (2009) Breaking the chains: structure and function of the deubiquitinases. *Nature reviews Molecular cell biology* **10:** 550-563

Komander D, Rape M (2012) The ubiquitin code. *Annual review of biochemistry* **81:** 203-229

Kumari S, Mg S, Mayor S (2010) Endocytosis unplugged: multiple ways to enter the cell. *Cell research* **20:** 256-275

Lampugnani MG, Orsenigo F, Gagliani MC, Tacchetti C, Dejana E (2006) Vascular endothelial cadherin controls VEGFR-2 internalization and signaling from intracellular compartments. *The Journal of cell biology* **174:** 593-604

Lanahan AA, Hermans K, Claes F, Kerley-Hamilton JS, Zhuang ZW, Giordano FJ, Carmeliet P, Simons M (2010) VEGF receptor 2 endocytic trafficking regulates arterial morphogenesis. *Developmental cell* **18:** 713-724

Larsen CN, Krantz BA, Wilkinson KD (1998) Substrate specificity of deubiquitinating enzymes: ubiquitin C-terminal hydrolases. *Biochemistry* **37:** 3358-3368

Larue L, Bellacosa A (2005) Epithelial-mesenchymal transition in development and cancer: role of phosphatidylinositol 3' kinase/AKT pathways. *Oncogene* **24:** 7443-7454

Lauwers E, Jacob C, Andre B (2009) K63-linked ubiquitin chains as a specific signal for protein sorting into the multivesicular body pathway. *The Journal of cell biology* **185:** 493-502

Lee JG, Baek K, Soetandyo N, Ye Y (2013) Reversible inactivation of deubiquitinases by reactive oxygen species in vitro and in cells. *Nature communications* **4:** 1568

Lemus L, Goder V (2014) Regulation of Endoplasmic Reticulum-Associated Protein Degradation (ERAD) by Ubiquitin. *Cells* **3:** 824-847

Leuchowius KJ, Weibrecht I, Landegren U, Gedda L, Soderberg O (2009) Flow cytometric in situ proximity ligation analyses of protein interactions and post-translational modification of the epidermal growth factor receptor family. *Cytometry Part A : the journal of the International Society for Analytical Cytology* **75:** 833-839

Levkowitz G, Waterman H, Ettenberg SA, Katz M, Tsygankov AY, Alroy I, Lavi S, Iwai K, Reiss Y, Ciechanover A, Lipkowitz S, Yarden Y (1999) Ubiquitin ligase activity and tyrosine phosphorylation underlie suppression of growth factor signaling by c-Cbl/Sli-1. *Molecular cell* **4:** 1029-1040

Levkowitz G, Waterman H, Zamir E, Kam Z, Oved S, Langdon WY, Beguinot L, Geiger B, Yarden Y (1998) c-Cbl/Sli-1 regulates endocytic sorting and ubiquitination of the epidermal growth factor receptor. *Genes & development* **12:** 3663-3674

Li J, Tan Q, Yan M, Liu L, Lin H, Zhao F, Bao G, Kong H, Ge C, Zhang F, Yu T, Li J, He X, Yao M (2014) miRNA-200c inhibits invasion and metastasis of human non-small cell lung cancer by directly targeting ubiquitin specific peptidase 25. *Molecular cancer* **13:** 166

Liang J, Saad Y, Lei T, Wang J, Qi D, Yang Q, Kolattukudy PE, Fu M (2010) MCP-induced protein 1 deubiquitinates TRAF proteins and negatively regulates JNK and NF-kappaB signaling. *The Journal of experimental medicine* **207:** 2959-2973

Lim JP, Gleeson PA (2011) Macropinocytosis: an endocytic pathway for internalising large gulps. *Immunology and cell biology* **89:** 836-843

Liu H, Buus R, Clague MJ, Urbe S (2009) Regulation of ErbB2 receptor status by the proteasomal DUB POH1. *PloS one* **4:** e5544

Liu LQ, Ilaria R, Jr., Kingsley PD, Iwama A, van Etten RA, Palis J, Zhang DE (1999) A novel ubiquitin-specific protease, UBP43, cloned from leukemia fusion protein AML1-ETO-expressing mice, functions in hematopoietic cell differentiation. *Molecular and cellular biology* **19:** 3029-3038

Liu Y, Ye Y (2012) Roles of p97-associated deubiquitinases in protein quality control at the endoplasmic reticulum. *Current protein & peptide science* **13:** 436-446

Liu Z, Zanata SM, Kim J, Peterson MA, Di Vizio D, Chirieac LR, Pyne S, Agostini M, Freeman MR, Loda M (2013) The ubiquitin-specific protease USP2a prevents endocytosis-mediated EGFR degradation. *Oncogene* **32:** 1660-1669

Lu A, Pfeffer SR. (2014) A CULLINary ride across the secretory pathway: more than just secretion. *Trends in cell biology* **24:** 389-399

Lu Z, Murray JT, Luo W, Li H, Wu X, Xu H, Backer JM, Chen YG (2002) Transforming growth factor beta activates Smad2 in the absence of receptor endocytosis. *The Journal of biological chemistry* **277:** 29363-29368

Luna-Vargas MP, Faesen AC, van Dijk WJ, Rape M, Fish A, Sixma TK (2011) Ubiquitin-specific protease 4 is inhibited by its ubiquitin-like domain. *EMBO reports* **12:** 365-372

Lund PK, Moats-Staats BM, Simmons JG, Hoyt E, D'Ercole AJ, Martin F, Van Wyk JJ (1985) Nucleotide sequence analysis of a cDNA encoding human ubiquitin reveals that

ubiquitin is synthesized as a precursor. *The Journal of biological chemistry* **260:** 7609-7613

Macia E, Ehrlich M, Massol R, Boucrot E, Brunner C, Kirchhausen T (2006) Dynasore, a cell-permeable inhibitor of dynamin. *Developmental cell* **10:** 839-850

Magnifico A, Ettenberg S, Yang C, Mariano J, Tiwari S, Fang S, Lipkowitz S, Weissman AM (2003) WW domain HECT E3s target Cbl RING finger E3s for proteasomal degradation. *The Journal of biological chemistry* **278:** 43169-43177

Maldonado-Baez L, Williamson C, Donaldson JG (2013) Clathrin-independent endocytosis: a cargo-centric view. *Experimental cell research* **319:** 2759-2769

Martinu L, Masuda-Robens JM, Robertson SE, Santy LC, Casanova JE, Chou MM (2004) The TBC (Tre-2/Bub2/Cdc16) domain protein TRE17 regulates plasma membrane-endosomal trafficking through activation of Arf6. *Molecular and cellular biology* **24:** 9752-9762

Maspero E, Valentini E, Mari S, Cecatiello V, Soffientini P, Pasqualato S, Polo S (2013) Structure of a ubiquitin-loaded HECT ligase reveals the molecular basis for catalytic priming. *Nature structural & molecular biology* **20:** 696-701

Massague J (1990) Transforming growth factor-alpha. A model for membrane-anchored growth factors. *J Biol Chem* **265:** 21393-21396

Mathie A (2007) Neuronal two-pore-domain potassium channels and their regulation by G protein-coupled receptors. *The Journal of physiology* **578:** 377-385

Matos CA, de Macedo-Ribeiro S, Carvalho AL (2011) Polyglutamine diseases: the special case of ataxin-3 and Machado-Joseph disease. *Progress in neurobiology* **95:** 26-48

Mayle KM, Le AM, Kamei DT (2012) The intracellular trafficking pathway of transferrin. *Biochimica et biophysica acta* **1820:** 264-281

McCullough J, Clague MJ, Urbe S (2004) AMSH is an endosome-associated ubiquitin isopeptidase. *The Journal of cell biology* **166:** 487-492

McCullough J, Row PE, Lorenzo O, Doherty M, Beynon R, Clague MJ, Urbe S (2006) Activation of the endosome-associated ubiquitin isopeptidase AMSH by STAM, a component of the multivesicular body-sorting machinery. *Current biology : CB* **16:** 160-165

McMahon HT, Boucrot E (2011) Molecular mechanism and physiological functions of clathrin-mediated endocytosis. *Nature reviews Molecular cell biology* **12:** 517-533

Meisenhelder J, Suh PG, Rhee SG, Hunter T (1989) Phospholipase C-gamma is a substrate for the PDGF and EGF receptor protein-tyrosine kinases in vivo and in vitro. *Cell* **57:** 1109-1122

Metzger MB, Pruneda JN, Klevit RE, Weissman AM (2014) RING-type E3 ligases: master manipulators of E2 ubiquitin-conjugating enzymes and ubiquitination. *Biochimica et biophysica acta* **1843:** 47-60

Meulmeester E, Kunze M, Hsiao HH, Urlaub H, Melchior F (2008) Mechanism and consequences for paralog-specific sumoylation of ubiquitin-specific protease 25. *Molecular cell* **30:** 610-619

Mevissen TE, Hospenthal MK, Geurink PP, Elliott PR, Akutsu M, Arnaudo N, Ekkebus R, Kulathu Y, Wauer T, El Oualid F, Freund SM, Ovaa H, Komander D (2013) OTU deubiquitinases reveal mechanisms of linkage specificity and enable ubiquitin chain restriction analysis. *Cell* **154:** 169-184

Meyer H, Bug M, Bremer S (2012) Emerging functions of the VCP/p97 AAA-ATPase in the ubiquitin system. *Nature cell biology* **14:** 117-123

Mizuno E, Iura T, Mukai A, Yoshimori T, Kitamura N, Komada M (2005) Regulation of epidermal growth factor receptor down-regulation by UBPY-mediated deubiquitination at endosomes. *Molecular biology of the cell* **16:** 5163-5174

Mizuno E, Kobayashi K, Yamamoto A, Kitamura N, Komada M (2006) A deubiquitinating enzyme UBPY regulates the level of protein ubiquitination on endosomes. *Traffic* **7:** 1017-1031

Mosesson Y, Shtiegman K, Katz M, Zwang Y, Vereb G, Szollosi J, Yarden Y (2003) Endocytosis of receptor tyrosine kinases is driven by monoubiquitylation, not polyubiquitylation. *The Journal of biological chemistry* **278:** 21323-21326

Nakamura M, Tanaka N, Kitamura N, Komada M (2006) Clathrin anchors deubiquitinating enzymes, AMSH and AMSH-like protein, on early endosomes. *Genes to cells : devoted to molecular & cellular mechanisms* **11:** 593-606

Nakamura T, Hillova J, Mariage-Samson R, Onno M, Huebner K, Cannizzaro LA, Boghosian-Sell L, Croce CM, Hill M (1992) A novel transcriptional unit of the tre oncogene widely expressed in human cancer cells. *Oncogene* **7:** 733-741

Nathan JA, Kim HT, Ting L, Gygi SP, Goldberg AL (2013) Why do cellular proteins linked to K63-polyubiquitin chains not associate with proteasomes? *The EMBO journal* **32:** 552-565

Niendorf S, Oksche A, Kisser A, Lohler J, Prinz M, Schorle H, Feller S, Lewitzky M, Horak I, Knobeloch KP (2007) Essential role of ubiquitin-specific protease 8 for receptor tyrosine kinase stability and endocytic trafficking in vivo. *Molecular and cellular biology* **27:** 5029-5039

Ogiso H, Ishitani R, Nureki O, Fukai S, Yamanaka M, Kim JH, Saito K, Sakamoto A, Inoue M, Shirouzu M, Yokoyama S (2002) Crystal structure of the complex of human epidermal growth factor and receptor extracellular domains. *Cell* **110:** 775-787

Ohayon S, Refua M, Hendler A, Aharoni A, Brik A (2014) Harnessing the Oxidation Susceptibility of Deubiquitinases for Inhibition with Small Molecules. *Angewandte Chemie*

Oka Y, Orth DN (1983) Human plasma epidermal growth factor/beta-urogastrone is associated with blood platelets. *J Clin Invest* **72:** 249-259

Oldham CE, Mohney RP, Miller SL, Hanes RN, O'Bryan JP (2002) The ubiquitin-interacting motifs target the endocytic adaptor protein epsin for ubiquitination. *Current biology : CB* **12:** 1112-1116

Ozkan E, Yu H, Deisenhofer J (2005) Mechanistic insight into the allosteric activation of a ubiquitin-conjugating enzyme by RING-type ubiquitin ligases. *Proceedings of the National Academy of Sciences of the United States of America* **102:** 18890-18895

Pal A, Young MA, Donato NJ (2014) Emerging Potential of Therapeutic Targeting of Ubiquitin-Specific Proteases in the Treatment of Cancer. *Cancer research* **74:** 4955-4966

Pareja F, Ferraro DA, Rubin C, Cohen-Dvashi H, Zhang F, Aulmann S, Ben-Chetrit N, Pines G, Navon R, Crosetto N, Kostler W, Carvalho S, Lavi S, Schmitt F, Dikic I, Yakhini Z, Sinn P, Mills GB, Yarden Y (2012) Deubiquitination of EGFR by Cezanne-1 contributes to cancer progression. *Oncogene* **31:** 4599-4608

Pearse BM, Robinson MS (1990) Clathrin, adaptors, and sorting. *Annual review of cell biology* **6:** 151-171

Peng J, Schwartz D, Elias JE, Thoreen CC, Cheng D, Marsischky G, Roelofs J, Finley D, Gygi SP (2003) A proteomics approach to understanding protein ubiquitination. *Nature biotechnology* **21:** 921-926

Pickart CM, Rose IA (1985) Functional heterogeneity of ubiquitin carrier proteins. *Progress in clinical and biological research* **180:** 215

Pintard L, Willis JH, Willems A, Johnson JL, Srayko M, Kurz T, Glaser S, Mains PE, Tyers M, Bowerman B, Peter M (2003) The BTB protein MEL-26 is a substrate-specific adaptor of the CUL-3 ubiquitin-ligase. *Nature* **425:** 311-316

Polo S, Di Fiore PP, Sigismund S (2014) Keeping EGFR signaling in check: ubiquitin is the guardian. *Cell cycle* **5:** 681-682

Polo S (2012) Signaling-mediated control of ubiquitin ligases in endocytosis. *BMC biology* **10:** 25

Polo S, Sigismund S, Faretta M, Guidi M, Capua MR, Bossi G, Chen H, De Camilli P, Di Fiore PP (2002) A single motif responsible for ubiquitin recognition and monoubiquitination in endocytic proteins. *Nature* **416:** 451-455

Posor Y, Eichhorn-Grunig M, Haucke V (2014) Phosphoinositides in endocytosis. *Biochimica et biophysica acta*

Poteryaev D, Datta S, Ackema K, Zerial M, Spang A (2010) Identification of the switch in early-to-late endosome transition. *Cell* **141:** 497-508

Prager D, Li HL, Yamasaki H, Melmed S (1994) Human insulin-like growth factor I receptor internalization. Role of the juxtamembrane domain. *The Journal of biological chemistry* **269:** 11934-11937

Puertollano R, Bonifacino JS (2004) Interactions of GGA3 with the ubiquitin sorting machinery. *Nature cell biology* **6:** 244-251

Puthenveedu MA, von Zastrow M (2006) Cargo regulates clathrin-coated pit dynamics. *Cell* **127:** 113-124

Raiborg C, Bache KG, Gillooly DJ, Madshus IH, Stang E, Stenmark H (2002) Hrs sorts ubiquitinated proteins into clathrin-coated microdomains of early endosomes. *Nature cell biology* **4:** 394-398

Ren X, Hurley JH (2010) VHS domains of ESCRT-0 cooperate in high-avidity binding to polyubiquitinated cargo. *The EMBO journal* **29:** 1045-1054

Reyes-Turcu FE, Ventii KH, Wilkinson KD (2009) Regulation and cellular roles of ubiquitin-specific deubiquitinating enzymes. *Annual review of biochemistry* **78:** 363-397

Rink J, Ghigo E, Kalaidzidis Y, Zerial M (2005) Rab conversion as a mechanism of progression from early to late endosomes. *Cell* **122:** 735-749

Roberts D, Pedmale UV, Morrow J, Sachdev S, Lechner E, Tang X, Zheng N, Hannink M, Genschik P, Liscum E (2011) Modulation of phototropic responsiveness in Arabidopsis through ubiquitination of phototropin 1 by the CUL3-Ring E3 ubiquitin ligase CRL3(NPH3). *The Plant cell* **23:** 3627-3640

Roepstorff K, Grovdal L, Grandal M, Lerdrup M, van Deurs B (2008) Endocytic downregulation of ErbB receptors: mechanisms and relevance in cancer. *Histochemistry and cell biology* **129:** 563-578

Rose IA, Warms JV (1983) An enzyme with ubiquitin carboxy-terminal esterase activity from reticulocytes. *Biochemistry* **22:** 4234-4237

Roskoski R, Jr. (2014a) The ErbB/HER family of protein-tyrosine kinases and cancer. *Pharmacological research : the official journal of the Italian Pharmacological Society* **79:** 34-74

Roskoski R, Jr. (2014b) ErbB/HER protein-tyrosine kinases: Structures and small molecule inhibitors. *Pharmacological research : the official journal of the Italian Pharmacological Society* **87:** 42-59

Rothberg KG, Heuser JE, Donzell WC, Ying YS, Glenney JR, Anderson RG (1992) Caveolin, a protein component of caveolae membrane coats. *Cell* **68:** 673-682

Row PE, Liu H, Hayes S, Welchman R, Charalabous P, Hofmann K, Clague MJ, Sanderson CM, Urbe S (2007) The MIT domain of UBPY constitutes a CHMP binding and endosomal localization signal required for efficient epidermal growth factor receptor degradation. *The Journal of biological chemistry* **282:** 30929-30937

Row PE, Prior IA, McCullough J, Clague MJ, Urbe S (2006) The ubiquitin isopeptidase UBPY regulates endosomal ubiquitin dynamics and is essential for receptor down-regulation. *J Biol Chem* **281:** 12618-12624

Roxrud I, Raiborg C, Pedersen NM, Stang E, Stenmark H (2008) An endosomally localized isoform of Eps15 interacts with Hrs to mediate degradation of epidermal growth factor receptor. *The Journal of cell biology* **180:** 1205-1218

Ruggiano A, Foresti O, Carvalho P (2014) Quality control: ER-associated degradation: protein quality control and beyond. *The Journal of cell biology* **204:** 869-879

Sabharanjak S, Sharma P, Parton RG, Mayor S (2002) GPI-anchored proteins are delivered to recycling endosomes via a distinct cdc42-regulated, clathrin-independent pinocytic pathway. *Developmental cell* **2:** 411-423

Sadowski L, Pilecka I, Miaczynska M (2009) Signaling from endosomes: location makes a difference. *Experimental cell research* **315:** 1601-1609

Salomon DS, Brandt R, Ciardiello F, Normanno N (1995) Epidermal growth factor-related peptides and their receptors in human malignancies. *Critical reviews in oncology/hematology* **19:** 183-232

Savio MG, Wollscheid N, Cavallaro E, Algisi V, Di Fiore PP, S. S, S. P (2014) USP9X controls EGFR fate by deubiquitinating the endocytic adaptors Eps15 and Epsin. **manuscript in preparation**

Schaefer H, Rongo C (2006) KEL-8 is a substrate receptor for CUL3-dependent ubiquitin ligase that regulates synaptic glutamate receptor turnover. *Molecular biology of the cell* **17:** 1250-1260

Schwanhausser B, Busse D, Li N, Dittmar G, Schuchhardt J, Wolf J, Chen W, Selbach M (2011) Global quantification of mammalian gene expression control. *Nature* **473:** 337-342

Schwickart M, Huang X, Lill JR, Liu J, Ferrando R, French DM, Maecker H, O'Rourke K, Bazan F, Eastham-Anderson J, Yue P, Dornan D, Huang DC, Dixit VM (2010) Deubiquitinase USP9X stabilizes MCL1 and promotes tumour cell survival. *Nature* **463:** 103-107

Scita G, Di Fiore PP (2010) The endocytic matrix. *Nature* **463:** 464-473

Scortegagna M, Subtil T, Qi J, Kim H, Zhao W, Gu W, Kluger H, Ronai ZA (2011) USP13 enzyme regulates Siah2 ligase stability and activity via noncatalytic ubiquitin-binding domains. *The Journal of biological chemistry* **286:** 27333-27341

Sharma DK, Brown JC, Choudhury A, Peterson TE, Holicky E, Marks DL, Simari R, Parton RG, Pagano RE (2004) Selective stimulation of caveolar endocytosis by glycosphingolipids and cholesterol. *Molecular biology of the cell* **15:** 3114-3122

Shenoy SK, Lefkowitz RJ (2003) Trafficking patterns of beta-arrestin and G protein-coupled receptors determined by the kinetics of beta-arrestin deubiquitination. *The Journal of biological chemistry* **278:** 14498-14506

Shenoy SK, Modi AS, Shukla AK, Xiao K, Berthouze M, Ahn S, Wilkinson KD, Miller WE, Lefkowitz RJ (2009) Beta-arrestin-dependent signaling and trafficking of 7-transmembrane receptors is reciprocally regulated by the deubiquitinase USP33 and the E3

ligase Mdm2. *Proceedings of the National Academy of Sciences of the United States of America* **106:** 6650-6655

Shields SB, Piper RC (2011) How ubiquitin functions with ESCRTs. *Traffic* **12:** 1306-1317

Shin KJ, Wall EA, Zavzavadjian JR, Santat LA, Liu J, Hwang JI, Rebres R, Roach T, Seaman W, Simon MI, Fraser ID (2006) A single lentiviral vector platform for microRNA-based conditional RNA interference and coordinated transgene expression. *Proceedings of the National Academy of Sciences of the United States of America* **103:** 13759-13764

Shoyab M, McDonald VL, Bradley JG, Todaro GJ (1988) Amphiregulin: a bifunctional growth-modulating glycoprotein produced by the phorbol 12-myristate 13-acetate-treated human breast adenocarcinoma cell line MCF-7. *Proc Natl Acad Sci U S A* **85:** 6528-6532

Sigismund S, Algisi V, Nappo G, Conte A, Pascolutti R, Cuomo A, Bonaldi T, Argenzio E, Verhoef LG, Maspero E, Bianchi F, Capuani F, Ciliberto A, Polo S, Di Fiore PP (2013) Threshold-controlled ubiquitination of the EGFR directs receptor fate. *The EMBO journal* **32:** 2140-2157

Sigismund S, Argenzio E, Tosoni D, Cavallaro E, Polo S, Di Fiore PP (2008) Clathrin-mediated internalization is essential for sustained EGFR signaling but dispensable for degradation. *Developmental cell* **15:** 209-219

Sigismund S, Confalonieri S, Ciliberto A, Polo S, Scita G, Di Fiore PP (2012) Endocytosis and signaling: cell logistics shape the eukaryotic cell plan. *Physiological reviews* **92:** 273-366

Sigismund S, Woelk T, Puri C, Maspero E, Tacchetti C, Transidico P, Di Fiore PP, Polo S (2005) Clathrin-independent endocytosis of ubiquitinated cargos. *Proceedings of the National Academy of Sciences of the United States of America* **102:** 2760-2765

Soncini C, Berdo I, Draetta G (2001) Ras-GAP SH3 domain binding protein (G3BP) is a modulator of USP10, a novel human ubiquitin specific protease. *Oncogene* **20:** 3869-3879

Sorkin A, Von Zastrow M (2002) Signal transduction and endocytosis: close encounters of many kinds. *Nature reviews Molecular cell biology* **3:** 600-614

Sorkin A, von Zastrow M (2009) Endocytosis and signalling: intertwining molecular networks. *Nature reviews Molecular cell biology* **10:** 609-622

Sousa LP, Lax I, Shen H, Ferguson SM, De Camilli P, Schlessinger J (2012) Suppression of EGFR endocytosis by dynamin depletion reveals that EGFR signaling occurs primarily at the plasma membrane. *Proceedings of the National Academy of Sciences of the United States of America* **109:** 4419-4424

Sowa ME, Bennett EJ, Gygi SP, Harper JW (2009) Defining the human deubiquitinating enzyme interaction landscape. *Cell* **138:** 389-403

Spratt DE, Walden H, Shaw GS (2014) RBR E3 ubiquitin ligases: new structures, new insights, new questions. *The Biochemical journal* **458:** 421-437

Springael JY, Galan JM, Haguenauer-Tsapis R, Andre B (1999) NH4+-induced down-regulation of the Saccharomyces cerevisiae Gap1p permease involves its ubiquitination with lysine-63-linked chains. *Journal of cell science* **112 (Pt 9):** 1375-1383

Staub O, Gautschi I, Ishikawa T, Breitschopf K, Ciechanover A, Schild L, Rotin D (1997) Regulation of stability and function of the epithelial Na+ channel (ENaC) by ubiquitination. *The EMBO journal* **16:** 6325-6336

Steinhauer WR, Walsh RC, Kalfayan LJ (1989) Sequence and structure of the Drosophila melanogaster ovarian tumor gene and generation of an antibody specific for the ovarian tumor protein. *Molecular and cellular biology* **9:** 5726-5732

Stenmark H (2009) Rab GTPases as coordinators of vesicle traffic. *Nature reviews Molecular cell biology* **10:** 513-525

Stern KA, Visser Smit GD, Place TL, Winistorfer S, Piper RC, Lill NL (2007) Epidermal growth factor receptor fate is controlled by Hrs tyrosine phosphorylation sites that regulate Hrs degradation. *Molecular and cellular biology* **27:** 888-898

Strachan L, Murison JG, Prestidge RL, Sleeman MA, Watson JD, Kumble KD (2001) Cloning and biological activity of epigen, a novel member of the epidermal growth factor superfamily. *J Biol Chem* **276:** 18265-18271

Sumara I, Maerki S, Peter M (2008) E3 ubiquitin ligases and mitosis: embracing the complexity. *Trends in cell biology* **18:** 84-94

Sumara I, Quadroni M, Frei C, Olma MH, Sumara G, Ricci R, Peter M (2007) A Cul3-based E3 ligase removes Aurora B from mitotic chromosomes, regulating mitotic progression and completion of cytokinesis in human cells. *Developmental cell* **12:** 887-900

Swanson JA (2008) Shaping cups into phagosomes and macropinosomes. *Nature reviews Molecular cell biology* **9:** 639-649

Terrell J, Shih S, Dunn R, Hicke L (1998) A function for monoubiquitination in the internalization of a G protein-coupled receptor. *Molecular cell* **1:** 193-202

Tosoni D, Puri C, Confalonieri S, Salcini AE, De Camilli P, Tacchetti C, Di Fiore PP (2005) TTP specifically regulates the internalization of the transferrin receptor. *Cell* **123:** 875-88.

Toyoda H, Komurasaki T, Ikeda Y, Yoshimoto M, Morimoto S (1995) Molecular cloning of mouse epiregulin, a novel epidermal growth factor-related protein, expressed in the early stage of development. *FEBS Lett* **377:** 403-407

Tsukazaki T, Chiang TA, Davison AF, Attisano L, Wrana JL (1998) SARA, a FYVE domain protein that recruits Smad2 to the TGFbeta receptor. *Cell* **95:** 779-791

Ullrich A, Schlessinger J (1990) Signal transduction by receptors with tyrosine kinase activity. *Cell* **61:** 203-212

Urbe S, Sachse M, Row PE, Preisinger C, Barr FA, Strous G, Klumperman J, Clague MJ (2003) The UIM domain of Hrs couples receptor sorting to vesicle formation. *Journal of cell science* **116:** 4169-4179

Valero R, Bayes M, Francisca Sanchez-Font M, Gonzalez-Angulo O, Gonzalez-Duarte R, Marfany G (2001) Characterization of alternatively spliced products and tissue-specific isoforms of USP28 and USP25. *Genome biology* **2:** RESEARCH0043

Valero R, Marfany G, Gonzalez-Angulo O, Gonzalez-Gonzalez G, Puelles L, Gonzalez-Duarte R (1999) USP25, a novel gene encoding a deubiquitinating enzyme, is located in the gene-poor region 21q11.2. *Genomics* **62:** 395-405

van Delft S, Govers R, Strous GJ, Verkleij AJ, van Bergen en Henegouwen PM (1997) Epidermal growth factor induces ubiquitination of Eps15. *The Journal of biological chemistry* **272:** 14013-14016

von Zastrow M, Sorkin A (2007) Signaling on the endocytic pathway. *Current opinion in cell biology* **19:** 436-445

Ventii KH, Wilkinson KD (2008) Protein partners of deubiquitinating enzymes. *The Biochemical journal* **414:** 161-175

Vieira AV, Lamaze C, Schmid SL (1996) Control of EGF receptor signaling by clathrin-mediated endocytosis. *Science* **274:** 2086-2089

Westergaard LG, Yding Andersen C, Byskov AG (1990) Epidermal growth factor in small antral ovarian follicles of pregnant women. *J Endocrinol* **127:** 363-367

Wilde A, Beattie EC, Lem L, Riethof DA, Liu SH, Mobley WC, Soriano P, Brodsky FM (1999) EGF receptor signaling stimulates SRC kinase phosphorylation of clathrin, influencing clathrin redistribution and EGF uptake. *Cell* **96:** 677-687

Wiley HS (1988) Anomalous binding of epidermal growth factor to A431 cells is due to the effect of high receptor densities and a saturable endocytic system. *The Journal of cell biology* **107:** 801-810

Wiley HS, Cunningham DD (1982) The endocytotic rate constant. A cellular parameter for quantitating receptor-mediated endocytosis. *The Journal of biological chemistry* **257:** 4222-4229

Wilkinson KD (2009) DUBs at a glance. *Journal of cell science* **122:** 2325-2329

Winkler ME, O'Connor L, Winget M, Fendly B (1989) Epidermal growth factor and transforming growth factor alpha bind differently to the epidermal growth factor receptor. *Biochemistry* **28:** 6373-6378

Woelk T, Oldrini B, Maspero E, Confalonieri S, Cavallaro E, Di Fiore PP, Polo S (2006) Molecular mechanisms of coupled monoubiquitination. *Nature cell biology* **8:** 1246-1254

Wollert T, Wunder C, Lippincott-Schwartz J, Hurley JH (2009) Membrane scission by the ESCRT-III complex. *Nature* **458:** 172-177

Wood, E. J. (1983), Molecular cloning. A laboratory manual by T Maniatis, E F Fritsch and J Sambrook. pp 545. Cold Spring Harbor Laboratory, New York. 1982. $48 ISBN 0-87969-136-0. Biochemical Education, 11: 82. doi: 10.1016/0307-4412(83)90068-7
Xu L, Wei Y, Reboul J, Vaglio P, Shin TH, Vidal M, Elledge SJ, Harper JW (2003) BTB proteins are substrate-specific adaptors in an SCF-like modular ubiquitin ligase containing CUL-3. *Nature* **425:** 316-321

Xu P, Duong DM, Seyfried NT, Cheng D, Xie Y, Robert J, Rush J, Hochstrasser M, Finley D, Peng J (2009) Quantitative proteomics reveals the function of unconventional ubiquitin chains in proteasomal degradation. *Cell* **137:** 133-145

Yamamoto H, Sakane H, Yamamoto H, Michiue T, Kikuchi A (2008) Wnt3a and Dkk1 regulate distinct internalization pathways of LRP6 to tune the activation of beta-catenin signaling. *Developmental cell* **15:** 37-48

Yao T, Cohen RE (2002) A cryptic protease couples deubiquitination and degradation by the proteasome. *Nature* **419:** 403-407

Yarden Y (2001) The EGFR family and its ligands in human cancer. signalling mechanisms and therapeutic opportunities. *European journal of cancer* **37 Suppl 4:** S3-8

Yen HC, Xu Q, Chou DM, Zhao Z, Elledge SJ (2008) Global protein stability profiling in mammalian cells. *Science* **322:** 918-923

Yu X, Riley T, Levine AJ (2009) The regulation of the endosomal compartment by p53 the tumor suppressor gene. *The FEBS journal* **276:** 2201-2212

Zeng S, Xu Z, Lipkowitz S, Longley JB (2005) Regulation of stem cell factor receptor signaling by Cbl family proteins (Cbl-b/c-Cbl). *Blood* **105:** 226-232

Zhong B, Liu X, Wang X, Chang SH, Wang A, Reynolds JM, Dong C (2012) Negative regulation of IL-17-mediated signaling and inflammation by the ubiquitin-specific protease USP25. *Nature immunology* **13:** 1110-1117

Zhong B, Liu X, Wang X, Li H, Darnay BG, Lin X, Sun SC, Dong C (2013a) Ubiquitin-specific protease 25 regulates TLR4-dependent innate immune responses through deubiquitination of the adaptor protein TRAF3. *Science signaling* **6:** ra35

Zhong H, Wang D, Fang L, Zhang H, Luo R, Shang M, Ouyang C, Ouyang H, Chen H, Xiao S (2013b) Ubiquitin-specific proteases 25 negatively regulates virus-induced type I interferon signaling. *PloS one* **8:** e80976